

THESIS ON POWER ENGINEERING,  
ELECTRICAL ENGINEERING, MINING ENGINEERING D68

**Research and Development of  
Trial Instrumentation for  
Electric Propulsion Motor Drives**

ANTON RASSÖLKIN

**TUT**  
PRESS

# TALLINN UNIVERSITY OF TECHNOLOGY

Faculty of Power Engineering  
Department of Electrical Engineering

**Dissertation was accepted for the defence of the degree of Doctor of Philosophy in Engineering on May 25, 2014**

**Supervisors:** PhD Hardi Hõimoja, Department of Electrical Engineering, Tallinn University of Technology

PhD Valery Vodovozov, Department of Electrical Engineering, Tallinn University of Technology

**Opponents:** Dr Tuomo Lindh, Faculty of Technology, Lappeenranta University of Technology, Finland

PhD Vitali Boiko, ABB AS, Estonia

Defence of the thesis: June 25, 2014

**Declaration:**

*Hereby I declare that this doctoral thesis, my original investigation and achievement, submitted for the doctoral degree at Tallinn University of Technology, has not been submitted for any academic degree.*

Anton Rassõlkin .....



European Union  
European Social Fund



Investing in your future

Copyright: Anton Rassõlkin, 2014

ISSN 1406-474X

ISBN 978-9949-23-634-3 (publication)

ISBN 978-9949-23-635-0 (PDF)

ENERGEETIKA. ELEKTROTEHNIKA. MÄENDUS D68

# **Elekterveoajamite katsekeskkonna uurimine ja arendamine**

ANTON RASSÕLKIN



## Table of Contents

Acknowledgement .....	7
List of abbreviations .....	8
Symbol index .....	10
1 Introduction.....	12
1.1 Motivation and Background .....	12
1.2 Main Objectives and Tasks of the Thesis .....	14
1.3 Contribution of the Thesis and Dissemination.....	15
1.4 Thesis Outline .....	15
2 Overview of Studies in the Field of Electric Propulsion Motor Drive .....	17
2.1 Comparative study of HEV and EV Topologies.....	17
2.2 Electric Drives and Motors for BEV Propulsion .....	23
2.3 Analysis of Power Electronic Devices for a Propulsion Drive .....	28
2.4 Analysis of Energy Storage Applications for a Propulsion Drive .....	31
2.5 Regenerative braking .....	38
2.6 Charging Systems for BEV.....	38
2.7 Summary of Chapter 2.....	40
3 Modelling of Propulsion Drive System .....	42
3.1 Model of the vehicle's propulsion drive load .....	42
3.2 Computer Model of the Propulsion Drive of BEV .....	47
3.3 A Test Bench to Study Propulsion Drives of BEV .....	51
3.4 Summary of Chapter 3 .....	58
4 Study of Electric Propulsion Motor Drives .....	60
4.1 Vehicle Testing Cycles .....	60
4.2 Library of Samples to Study BEV Drive Behavior.....	63
4.3 Tuning of propulsion motor drive.....	67
4.4 Study of the Propulsion Drive Regarding Speed Reference .....	69
4.5 Study of the Propulsion Drive Regarding Load.....	72
4.6 Dynamic load for electric motor drive testing on the test bench .....	74
4.7 Summary of Chapter 4.....	78
5 Future Work. Extended application of the BEV propulsion drive system.....	79
5.1 STATCOM as a Part of BEV Propulsion Drive System .....	79
5.2 PSIM Model of Topology .....	81
5.3 Experimental Verification of Topology Application .....	84
5.4 Summary of Chapter 5 .....	86
References.....	87
List of Author's Publications .....	93
Abstract.....	95
Kokkuvõte.....	97

Elulookirjeldus.....	99
Curriculum Vitae .....	101
Appendix 1. MATLAB/Simulink model of test bench.....	103
Appendix 2. Adaptive programs .....	105
Appendix 3. Results observed from MATLAB/Simulink simulation and test bench experiments .....	113

## Acknowledgement

My research for the degree of PhD was conducted at Tallinn University of Technology, the Department of Electrical Drives and Power Electronics (Department of Electrical Engineering from 01.01.2013) during four years of study. First of all, I would like to express my appreciation to my supervisors Prof. Valery Vodovozov and Dr. Hardi Hõimoja for their help and encouragement during the years of my research.

Doctoral School of Energy and Geotechnology II (DAR8130), DoRa Doctoral Studies Programme, Kristjan Jaak Scholarships Programme and Project ETF9350 are gratefully acknowledged for their financial support.

Also, I would like to thank my colleagues Dr. Sc. Dmitri Vinnikov, Dr. Sc. Janis Zakis, Dr. Tanel Jalakas, Dr. Viktor Beldjajev, Dr. Alexandr Suzdalenko, PhD student Liisa Liivik, PhD student Levon Gevorgov PhD student Andrii Chub and everyone who helped me with their invaluable advice and criticism regarding to scientific work and article publishing. Furthermore, I am thankful to them for creating a favourable atmosphere for my work.

Moreover, I would like to thank Mare-Anne Laane for revising and editing English texts in my articles and the thesis.

In addition, I would like to express my sincere thanks to all other colleagues from Tallinn University of Technology, Department of Electrical Engineering, for their versatile help and support during the four years of research.

My special thanks are due to my family and my friends for their support, patience and care throughout the years of my study.

Thank you all!

Anton Rassõlkin

## List of abbreviations

AC	Alternating Current
BAT	Batteries
BEV	Battery Electric Vehicle
BLDCM	Brushless DC Motor
CSI	Current Source Inverter
DC	Direct Current
DIFF	Differential
DTC	Direct Torque Control
ECE-R15	Europe urban driving cycle
EM	Electric Machine
EREV	Extended-Range Electric Vehicle
ESS	Energy Storage System
EUDC	Extra Urban Driving Cycle
EV	Electric Vehicle
FC	Fuel Cell
FCEV	Fuel Cell Electric Vehicle
FES	Flywheel Energy Storage
FTP-75	(Federal Test Procedure 75) - US Driving Cycle
G2V	Grid-to-Vehicle
GCEV	Grid-connected Electric Vehicle
GEAR	Mechanical Coupling (Gearbox)
HEV	Hybrid Electric Vehicle
ICE	Internal Combustion Engine
ICEV	Internal Combustion Engine Vehicle
IEEE	Institute of Electrical and Electronics Engineers
IGBT	Integrated Gate Bipolar Transistor
IM	Induction Motor
JC08	Japan Driving Cycle
KAIST	Korea Advanced Institute of Science and Technology
KERS	Kinetic Energy Recovery Systems
MOSFET	Metal-Oxide-Semiconductor Field-Effect Transistor
NEDC	New European Driving Cycle
OICA	International Organization of Motor Vehicle Manufacturers
OLEV	Online Electric Vehicle
PE	Power Electronic Converter
PHEV	Plug-in Hybrid Electric Vehicle
PM	Permanent Magnet
PMR	Power-to-mass ratio
PMSM	Permanent Magnet Synchronous Machine
PWM	Pulse-Width Modulation
RES	Renewable Energy Sources
RFB	Reduction-oxidation (redox) Flow Batteries
RPA	Relative Positive Acceleration

rms	root mean square
SC	Supercapacitors
SEPIC	Single-Ended Primary-Inductor Converter
SG	Smart Grid
SMES	Superconducting Magnetic Energy Storage
SOC	State of Charge
SRM	Switched Reluctance Motors
STATCOM	Static Synchronous Compensator
SVC	Static var Compensator
TUT	Tallinn University of Technology
UPS	Uninterruptible Power Supply
V2G	Vehicle-to-Grid
V2H	Vehicle-to-Home
VSI	Voltage Source Inverter
WLTC	World-wide harmonized Light duty driving Test Cycle

## Symbol index

$A$	frontal area of the vehicle
$a$	linear acceleration of the vehicle ( $a=dv/dt$ )
$C$	capacitance
$C_{(n)}$	dynamic load coefficients
$C^*_{(n)}$	dynamic load coefficients related to linear vehicle speed
$C_d$	coefficient of drag
$C_n$	capacity of the single capacitor
$C_{rf}$	coefficient of rolling friction between the tire and the road
$F_{ACC}$	acceleration force
$F_{AD}$	aerodynamic drag
$F_{CR}$	climbing resistance force
$F_N$	normal force
$F_{RL}$	road load
$F_{RR}$	rolling resistance
$F_{TE}$	tractive effort
$g$	gravitational acceleration ( $g \approx 9.81 \dots \text{m/s}^2$ )
$GR_{DIFF}$	differential gear ratio
$GR_{TRANS}$	transmission gear ratio
$J_{eq}$	equivalent inertia moment of the system reduced to propulsion motor shaft
$J_{motor}$	inertia moment of the motor
$k$	required amplitude level
$K_i$	integral coefficient of PI regulator
$K_p$	proportional coefficient of PI regulator
$m$	mass of the vehicle
$n_{motor}$	frequency of rotation of the motor
$P$	active power
$Q$	reactive power
$t_{(n)}$	time slot
$T_{axle}$	wheel axle torque
$T_{motor}$	torque developed by motor
$t_n$	time point
$U_{grid}$	voltage magnitude of the grid
$U_{STATCOM}$	voltage magnitude of STATCOM
$v$	velocity of the vehicle
$W_{C(s)}$	converter transfer function
$W_{F(s)}$	feedback speed sensor transfer function
$W_{k,motor}$	kinetic energy stored rotating parts of motor
$W_{k,trans}$	kinetic energy stored in the moving vehicles transmission
$W_{k,vehicle}$	kinetic energy stored in the moving vehicle
$W_{M(s)}$	motor transfer function
$W_{R(s)}$	speed regulator transfer function

$X_L$	reactance of coupling reactor
$y^*$	step signal
$\alpha$	slope angle
$\gamma$	phase difference between the voltages
$\delta$	signal processing
$\varepsilon$	angular acceleration ( $\varepsilon=d\omega/dt$ )
$\eta_{diff}$	differential efficiency
$\eta_{trans}$	transmission efficiency
$\pi$	mathematical constant ( $\pi\approx 3.14.. m/s^2$ )
$\rho$	air density
$\tau$	signal period
$\omega^*$	speed set-point
$\omega_{axle}$	angular velocity of the wheel axle
$\omega_{motor}$	angular velocity of the motor

# 1 INTRODUCTION

## 1.1 Motivation and Background

World population already exceeds seven billion people and the number of vehicles in operation has surpassed one billion units. According to OICA (International Organization of Motor Vehicle Manufacturers) statistics, more than 87 million vehicles were produced in 2013, and the number is increasing each year. With further globalization, industrialization and urbanization, the trend of fast growth of the number of vehicles worldwide is inevitable. The main issues due to increasing vehicle numbers are limited volume of oil and the emissions from burning oil products. The world consumes approximately 85 million barrels of oil every day but there are only 1300 billion barrels of proven reserves of oil [1]. At the current rate of consumption, the world will run out of oil approximately in the next 40 years [2]. The emissions from burning fossil fuels increase the carbon dioxide (CO<sub>2</sub>) in the Earth's atmosphere [2]. The increase of CO<sub>2</sub> is a cause of greenhouse effect and climate change. As a consequence, it will lead to instability of ecosystems and, perhaps, rising sea levels. Reducing fossil fuel usage and as a result, reducing carbon emissions are the main goals of humanity nowadays. Hybrid Electric Vehicles (HEVs) in use instead of Internal Combusting Engine Vehicles (ICEVs) could notably decrease the atmospheric pollution. The effect of using of an Electric Vehicle (EV) could be still better.

The production of electricity, a complex process, is not always friendly to the environment, being often connected with burning of fossil fuels. Well-to-wheel studies show that even if the electricity is generated from petroleum, the equivalent kilometres that can be driven by 1 litre of petrol are 46 km in an electric car, compared to 14 km in an ICEV [2]. As compared to petrol price per kilometre, driving an EV (ca 15-20 kWh/100 km, i.e. about 1.5-2 €/100 km), is cheaper than with an ICEV (ca 5-6 l/100 km, i.e. about 8-11 €/100 km). Moreover, the size of petrol-to-electric transmission is more compact, while with a pure mechanical transmission from the engine to the wheels, a large number of gears are required and with a generator-motor traction system, a wide range of operating speeds are available.

The block diagram in Figure 1.1 describes the energy management between different parts of an electric propulsion vehicle. The propulsion motor drive of an EV consists of a power electronics converter (PE(2)), a vehicle propulsion motor (MOTOR), mechanical transmission or differential (DIFF), and a control system (CONTROL). The energy storage system (ESS) and a vehicle's load, incl. aerodynamic drag, road friction, road slope etc. (LOAD) are not a part of a propulsion motor drive system, but their features have influence on the propulsion drive system, particularly on such portable systems, as a vehicle. The propulsion motor drive system is shown in Figure 1.1 inside the green dashed line. It means that their particular qualities should be taken into account. The EV is a rather complex system for accurate mathematical description,

monitoring, and validation. However, today much attention is paid to the studies of different parts of EVs. The laboratory studies with test benches, combining advantages of software models and real equipment, contribute to the reduction of the number of vehicle test runs and safe maintenance. By using a variety of different test benches, separate parts of an EV could be studied and improved. Each wide arrow in Figure 1.1 describes some energy conversion, which means that different test benches could be created for each energy conversion.

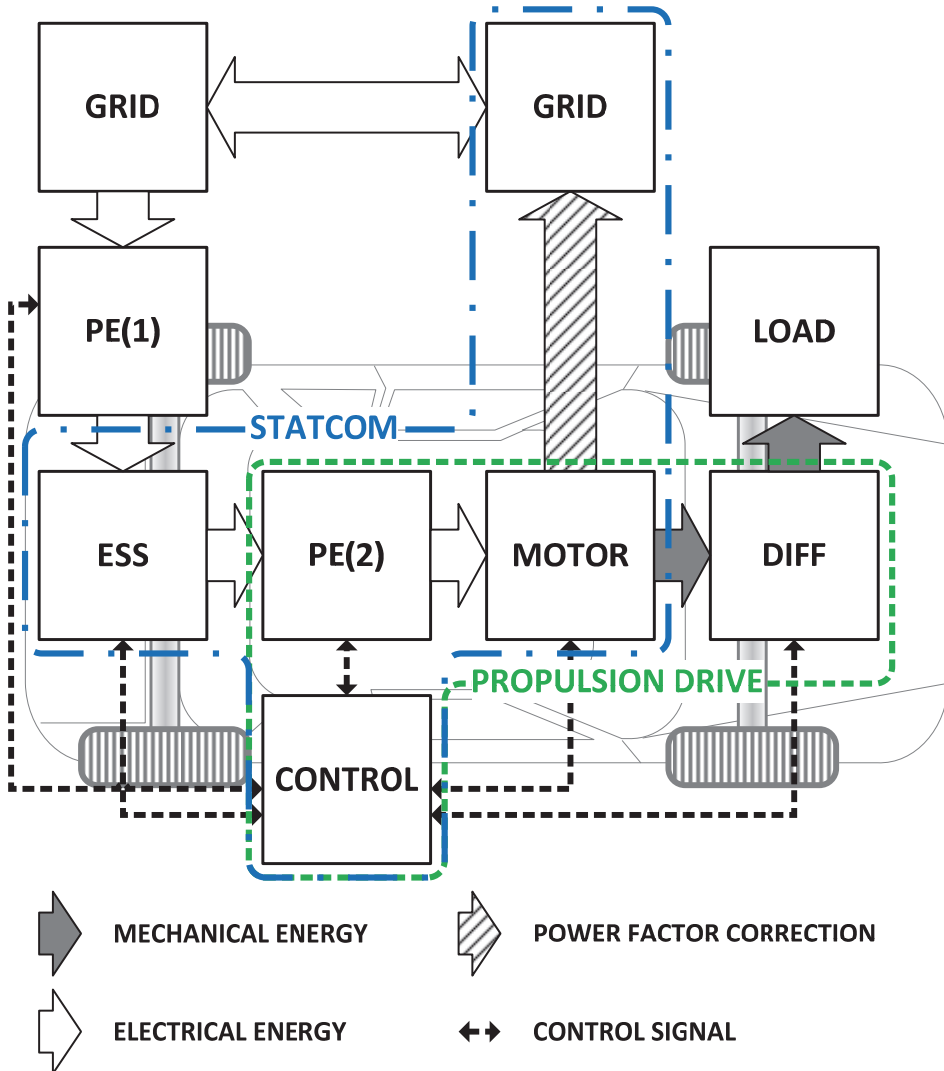


Figure 1.1. Power flow diagram of an EV including grid connection and control system

Currently used electric grids have some disadvantages and complaints and criticisms are frequent. They are losing their reliability because of a wide range

of renewable energy sources (RESs) and availability of ESSs today. The combination of RESs with ESSs brings new features to the electric grids and converts them into smart electric grids. Hereby the consumer role of the EV/HEV is changing to the “smart consumer” role, or so-called prosumer (combined producer and consumer device). Prosumer could become a part of an electric grid in different ways – as a usual consumer when the EV/HEV is plugged in to the charging point and consumes power from the grid; or as a buffering energy storage element when the battery of the EV/HEV is used as an energy storage device for energy exchanging between the elements of the distributed energy grid. However, another solution how to use an EV/HEV in today’s electric grid has emerged - a smart producer for power quality improvement. A static synchronous compensator or STATCOM could be used for that. STATCOM is a promising technology for reactive power control, voltage regulation and other power quality improvement features. Connection of an EV to the electric grid is presented in Figure 1.1 inside the blue dot-dashed line. The electric grid (GRID) is connected to the ESS through a charging system (PE(2)). An additional feature, the power factor correction of the propulsion motor drive system, is shown with the hatched wide arrow.

Within the variety of electric motors used in today’s EV/HEV, induction motors stand out. The application topology of the induction motors widely used in other electric drives is rarely used for propulsion drive systems, because their working mode is unstable and controllability is low at a low speed range. Technologies used in ESSs and power converters allow using different algorithms and methods for induction motor control. It means that induction motors with their very simple construction and high reliability and performance have good prospects to become a leading motor type to be used in EV/HEV propulsion drives. Regarding to the induction motors studies, the best solution for a power converter is the voltage source inverter with a possibility to change the control mode (frequency and flux control modes). Essentially, an induction motor based propulsion motor drive system has a potential possibility to be used in the vehicle-to-grid and the grid-to-vehicle systems. In addition, today’s power grids and charging systems need to have updated new requirements arising from energy consumers. The role of the EV/HEV connected to the grid is transforming to the prosumer role. The prosumer could become a part of the electric grid in different ways and applications, so some additional features could be added to the actual systems. Thus, studies in that area are necessary.

## **1.2 Main Objectives and Tasks of the Thesis**

The major objective of the thesis is to develop and implement the novel framework for exploring, modelling, identification and assessment of multiple EV drive configurations aiming to provide fast and concise information about their most important indicators.

Another objective of the studies is to develop extended application topologies for propulsion motor drive system upgrade.

***The main research tasks of the PhD thesis were as follows:***

- to analyse of the current state-of-the-art technologies and development trends in the field of electric propulsion vehicles and to identify the challenges;
- to develop a computer model and test bench for propulsion motor drive studies related to road, landscape and driving conditions;
- to design the library of models for electric propulsion motor drive studies based on the test bench and to propose a methodology of their joint use;
- to study propulsion motor drive system side applications.

### **1.3 Contribution of the Thesis and Dissemination**

New scientific contributions of the thesis can be summarized as follows:

#### ***Scientific Novelty***

Scientific novelty of the doctoral thesis includes:

- library of speed control and disturbance models intended for study and analysis of electric propulsion motor drives;
- methodology for tuning of the propulsion motor drives proposed to explore the drive responses under changeable control and disturbance signals;
- mathematical model of the dynamical load of electric propulsion motor drive developed for laboratory exploring of the real road conditions under variable speed.

#### ***Practical Novelty***

The practical novelty of the doctoral thesis includes:

- original experimental test bench for research, assessment and tuning of the propulsion electric motor drives;
- prospective methodology of the grid power factor correction in the vehicle-to-grid system;
- based on the developed test bench, a laboratory course for graduate students.

#### ***Dissemination of the Results***

The results of the doctoral thesis have been presented by the author at 16 international conferences. The author has published 18 international scientific papers, 7 of which are directly associated with the thesis. Three of them are available in the *IEEE* database, one in *IFAC* database and three have been published in the international peer-reviewed journals. In addition, one tutorial manual for graduate students was published.

### **1.4 Thesis Outline**

Chapter 2 presents the basic components of the electric propulsion motor drive technologies and the propulsion drive segments are studied in more detail. Attention is paid to the study of HEV/EV topologies, electric motors, power

electronic devices, energy storage applications for the propulsion drive systems as well as regenerative braking and charging systems.

Chapter 3 consists of three models: the load model of the propulsion drive, the computer model of the propulsion drive system and experimental setup. All the models are scaled to the real vehicle.

Chapter 4 sets the requirements related to control restrictions and tuning possibilities of the EV/HEV propulsion drives. The goal is to propose a methodology for adjusting the electric drives under the test cycles different from the standard testing cycles. By estimating the drive responses, the discussed methodology helps to measure the steady-state and transient vehicle quality and to recommend approaches to the drive regulator tuning, control looping, sensor allocation, and feedback arrangements. The methodology can be recommended to adjust the electric drives for different kinds of testing equipment, including the synchronous, induction, and direct current machines. Experimental validation of the described approach has demonstrated broad possibilities for the steady-state and transient modes of vehicle quality evaluation.

The topology proposed in Chapter 5 enables the use of part of the traction system of the EV/HEV as STATCOM. The topology offers an opportunity to improve even existing vehicle propulsion motor drive systems. A simple and quick solution for controlling the power factor is proposed.

The conclusive list of references consists of 109 external publications and 8 author's publications.

## **2 OVERVIEW OF STUDIES IN THE FIELD OF ELECTRIC PROPULSION MOTOR DRIVE**

### **2.1 Comparative study of HEV and EV Topologies**

The efficiency of the internal combustion engine (ICE) commonly ranges from 20 to 40% and in a very small area of the engine map. Usually the best performance ICE is revealed during highway cruising, thus it is worse for urban cruising. Many different ways are available to combine an ICE with an electric machine (EM). The electric machine is designed to handle transient power variations and helps the engine to operate more constantly, so that higher efficiency and lower tailpipe emissions can be achieved [3]. The variety of ICE/EM connection topologies and designs of the power train can be varied by the traction effort proportion, operating time and total provided power. The topologies most widely used today are presented below.

#### ***Assist HEV***

The electric motor is essentially a very large motor which operates not only when the engine needs to be turned over, but also when the driver presses the throttle pedal and requires extra power [4]. Because of the small range of the electric drive, the assist hybrid cannot operate in pure electric mode, but it can be used as an assist motor in a wide range of controlled torques and speeds. In addition, part of kinetic energy could be converted into electric energy during regenerative braking while the vehicle decelerates. The size of the electric battery used in assist hybrids has extended as compared to the ICEV, which increases the total weight of the vehicle.

#### ***Mild HEV***

The advanced version of the assist HEV is called a mild HEV. The mild hybrid has a small electric motor that is mostly used as a starter and a charging generator, sometimes it does operate as a traction motor as well. Usually, the power rating of the electric motor may be in the range of about 10% of the engine power rating [5]. The mild hybrid could operate as a pure EV (the combustion engine is switched off in that mode) only in a small speed range, up to 10 km/h. The design of the traction part of the mild hybrid is similar to the IECV traction system. The main difference is the extended battery storage system, like in assist hybrids. The proportional schematic of the mild HEV is shown in Figure 2.1.a.

#### ***Full HEV***

Full hybrids are a type of the vehicles that can use pure electric traction mode, proportionally EM and ICE are equal, which notably reduces CO<sub>2</sub> emission. The hybrid-drive concept appears in many forms depending on the mix of energy sources and propulsion systems used on the vehicle [6].

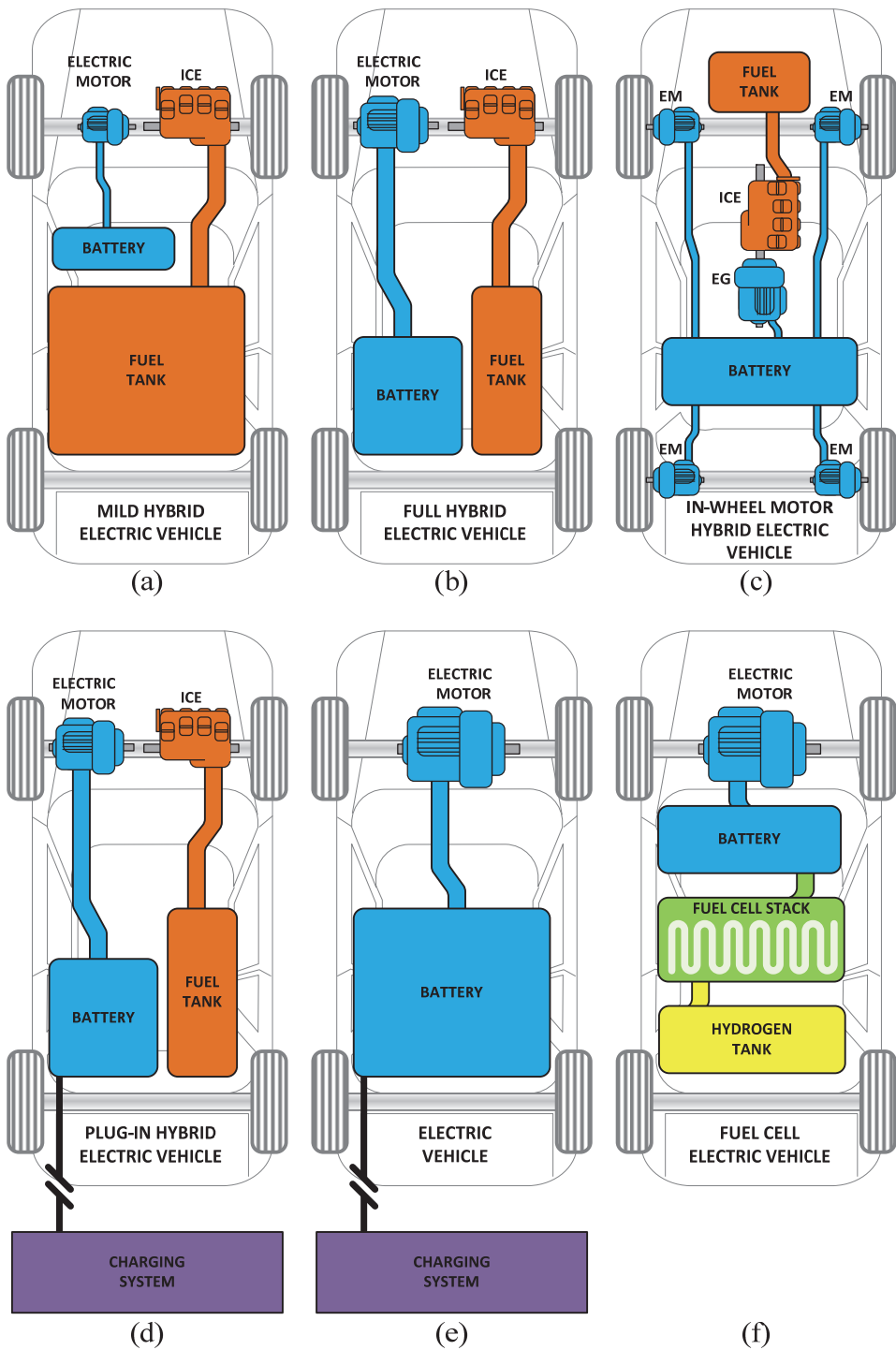


Figure 2.1. Hybrid and electric vehicle topologies: a) mild hybrid electric vehicle; b) full hybrid electric vehicle; c) in-wheel motor hybrid electric vehicle; d) plug-in hybrid electric vehicle; e) electric vehicle; e) fuel cell electric vehicle

The energy required for traction could be received from two separate energy sources: EM and ICE; there are several combinations of these available. Schematically, the full HEV is shown in Figure 2.1.b.

### **Series HEV**

Series HEV uses only electric drive for traction. An ICE is decoupled from mechanical transmission and used to produce kinetic energy for the generator that converts it into electrical energy. That means the traction system requires double energy conversion: mechanical-electrical-mechanical. A weakness of a series hybrid system is that series hybrids require a separate motor and generator portions which can be combined in some parallel hybrid engines; the combined efficiency of the motor and generator will be lower than that of a conventional transmission, thereby offsetting the efficiency gains that might otherwise be realized [4]. Schematically, the configuration of a series HEV is shown in Figure 2.2. Some part of energy disengaged during the braking could be regenerated and returned to the battery, only a small amount of braking energy, up to 35%, could be returned back to the battery [7].

Sometimes series HEVs are referred to as extended-range electric vehicles (EREVs).

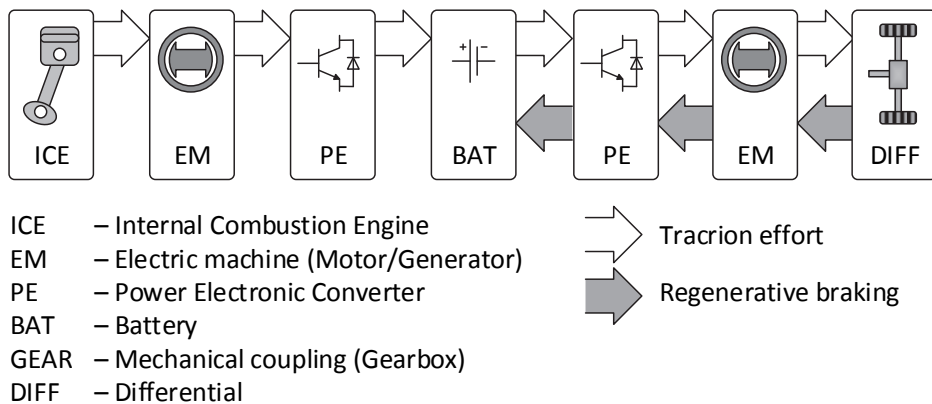


Figure 2.2. Functional diagram of series hybrid electric vehicle

### **Parallel HEV**

A parallel HEV is only a hybrid vehicle that can switch between two types of drives and could be used separately or simultaneously, depending on the traction mode. Schematically, the configuration of the parallel HEV is shown in Figure 2.3, the conventional signs are the same as in Figure 2.2. Parallel HEVs have the same features as series HEVs while regenerative braking. Moreover, an EM can also be used as a generator to recharge the batteries when the engine produces more power than is needed to propel the vehicle [8]. An ICE and an EM are coupled mechanically by a special gear construction and could be unplugged by reswitching of a clutch. A parallel hybrid uses mostly the electric drive in urban areas because of the specific qualities of urban driving: fast

acceleration/deceleration and short-time duty cycles. During highway cruising, the ICE is commonly used, while it has its best performance without speed and torque variations. The main drawbacks of the parallel HEV are a doubled traction system, which increases the price of the vehicle as well. Flexibility and the number of combinations of the working modes of the parallel HEV makes it the most used technology for today's lightweight hybrid vehicles.

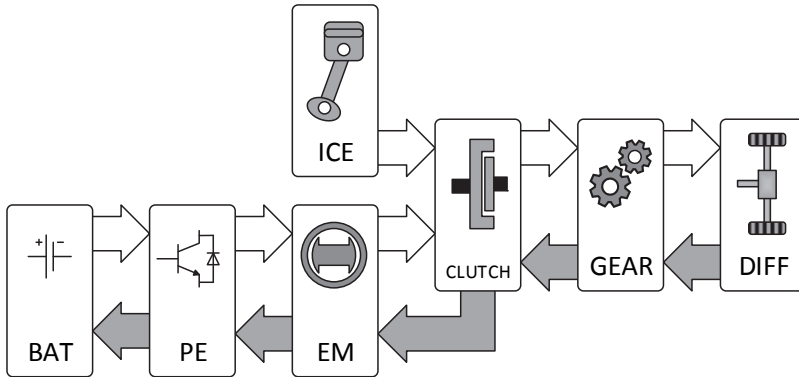


Figure 2.3. Functional diagram of parallel hybrid electric vehicle

### ***Series-parallel HEV***

Series-parallel HEV has two couplings: mechanical and electrical, which allows overcoming the drawbacks of both technologies and using their benefits with best performance. Schematically, the configuration of the series-parallel HEV is shown in Figure 2.4, the conventional signs are the same as in Figure 2.2.

The main aim of such systems is to reduce the fuel consumption [9]. In addition, drivability can be optimized based on the vehicle's operating condition [1]. The main drawback of the series-parallel hybrid is higher vehicle price as compared to other hybrids.

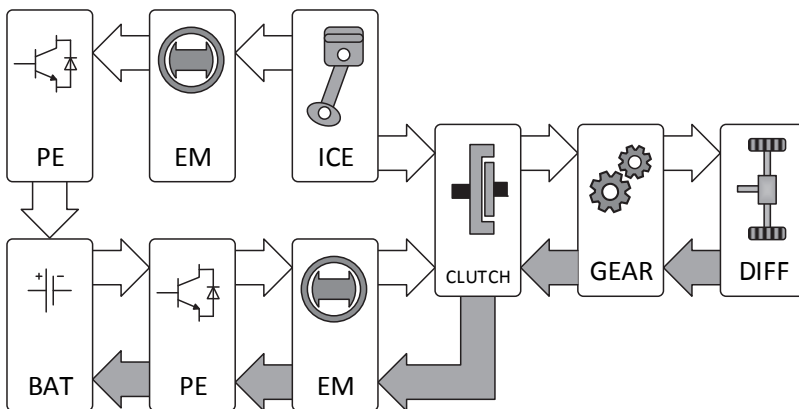


Figure 2.4. Functional diagram of series-parallel hybrid electric vehicle

### ***In-wheel motor HEV***

Some variations of the series HEV have separate small electric in-wheel motors (sometimes called hub motors) installed independently at each wheel. That allows separate control of the power delivery to each wheel, and therefore it simplifies the traction control of the vehicle [4]. The acceleration/deceleration torque and speed values are regulated independently for each wheel. The proportional schematic of the in-wheel motor HEV is shown in Figure 2.1.c. The mechanical part could be reduced even more than in the series HEV, i.e. additional batteries can be installed on the free space that has been occupied by the transmission, which helps to increase the driving range per charge [10]. Most conventional electric machines (such as ac excited or brushed dc motors) are not suitable for applications of in-wheel motor drive because of their poor torque density and overload capability [11]. For that reason, in-wheel hybrids require specially designed motors like axial-flux ironless permanent magnet motors or synchronous permanent magnet outer rotor motors.

### ***Plug-in Hybrid Electric Vehicles (PHEVs)***

The only difference of the PHEV from the HEV is the presence of the connection with an electric grid. Depending on the energy flow direction, plug-in systems could be divided into several parts: grid-to-vehicle (G2V) if the batteries are charged from the grid; vehicle-to-grid (V2G) if the energy flow goes to the grid from the vehicle, some solution are called vehicle-to-home (V2H), if the vehicle is connected to the Smart Grid (SG). G2V allows recharging the batteries without using the ICE that makes daily used lightweight PHEV more environmentally friendly. The proportional schematic of the PHEV is shown in Figure 2.1.d.

The basic concept of V2G(V2H) power is used in electric drive vehicles to provide electric power to the grid while the vehicle is parked [12]. It means that the batteries on parked and plugged-in vehicles could be recharged during the lean hours and discharged during the peak hours of loads, if necessary. To allow such bi-directional energy flow, the charging systems should be specifically designed and optimized. In that case, the vehicle is used as a smart consumer, so-called prosumer (combined producer and consumer) and can be used as a part of a smart electric grid. A PHEV connected to the smart grid could bring new features into the grid like STATCOM, an active filter or even a portable power plant [PAPER-IV].

### ***All Electric Vehicles (EVs)***

EVs use chemical battery as a primary energy storage and an EM only for traction. It means that they have zero tailpipe emission and are more friendly to the environment than other types of vehicles.

The EV has many advantages over the conventional ICEV, such as zero emissions, high efficiency, independence of fossil fuels, and quiet and smooth operation [5]. Usually EV simplifies the mechanical motor-to-wheel

transmission part that is similar to the series HEV or the in-wheel HEV. The design and parameters of the traction system of the EV depend mostly on the speed-torque and speed-power characteristics. The proportional schematic of an EV is shown in Figure 2.1.e.

All of the major automotive manufacturers are producing EVs, many of which are available for sale or lease to the general public [13]. While the EV is a novel technology, many challenges have emerged in its development and research areas. New standards and requirements should be prepared before mass implementation of the EVs. Moreover, public recharging infrastructure is required and is being used nowadays, electrical grids need to be renewed or even rebuilt to withstand the increasing consumption load. Due to European Union directives, the governments support the idea of the EV/HEV with taxes cuts and other benefits for EV/HEV owners. However, it seems that the main problem is the driver habits on vehicle use and refuelling.

### ***Fuel Cell Electric Vehicle (FCEV)***

A Fuel Cell (FC) is a galvanic cell in which the chemical energy of a fuel is converted directly into electrical energy by means of electrochemical processes [5]. There are special tanks required to store the fuel, which usually is hydrogen. It makes the FCEV more similar to the series hybrid but with fewer energy conversion stages. A FCEV is schematically shown in Figure 2.1.f.

The main benefits and drawbacks of the FCEV relate to the FC, but vehicles powered solely by the FC have some other drawbacks, such as a heavy and bulky power unit caused by the low power density of the fuel cell system, long start-up time, and slow power response [5]. To overcome these drawbacks, some hybrid solutions are presented, where the FCEVs are combined with some other vehicle technologies, such as supercapacitors (SC) [14]–[17]. The FC presents a novel technology that can be used not only for ground vehicle technology, but also for airplane solutions [18].

### ***Online Electric Vehicle (OLEV)***

An online electric vehicle (OLEV) is an EV that uses electromagnetic induction to receive energy required for traction. Battery problems on an EV can be solved by the OLEV developed by Korea Advanced Institute of Science and Technology (KAIST) [19]–[21]. Two OLEV buses run an inner city route between Gumi Train Station and In-dong district, for a total of 24 km roundtrip, a single bus receives 20 kHz and 100 kW (136 HP) electricity at an 85 % maximum power transmission efficiency rate while maintaining a 17 cm air gap between the underbody of the vehicle and the road surface [22].

### ***Grid-Connected Electric Vehicle (GCEV)***

Grid-connected electric vehicles (GCEVs) like trams, trolley buses, electric trains and metros are directly connected to the power grid. Their low at-vehicle energy consumption and ability to use a wide range of renewable energy sources make them strong contenders for urban and interurban transport systems

in an era of energy constraints that favours use of renewable fuels, which may lie ahead [23]. For megacities with a huge population, ICEVs will lead to pollution cataclysm, so the GCEV decreases the CO<sub>2</sub> emission and makes the urban environment more liveable. Some of the applications use additional energy storage devices, like batteries and supercapacitors, to increase the performance of the GCEV [24]–[26]. The GCEV is used in public transportation and it is a challenge to implement the GCEV for private use.

### ***Other EV/HEV Solutions***

Low power range EVs/HEVs are presented by bicycles and motor scooters. The rider of an electric bicycle can choose from three riding modes: pedalling only, pedalling and electric motor at the same time, which relies on the electric motor completely. Performance range and the specifications of electric bicycles vary according to the bicycle design and the riding conditions for which the electric bicycle is designed [27]. The light weight and easy design require a special motor type and energy storage system (ESS) design.

Because of the high controllability performance of the electric motor, that topology reduces the size of the gearbox and mechanical transmission. That is the reason for the series HEV wide use in heavy industrial vehicles like excavators and diesel-electric locomotives and for urban vehicles like public buses and delivery cars that require frequent stop duties.

### ***Resume***

As it can be seen from Figure 2.1, all the EVs/HEVs have a common electric part that is fed from a battery. To specify the field of study, all vehicles that use batteries for propulsion could be named battery electric vehicles (BEVs).

The variety of BEV topologies is based on the proportional usage of electric motors and combustion engines. The vehicles made to achieve different goals require different components, including a propulsion drive, a power electronics converter and an energy storage. For example, in assisted hybrids like mild or parallel HEVs, the size and dimension of the propulsion part could be reduced and optimized to help an ICE increase the working area of the engine map. In the vehicles that use an electric drive as a primary propulsion system (series HEV, EV, FCEV, etc.), the acceleration and braking modes should be taken into account.

Another direction of the BEV development is reducing the harmful effect of the ICEV on the environment pollution. Research is essential here to reduce the environmental footprint from manufacturing and BEV use.

## **2.2 Electric Drives and Motors for BEV Propulsion**

The electric drive has relative benefits and drawbacks in comparison with the traditional ICE. It is clear that the electric drive is more efficient and has zero emission, but a major advantage of the electric drive is that torque generation is very quick and accurate. That makes the BEV more controllable and manoeuvrable in urban areas.

By the classical definition, an electric drive consists of a power electronic converter, an electric motor, transmission, and a control device. Commonly, power supply and load are regarded only in terms of the influence on the working processes of an electric drive. The same statements are valid for the propulsion motor drive of a BEV, but while a BEV is a portable device, energy storage systems (ESSs) used in the BEV and their influence on the propulsion motor drive system should be analysed. The main drawback of ESSs is that they are usually short-term storage devices and that limits the driving range of the vehicle.

Propulsion motors and drives experience very harsh environmental conditions, such as a wide temperature range ( $-30$  to  $60$  °C), severe vibration and shock, high electromagnetic noise, size and weight constraints, stringent safety and reliability requirements; as a result, there are many unique aspects in the design, development, analysis, manufacturing, and research of electric motors and drives for propulsion applications, which are all-important aspects [1]. While the type of the propulsion motor determines the parameters of the whole drive system, the motors could be studied apart. Several types of direct current (DC) and alternating current (AC) electric motors are used in propulsion motor drives and it is necessary to address their classification and characteristics.

### ***Brushed DC Motors***

The brushed DC motors were used in the last century in electric transportation due to their developed status and suppleness of speed control. The series excited DC motor speed-torque characteristics are an excellent match with the road load characteristics. Therefore, they were widely used in public transport: tramway cars, trolleybuses, electric trains and diesel-electric locomotives. A number of early prototypes of BEV cars in the 1980s and earlier were built based on the DC series motors as well. However, the size and maintenance requirements of DC motors make their use obsolete, not just in the automotive industry, but in all motor drive applications [13].

The main drawback of the DC motor is a brushed collector that is required to change the direction of the current inside the rotating part of the motor (armature). The high friction between the brush-contacts and the collector results in high friction losses, temperature rise in the machine, low reliability, lower lifecycle, and low efficiency.

### ***Permanent Magnet AC Motors***

Permanent magnet (PM) brushless DC motor (BLDCM) is a motor with an independent excited magnet. The speed-torque diagram of a BLDCM is close to the parallel excited DC motor. This type of the motor usually has high efficiency, compactness, ease of control and cooling, low maintenance, great longevity, reliability, and low noise emission. Because of the limited PM technologies, the power range of the BLDCM is quite small. These drawbacks make the PM DC motor unsuitable for high power traction applications. Also,

the price of the BLDCM is quite high, the PM can be demagnetized and the construction is dangerous. Moreover, because of the PMs on the rotor, the BLDCM presents major risks in the case of short-circuit failures of the inverter [5].

Usually, the PM AC motor has three phase (rarely one phase) windings and the permanent magnet excite rotor. For BEV applications, motor size is relatively large compared to the other smaller power applications of PM motors, which amplifies the cost problem [13]. However, the PM AC motors could be used in the assist and mild HEV. The benefit of this motor is that currents do not need to be induced in the rotor (like in induction motors), making them somewhat more efficient and giving slightly greater specific power, at the same time, the drawback is that it is more expensive due to the presence of a PM [4]. PM motors face the possibility of demagnetization at extremely high temperatures, limited speed range and difficulty in protecting the powertrain during a fault condition [1].

### ***Switched Reluctance Motors (SRMs)***

SRMs are also known as doubly salient machines that have a simple construction and excellent fault tolerance characteristics. The stator and the rotor of the SRM are made of iron, which is magnetized by the current through the stator winding. These motors have no windings, magnets, or cages on the rotor, which helps to increase the torque and inertia rating. The motor speed-torque characteristics are an excellent match with the road load characteristics, and performance of switched reluctance motors for BEV applications has been found to be excellent [13].

The main drawback of SRMs is that the timing of the turning-on and turning-off of the stator currents must be much more carefully controlled [4], and a more complex control device is required. In addition, SRMs have such challenges as torque ripple.

### ***Induction Motors (IMs)***

The relatively mature AC IM technology has advanced fast with the progress of power electronics in the last 30 years. A squirrel cage IM has a very simple rotor construction, which increases the reliability and performance of the motor. Absence of the friction parts (except bearings) increases the efficiency of the IM. In contrast to the SRM, the rotor winding of the IM is made from copper, which increases the price of a single device. Vector control of the IM can decouple its torque control from the frequency control. This allows the motor to behave in the same manner as a separately excited DC motor [28].

Because of low stability and overheating at low speed, the IM is mostly applied in high-speed vehicles, otherwise some additional mechanical transmission is required for speed reduction. The efficiency of the IM in no-load or light-load operation modes is very small - ca 20..30%, but it increases gradually with the rated load and reaches ca 75..92% [29]. Drawbacks of the IM

are limited torque capabilities at low speeds, lower torque density and lower efficiency and noise due to stator/rotor slot combinations [1].

### ***Synchronous Permanent Magnet Outer Rotor (In-Wheel) Motor***

Usually an in-wheel motor is used in the permanent magnet synchronous machine (PMSM), which has high torque density, excellent efficiency and overload capability [30]. The main advantage of the in-wheel motor is the controllability of the vehicle, propulsion torque for each wheel could be specified separately. In addition to all the drawbacks of the PM machines, like limited power and demagnetization, there may also be risks of mechanical damage of the rotor's magnets in extreme driving conditions [31].

Usually, in addition to the motor, the assembly configuration of the in-wheel motor system contains also a reduction gear, a mechanical brake and a wheel. Today in-wheel motors are widely used in military and special purpose vehicles [32].

### ***Comparison of propulsion motor drive systems***

The diagram in Figure 2.5 compares the attributes of various propulsion systems. At the price axis, the cost of the EM/ICE parts is estimated, at high points cheaper solutions are presented. Simple construction and the resulting low price are the main advantages of the IM. SRMs have simpler construction than IMs and instead of relatively expensive copper iron is used. The production of ICEs has been worked out and established, but it still requires more attention to small parts of the engine (like injection and ignition system, pistons etc.) that could reduce the total price of the engine. The relatively high price of the rare-earth magnets affects the high price of the motors that use a PM (BLDCM, In-Wheel motor, some DC motors).

More noisy propulsion systems are estimated with low points on vibration and noise axis. The most noiseless motor is the SRM. PM machines could be named as low-noise machines. IMs produce some noise due to stator/rotor slot combinations. Existence of brushed collector in DC motors makes them noisier, the friction of brushes increases the vibration. As compared to EMs, ICEs are more noisy and subjected to vibration.

The efficiency of the propulsion motor is presented on the associated axis. It depends strongly on the construction, power range and operating point of the motor. The ICE has the lowest efficiency among electric motors; today they operating at about 30-40% efficiency. The efficiency of the motors with a PM is usually above 90%, i.e. higher than the efficiency of the IM, usually little below 90% [33]. Today's DC motors have also an efficiency range of about 70-90%.

Reliability axes show low reliability motors with low grade and high reliability motors accordingly with high grade. ICEs have many different complex parts, crash of one of that part failure the whole system. Out of EMs, DC motors have the lowest reliability. Motors with simpler construction (IM, BLDCM) show better reliability performance, SRMs showing the best

reliability. Due to harsh environmental conditions, the reliability of an in-wheel motor is lower than that of other PM machines.

Complication of the control devices for a propulsion system is estimated by the controllability axis. The speed of a DC motor could be controlled by adding an additional resistance in series with armature winding (deceleration) or excitation winding (acceleration). Frequency converters are widely used for AC motor speed control (BLDCM, SRM, in-wheel motor, IM). Use of power electronic devices for speed control is more complicated than DC motor speed control, this explains the lower grade of AC motors. ICEs have the most complicated control strategy, except injection and ignition control system, ICEs require mechanical transmission for speed control.

The match condition with a typical vehicle load diagram is estimated by the torque-speed characteristic. Series excited DC motors and SRMs have more suitable speed-torque characteristics for propulsion drive systems. BLDCMs and in-wheel motors have a hard control characteristic. Without feedback IMs have softer control characteristic than PM machines.

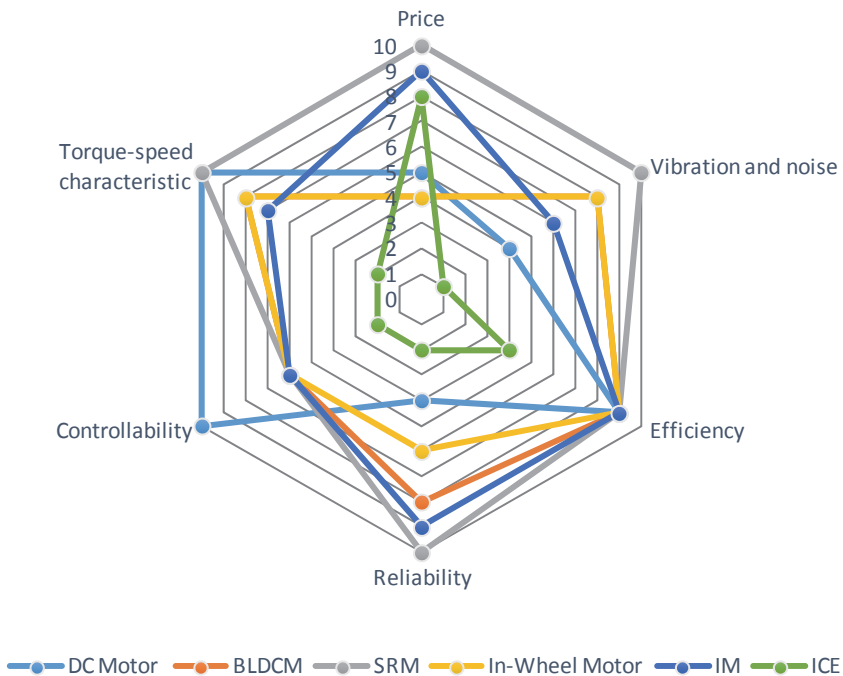


Figure 2.5. Comparison of attributes of various propulsion systems

## ***Resume***

Electric motor and the related controller are the determining parts of the propulsion motor drive system. With a variety of available EM types, different topologies and systems could be used in BEV propulsion drives, depending on the required performance. In today's BEVs different types of drives are used, for example, Nissan Leaf uses the PM AC motor for propulsion and Tesla Roadster a squirrel cage IM [34].

Figure 2.5 shows that the SRM and the IM have the widest area of application. Therefore, those motor types should provide the highest scientific interest. Nowadays their use in light vehicles is quite rare, but their application in public transportation like in trams, trolleybuses and electric trains is increasing.

## **2.3 Analysis of Power Electronic Devices for a Propulsion Drive**

Portable ESSs are mostly DC energy sources, so some power electronic converters are required to provide the electric energy conversion between the ESS and the propulsion system of the BEV. Inverters are required to provide connection between AC propulsion motors and the batteries. Rectifiers are used to apply AC generators as a kinetic-to-electrical energy converter. DC/DC converters equal the DC link voltage from all energy sources if more than one is used. Moreover, the charging systems require special attention, while they have specific requirements and standards. The main issues in the design of BEV power electronics circuits are [1]: electric design; control algorithm design; magnetic design; EMC design; mechanical and thermal design.

### ***Rectifiers***

In series and series-parallel HEVs, a synchronous generator is frequently used to convert mechanical energy produced by the ICE into electrical one. Rectifiers are required to convert the output AC of a synchronous generator into DC for a battery. There are four common rectifier circuits in series HEV: PWM voltage-source current-controlled rectifier, uncontrolled full-bridge diode rectifier, uncontrolled full-bridge diode rectifier with a DC/DC boost converter and controlled full-bridge thyristor rectifier [35]. Topologies of 3-phase rectifiers are shown in Figure 2.6. Single-phase rectifiers are more rare than 3-phase, used only in auxiliary circuits.

The rectifier presented in Figure 2.6.a is bidirectional, i.e. the energy flow could be directed from the ESS to the propulsion motor, or in the opposite direction. That feature could be used during regenerative braking, while propulsion motor works as a generator. The rectifier presented in Figure 2.6.b is an uncontrolled unidirectional rectifier, which does not allow the bidirectional energy flow. Rectifiers presented in Figure 2.6.c, d are controlled rectifiers, they allow output voltage adjustment. To apply fully controlled thyristor bridge rectifier (Figure 2.6.d) as a bidirectional rectifier, special additional circuits are required to close thyristors under DC current.

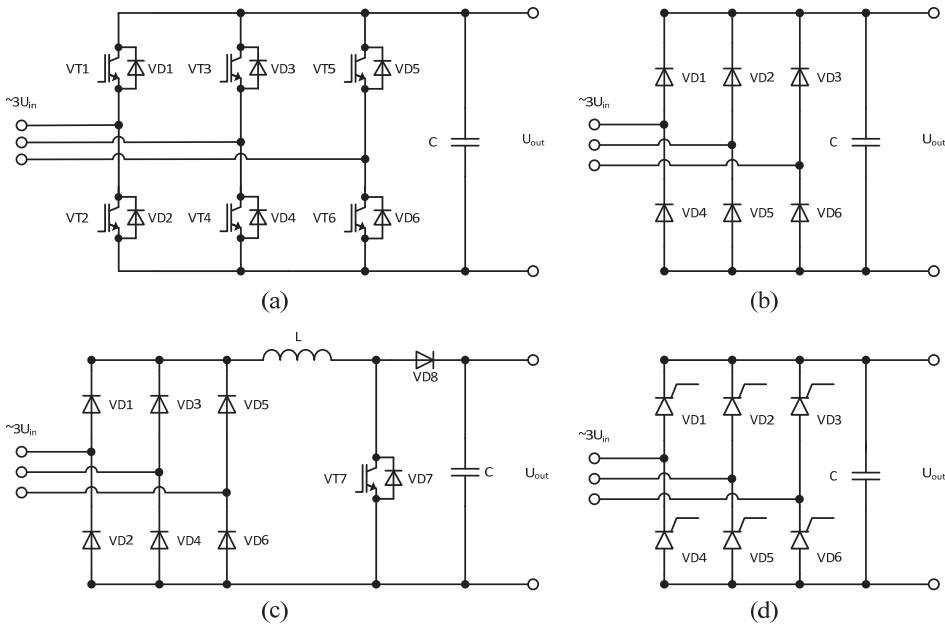


Figure 2.6. Rectifiers used in a BEV: a) PWM voltage-source current-controlled rectifier; b) uncontrolled diode bridge rectifier; c) diode rectifier with boost DC/DC converter; d) fully controlled thyristor bridge rectifier

### Inverters

While most of the energy storage devices are voltage sources, the voltage source inverter (VSI) is the most common in BEV applications, but it presents difficult hurdles for the automakers to address the important issues on the system cost, weight, volume, and reliability [36]. VSIs are used to control the speed of induction motors and PM AC motors. The switches are usually IGBTs for high voltage, high-power hybrid configurations or MOSFETs for low voltage designs [1]. Voltage surges caused by rapid voltage transitions made by the pulse-width modulation (PWM) control technique can cause motor insulation degradation, bearing failure due to the resulting shaft leakage current, and unacceptable electromagnetic interference effects upon the control circuits, as well as acoustic noises in the motor [36]. Nowadays many different torque control techniques are used for AC motors (IM, SRM, PM AC motor). The main benefit of such techniques is the direct control of the motor flux that has direct influence on the torque developed by the motor that increases the motor controllability.

The current source inverter (CSI) uses an inductor for energy boosting as distinct from the VSI that uses a capacitor. It has several inherent advantages that include its voltage boosting capabilities, its natural shoot-through and short-circuit protection capability, and a sinusoidal output voltage due to the effect of the output AC filter capacitors, which are much smaller than the VSI's DC capacitor [36]. Inverter topologies used in the BEV are shown in Figure 2.7.

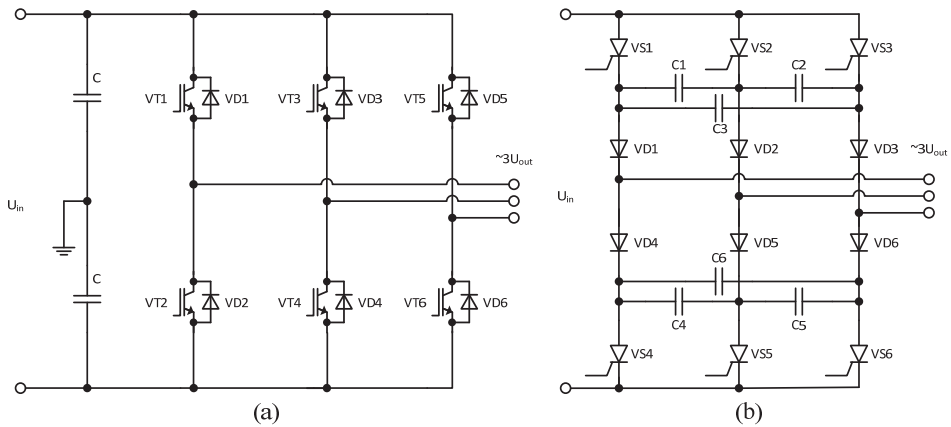


Figure 2.7. Inverters used in a BEV: a) voltage source inverter; b) current source inverter

### DC/DC Converters

The variety of DC/DC converter topologies used in the BEV is higher than the rectifier or inverter topologies, some circuits are shown in Figure 2.8.

The typical application of a buck converter in a BEV is to step down the high voltage battery voltage (typically 200 – 400 V) to charge the auxiliary battery (14 V) [1]. At such high step-down voltage rate, the duty cycle of the buck converter is small and that affects the design of the inductor and the capacitor, as well the current and voltage ripples. Moreover, control and regulation of the buck converter output voltage becomes more difficult.

A boost converter or a non-isolated bidirectional DC/DC converter is used to step up the high voltage battery up to the DC bus. The best operating voltage for a VSI that controls the traction motor is around 600 V. In addition, that converter allows the backward energy flow from the DC link back to the battery during the regenerative braking. The non-isolated converter type is generally used where the voltage needs to be stepped up or down by a relatively small ratio (less than 4:1) [37].

In some cases a non-galvanic isolation between the battery and the DC link is required. That fore, isolated unidirectional or bidirectional DC/DC converters with a high frequency AC link are used. Usually the ratio of stepping down or stepping up the voltage of the bidirectional DC/DC converters is high.

### Resume

An overview of power electronics converters used in the BEV was presented in this section. Usage of the topology of the power electronic converter depends on the parts it is connected with, the motor and the ESS.

The main requirements for that part of the propulsion drive are high efficiency, fault-tolerance, light weight, small volume, a wide range of power and a possibility of bidirectional energy flow between the parts of the drive. Each converter topology has advantages and drawbacks. Today's power electronic devices have the possibility to improve the performance of the BEV.

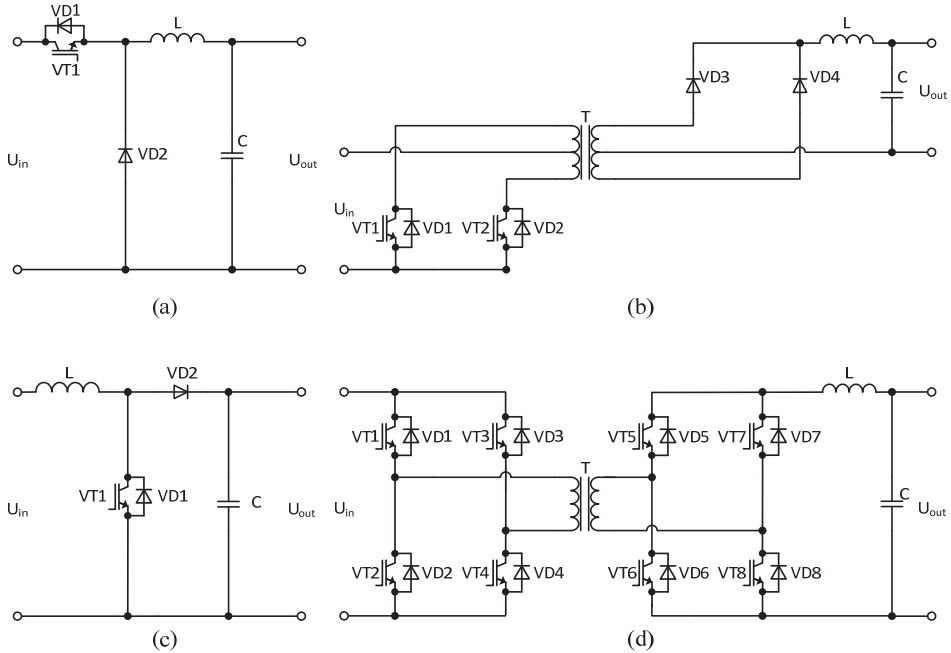


Figure 2.8. DC/DC Converters used in a BEV: a) buck converter; b) boost converter; c) isolated unidirectional half-bridge DC/DC converter; d) isolated bidirectional full-bridge DC/DC converter

## 2.4 Analysis of Energy Storage Applications for a Propulsion Drive

An ESS is not a part of the propulsion drive system, but its features have influence on the system, particularly on such portable systems, as a vehicle. There are many different energy storage solutions available today, such as ESS, like water dumps, thermal reservoirs, compressed air systems that could be used in SG systems, but their application in the BEV or other vehicles is on a competitive basis. Some of them allow to store a large volume of energy for quite a long time (e.g. fuel tanks), but other ones can save energy just for a couple of seconds (e.g. supercapacitors, SMES), which limits their usage as primary energy sources. There are some solutions that do not need to cover long distances, and a few-second acceleration is enough to reach the required speed of the vehicle. The diagram in Figure 2.9 [38] shows energy management of today's energy sources. The section describes the ESS that can be possibly used to store energy in the BEV.

### *Fuel Tanks*

Fuel tanks are reservoirs that are used to store the fossil fuels. Diesel and petrol produced from crude oil are the most common fuels used in the world. In addition, natural gas and biomass can serve as fuels. The reason of using combustible fuels is simple - huge volumes of energy could be stored in tanks for a long time with no additional efforts and losses. On the other hand, the fossil fuels have many disadvantages. To take out energy, they should first be

combusted, which means huge heat losses, a small efficiency factor and CO<sub>2</sub> emission. Moreover, to generate electric energy, an additional converter in the form of a generator is required, which reduces further the low efficiency factor of the ICE significantly.

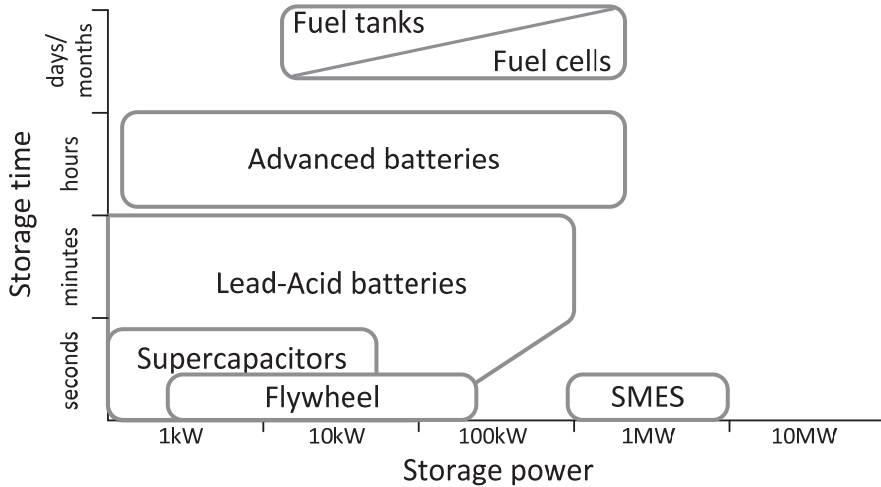


Figure 2.9. Energy management of today's energy sources

Fuel tank is a well-known technology that is currently used in ICEVs and HEVs, the size and volume of the fuel tank depend on the type of the vehicle and on the ICE to EM ratio.

### **Fuel Cells (FCs)**

A FC is an electrochemical device, much like a battery, that produces electricity by chemical reaction. FC can produce electricity as long as fuel (usually hydrogen) is supplied, which means they also need some reservoirs to store fuel. Fuel cells that are used in commercial applications could be divided by different temperature ranges. The first range is at an operating temperature up to 250 °C (Alkaline Fuel Cell, Proton Exchange Membrane Fuel Cell, Direct Methanol Fuel Cell, Phosphoric Acid Fuel Cell) [39]. They usually have low power range and low efficiency. The high temperature fuel cells, at an operating temperature higher than 600 °C (Molten Carbonate Fuel Cell, Solid Oxide Fuel Cell) [39] are mostly used in high power generation, as they have higher efficiency and output power. Hydrogen, the main fuel for the FC, has all advantages of fossil fuels. Moreover, the main benefits of the FC are – low zero emission, as the sole product of reaction is water; high electric efficiency, up to 60 %; very simple construction. The only drawback of a fuel cell for today is its high price and limited technologies.

Hydrogen used in FC applications is usually stored in the fuel tanks. Some topologies allow the use of a FC as an electrolyser and convert water to hydrogen. There are five basic methods for hydrogen storage: compressed and stored in a pressure tank; cooled to a liquid state and kept cold in an insulated

tank; physisorbed in carbon; metal hydrides; and complex compounds [40]. FCs are mostly used as a primary energy source in the FCEV, or as an additional energy source in some application. FC technologies could be implemented not only in surface transport, but also in aircraft technologies [18].

### ***Batteries (BATs)***

Batteries are well known assemblies of electrochemical cells that convert stored chemical energy into electricity. Different battery technologies are addressed to small portable applications, but there are some difficulties in using them in high-power applications because of the high weight-power relation and self-discharge. The most common lead-acid batteries are used in renewable energy applications, providing standby energy or working on regular basis in hybrid systems [41]. The main benefits of the lead-acid batteries are good efficiency; low maintenance level; easy installation and low investment price. The main drawback is: sensitivity to extreme operating conditions such as extreme temperatures and overcharging.

Advanced batteries differ from usual batteries. There is a wide range of advanced nickel batteries [42]: nickel-cadmium (NiCd), nickel-metal-hydrate (NiMH), and nickel-zinc (NiZn). Good temperature operating range, low cost and high power output are the advantages of nickel batteries. The main applications of nickel batteries are automotive application BEVs, railroad services, switchgear operation, telecommunications, emergency lighting and UPS (uninterruptible power supply) systems.

Different types of metal-air batteries have been developed in the last years including zinc-air [43], [44], aluminium-air [44], [45], magnesium-air [46], iron-air [44], and lithium-air batteries [47]. The main benefits of that type of batteries are: long shelf life; relatively low cost; capacity independent of load and temperature when working within normal operation range. There are also some drawbacks, such as limited output power; low current density obtainable; limited operating temperature range.

Zebra batteries operate at high temperature (250 °C ... 350 °C) and utilize molten sodium aluminium chloride ( $\text{NaAlCl}_4$ ) [48]. Due to the high energy density, they are used in automotive and railway applications. The benefits of Zebra batteries are [48]: high efficiency; low self-discharge and the fact that the cells are fully sealed and maintenance-free; discharge capacity is independent of the rate of discharge. The drawbacks are: limited range of available sizes and capacities; high operating temperature; using ca 14% of its own capacity per day to maintain temperature when not in use; thermal management needed.

The reduction-oxidation (redox) flow batteries (RFBs) are the advanced ones in which the chemical energy is converted into electricity by the transmission of solid electro-active components through power cells [49]. The main technologies of the RFB are based on vanadium and bromine. The main benefits of the RFB are: no memory effect; no self-discharge; high power rating; long energy storage time; no degradation for deep discharge. Their drawbacks are:

limited temperature range and capacity limitation by the number of ions in the electrolyte. Also, RFB has small specific power and energy.

BATs are mostly used as an ESS for the BEV because of their portability, performance, ruggedness and low cost.

### ***Flywheel Energy Storage (FES)***

Flywheel energy storage (FES) systems are electromechanical storage devices that store kinetic energy of a rotating body. FES consists of a rotating element with a large moment of inertia that keeps the torque for some time. A rotor is suspended by bearings; usage of magnetic bearings instead mechanical reduces the friction of the system and increases energy storage time. The kinetic energy stored in the flywheel could be used as mechanical energy, or converted into electric energy. FES can be used in different applications from network stabilization and network frequency regulation to energy-stored elements in vehicles [50], [51] and even in Uninterruptible Power Supply (UPS) systems [52]. Also, FES systems are widely used in vehicles [53]: road cars, buses, trucks, motorsport, and rail road applications. Moreover, a special FES, so called kinetic energy recovery systems (KERS), is used in formula one cars. KERS works by harnessing waste energy created under braking and transforming it into electric energy, providing an additional 60 kW of power for up to 6.67 seconds per lap [54]. The main benefits of the flywheel are: low price; fault-tolerance and durability; high efficiency factor. The drawbacks are: short energy storage time; design limitations; high-energy losses with mechanical bearings.

FES is used in high power applications such as locomotives together with the BAT ESS and also in space applications where the friction does not exist and the efficiency of the FES is maximal.

### ***Supercapacitors (SCs)***

An electric double-layer capacitor, or just a supercapacitor (SC), is a capacitor with a high power density, with a capacitance up to kilofarads. In comparison with batteries, the charging/discharging times of SCs are significantly shorter, which makes them an ideal solution for the devices that use electric motors to smoothen the start-up current and voltage peaks. The main benefits of supercapacitors are high specific power and high efficiency, low self-discharge, long life lifetime, low cost per cycle. The main drawbacks of the supercapacitors are: low voltage of a single device; to increase the voltage, several capacitors should be connected in series, which decreases the total capacity, calculated by (2.1), where  $n$  is the number of connected capacitors in a series and  $C_n$  is the capacitance of the single capacitor.

$$C = \frac{1}{\sum_n \frac{1}{C_n}} \quad (2.1)$$

Usually SCs in BEV applications are used as hybrid energy sources together with other energy storage devices, mostly batteries [15], [55], [56], the same solutions could be used for more powerful vehicles such as locomotives [57], [58].

### ***Superconducting magnetic energy storage (SMES)***

Superconducting magnetic energy storage (SMES) is a device that stores energy in the magnetic field produced by direct current in the overcooled to cryogenic temperature coil. Since energy is stored as circulating current, it can be drawn from an SMES unit with almost instantaneous response within periods ranging from a fraction of a second to several hours [59]. To reach the cryogenic temperature, a liquid helium or nitrogen is commonly used. The operating temperature used for a superconducting device is a compromise between the cost and the operational requirements [59]. The main benefit of the SMES is the extremely short charging/discharging time, which means the storage power is available almost instantaneously and high-energy output can be reached. The main drawbacks are: very short energy storage time and the high price; the cryogenic temperature can be a challenge as well. SMES could be used as a part of BEV ESS [60], or a part of a V2G system [61], [62].

### ***Contact connection***

The main advantage of a GCEV is that the renewable energy could be used directly for feeding the propulsion system of the vehicle. There are different standards for GCEV wires, depending on the technology used and the grid options. A wide range of voltages (including AC and DC) and frequencies (for AC) are used. In Estonia 400 VDC for trams and trolley buses and 3000 VDC for electric trains are used. The main challenges of contact connection energy are related to energy transportation and quality.

The main drawback of the GCEV is limited and narrow vehicle path. Some public transportation use contact connection together with the ESS [63] to free the vehicles from wires on some part of their path.

### ***Comparison of energy storage systems***

Figures 2.10 and 2.11 compare different types of ESSs. A wide range of different types of battery technologies are used today, so it is reasonable to compare them separately from other ESSs. Comparison of ESSs is based on the literature review [1], [40], [59], [64]–[67].

Specific energy means how much electrical energy can be stored per unit mass of a battery [1]. Specific energy density of a SC is the lowest (5–7 Wh/kg). Lithium and zinc-air batteries are promising energy storage devices due to their light weight, high specific energy and high specific power. The highest specific energy rate is shown by liquid hydrogen (39720 Wh/kg).

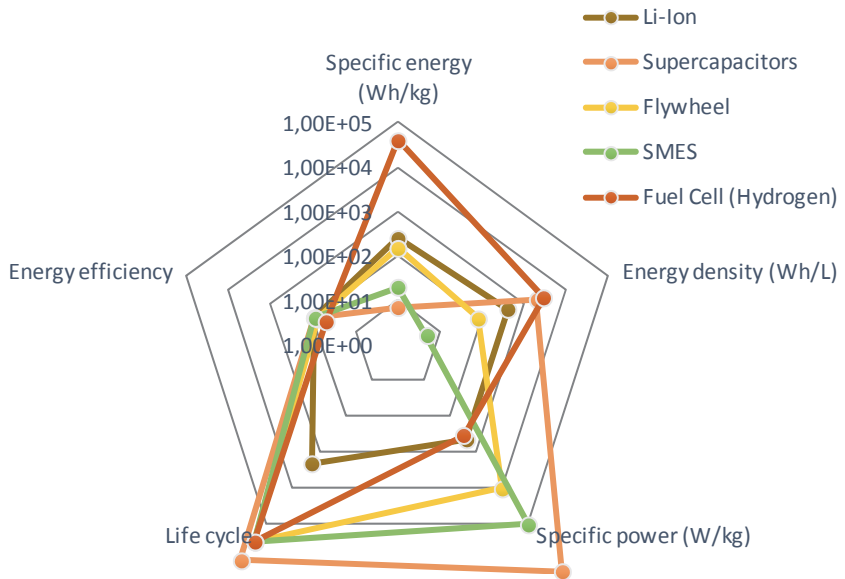


Figure 2.10. Comparison of attributes of various ESS technologies

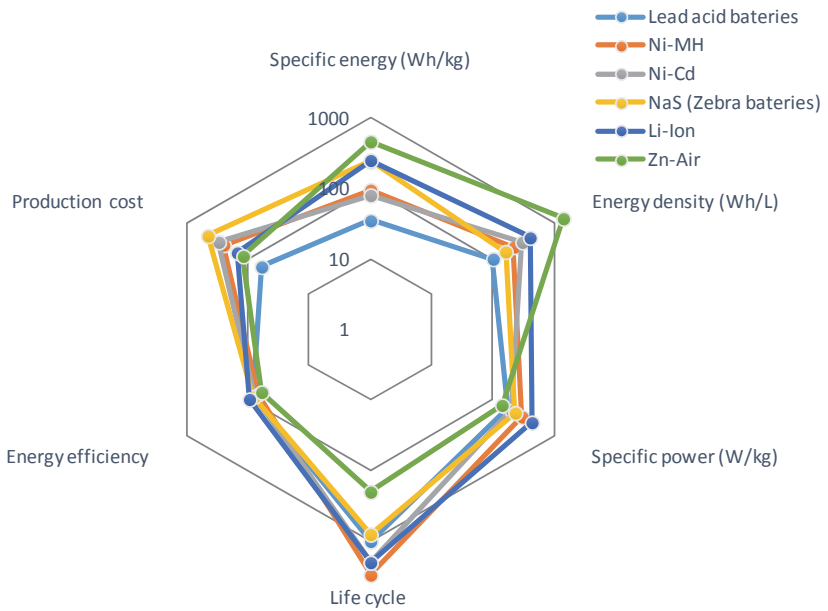


Figure 2.11. Comparison of attributes of various battery technologies

Energy density means how much electrical energy can be stored per cubic meter of the battery volume [1]. A zinc-air battery has higher energy density (1400 Wh/l) than a lithium battery (400 Wh/l). Nickel-cadmium (Ni-Cd) has higher energy density than most types of batteries (300 Wh/l). SC (2000 Wh/l) and a FC with liquid hydrogen (2800 Wh/l) show the best energy density.

Specific power means how much power can be supplied per kilogram of a battery [1]. Zinc-air battery has low specific power (140 W/kg), which is the main drawback of that technology. The specific power density for a SC is around 1000–2000 kW/kg. A lithium battery has also high specific power (430 W/kg). FES shows the best specific power (10 kW/kg), SMES (100 kW/kg) and SC (2 MW/kg).

By the life cycle, the number of recharge cycles is taken into account. Nickel batteries are more environment-friendly, as compared to other batteries and have longer life cycle (Ni-MH 3000 and Ni-Cd 2000). Life cycles of mechanical devices, like FESs, depend on the reliability of their parts, but they have a huge amount of recharging cycles (around 300,000). The number of recharging cycles of a SC and a SMES is noticeably higher than that of other devices and it is usually measured in 40 years for a SC and 15 for a SMES, which corresponds to 1,000,000 recharge cycles for a SC and around 300,000 for a SMES, but their volume of energy is lower than that with batteries. It is not always appropriate to speak about a FC life cycle, but it would be appropriate to refer to the lifetime of different construction parts of a FC, so the lifetime of FC devices is around 15 years, i.e. around 300,000 cycles.

This important quantity indicates the energy conversion efficiency of the ESS [1]. The efficiency of energy from braking to the FES is 70%, which is the double of the efficiency of the energy transformed from braking to electric energy and then to the FES. The overall FES mechanical efficiency can peak up to 97% and the round-trip efficiency up to 85% if magnetic bearings and vacuum are used [64]. FCs in transportation applications provide the capability of operating at high efficiency.

Production costs combine raw material and labor. Different ESSs require different materials, manufacturing methods and technologies. Thus, it might be irrelevant to compare production costs of single devices, instead the comparison of production costs of batteries would be reasonable. Production costs for batteries are presented in \$/kWh according to [64].

### ***Resume***

The goal of ESS producers is to provide portable energy sources with a high power resource, long-term storage possibilities and large stock of life cycles. Today's single ESSs cannot provide for the requirements necessary, therefore different combinations of energy storage devices are used. In EVs, batteries are used as main ESSs and SCs and FESs (rarely SMES) are used as additional ESSs. In the HEV the fuel tank is used as a primary energy source and the battery as an additional ESS, except the PHEV where the battery can be a

primary energy source and the fuel tank is used to extend the driving range of the vehicle.

As it can be seen from the diagram in Figure 2.10, the widest areas are covered by BATs, FCs and SCs, the main ESSs that are used nowadays. SMES and FES are used more as additional ESSs for BEVs. The diagram in Figure 2.11 shows the comparison of the attributes of various battery technologies. According to the diagram, the Li-ion technology shows the best performance (the widest covered area).

## **2.5 Regenerative braking**

If the rotating speed of the motor and the motor output torque have the same direction, then the EM works in the motor mode. In case the motor's rotating speed and the output torque have opposite directions, the EM works in the generator mode and starts to produce electric energy. The kinetic energy from the moving vehicle generating back to the energy supply side is known as the regenerative braking mode. If the power electronics part allows, recuperated energy could be stored in the ESS of the BEV. Currently, there are four ways to capture the energy generated by regenerative braking: the electricity generated is stored directly into the ESS; hydraulic energy in a small canister through compressed air (hydraulic motors required); in the FES as rotating energy; as gravitational energy (potential energy) through a spring [64]. Today the energy produced through regenerative braking is only suitable for a BEV with high ESS capacity.

Regenerative braking is regarded as one of the main benefits of a BEV that can extend the driving range of the vehicle. Studies have found that the share of energy at the wheels used for braking is at the range of 12% to 63% (with an average of 30%), engine braking could however reduce the amount of recoverable energy to about 16% [7]. The reason of such small range is that regenerative braking operates together with the friction brakes when the vehicle decelerates.

Further, in the HEV, in the regenerative mode, it is in principle possible to run the engine as well, and provide additional current to charge the battery faster (while the propulsion motor is in the generator mode) and commands its torque accordingly to match the total battery power input; in this case, the engine and motor controllers have to be properly coordinated [1].

Regenerative braking could be achieved by proper use and tuning of the propulsion motor drive, so it could indirectly refer to the propulsion drive system.

## **2.6 Charging Systems for BEV**

The charging system of the BEV is not a part of a propulsion drive as power electronic devices described in Section 2.3, but in some cases, they affect the propulsion drive topology, i.e. they need to be reviewed separately. Charging systems could be divided into on-board and off-board systems. In the case of an

on-board charger, the whole weight of the BEV as well as the load on the propulsion system are increasing. Typical on-board chargers limit the power because of weight, space, and cost constraints and are intended to charge the battery for a long period; an off-board battery charger is less constrained by size and weight [68].

The charging mode describes the safety communication protocol between the BEV and the charging station. The standard lists the charging modes defined in IEC61851-1, which includes:

- Mode 1 - slow charging from a household-type socket-outlet;
- Mode 2 - slow charging from a household-type socket-outlet with an in-cable protection device;
- Mode 3 - slow or fast charging using a specific EV socket-outlet with control and protection function installed;
- Mode 4 - fast charging using an external charger.

Similarly to power electronic devices used in propulsion motor drive converters (Chapter 2.3), charging systems could be divided into unidirectional and bidirectional topologies. There are many different schematic topologies available for charging systems. A general topology is presented in Figure 2.12.

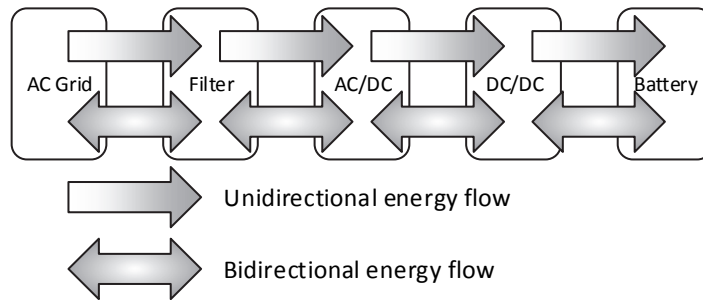


Figure 2.12. General unidirectional and bidirectional topology

Generally, DC/DC converters are used for unidirectional charging systems based on diodes and mostly bridges schemes with cascade. DC/DC converters present a wide variety: buck, boost, flyback, forward, push-pull, half-bridge, full-bridge, Single-Ended Primary-Inductor Converter (SEPIC), and Cuk converter. Unidirectional charging systems with active front ends can provide local reactive power support by means of current phase angle control without having to discharge a battery [68]. That can be used for the power quality correction of a grid.

Bidirectional power flow is necessary in order to realize V2G and G2V functions. In that case the plugged-in BEV becomes a part of the grid and the battery of the BEV is used as an energy storage device for energy exchange between the elements of the distributed energy grid. In that case, BEVs bring new features to the electric grid and could be used as a prosumer (combined producer and consumer) device.

Plug-in charging systems have several drawbacks[69]:

- the cable and connector typically deliver 2-3 times more power than standard plugs at home and this increases the risk of electric shock especially in wet environments, that means existed power sockets are not ready to be used for BEV charging;
- the long wire poses a trip hazard and results in poor aesthetics for such systems;
- in harsh climates that commonly have snow and ice, the plug-in charge point may become frozen onto the vehicle.

To overcome these drawbacks and inexistence of physical contact between the source and the load, wireless inductive charging systems could be used. The main benefits of wireless charging systems are: the galvanic isolation requires less maintenance, high output power and possible usage in harsh environments (that is important for such north regions as Estonia). The main drawbacks that can be pointed out are: resonant circuits hard to tune, electromagnetic interference, magnetic field does not penetrate metals (metallic objects in the middle of the magnetic connection increase the losses and the system may not work), and magnetic radiation [70].

GCEV systems could be referred to as charging systems because of the similarity of the topologies. Country standards and distance ranges determine the variety of GCEV voltage ranges. There are four main standards for electric trains used in Europe: 1.5 kV and 3 kV for DC and 15 kV  $16^{2/3}$  Hz and 25 kV 50Hz and 600 VDC or 750 VDC systems are used for trams and trolleybuses [71].

## 2.7 Summary of Chapter 2

Chapter 2 describes the basic components of the BEV technologies and propulsion drive segments are studied in more detail. From the variety of EM used in the BEV today, an IM stands out. The topology widely used in other electric drive applications of the IM is rarely used for propulsion drive systems because of its unstable working mode and low controllability in the low speed range.

Technologies used in the ESSs and power converters allow using different algorithms and methods for IM control. It means that its very simple construction and high reliability and performance could make the IM a leading motor type used in the BEV propulsion drives. A VSI with a possibility to change the control mode (frequency and flux control modes) is the best solution for a power converter. A VSI is required in the DC voltage supply, i.e. to study the propulsion motor drive system of the IM, ESS for the VSI could be replaced with a stable DC energy supply.

Essentially, the IM propulsion motor drive system has a potential possibility to be used in the V2G and G2V systems. Further, the power grid and charging systems used today need to be updated according to new requirements from

energy consumers. The role of the grid connected to the BEV is transformed to the prosumer role. The prosumer could become a part of the electric grid in different ways and applications, thus, some additional features could be added to actual systems. Further studies are required in that field.

### 3 MODELLING OF PROPULSION DRIVE SYSTEM

#### 3.1 Model of the vehicle's propulsion drive load

In this section the vehicle is modelled as a road load, the vehicle and the associated forces are illustrated in Figure 3.1. Calculations are based on [1], [5], [6]. The behavior of the road load model depends on the vehicle geometry, i.e. on this step of the vehicle mode, the modelling type of the propulsion system (ICEV, HEV and EV) does not matter, until the road load is applied to the propulsion motor.

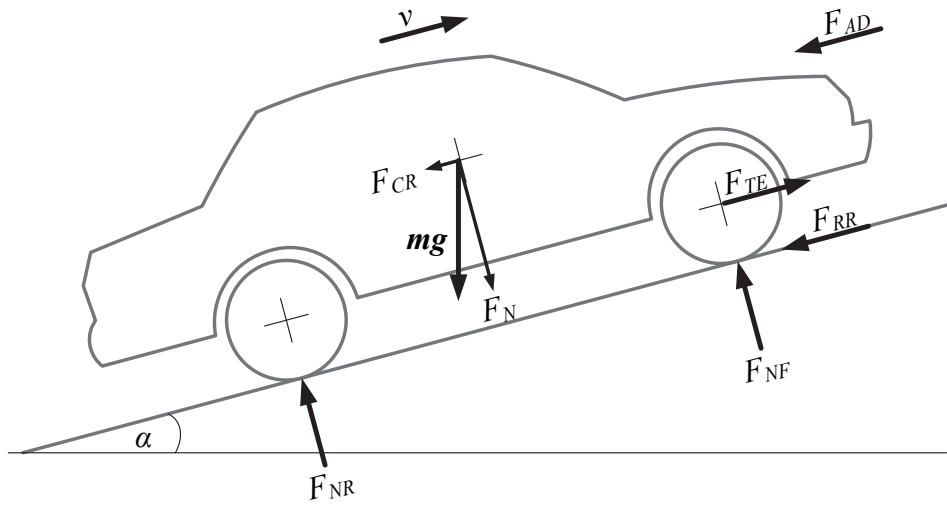


Figure 3.1. Forces applied to a vehicle

Consider a vehicle of mass  $m$ , moving at a velocity  $v$ , up a slope of angle  $\alpha$  (in degrees). The propulsion force for the vehicle to move forward is termed the tractive effort  $F_{TE}$ . This force has to overcome rolling resistance  $F_{RR}$ , aerodynamic drag  $F_{AD}$ , the climbing resistance force  $F_{CR}$ , and the accelerating force vehicle (if the velocity is not constant). In that case, the base road load  $F_{RL}$  is a sum of rolling resistance, aerodynamic drag and climbing resistance force as follows:

$$F_{RL} = F_{RR} + F_{AD} + F_{CR} . \quad (3.1)$$

The rolling resistance is the force resisting the tire at the roadway surface. Under most circumstances, rolling resistance depends on the coefficient of rolling friction between the tire and the road  $C_{rf}$ , the normal force  $F_N$  due to the vehicle's weight  $mg$ , and the gravitational acceleration  $g$ :

$$F_{RR} = -F_{TE} , \quad (3.2)$$

$$F_{RR} = -C_{rf} mg \cdot \cos\left(\frac{\alpha\pi}{180^\circ}\right). \quad (3.3)$$

However, if the vehicle is at rest and the force applied to the road is not strong enough to overcome the rolling resistance, then the rolling resistance must cancel out the applied tractive force accurately to keep the vehicle from moving. Thus, the equation for rolling resistance is

$$\text{if } v = 0 \text{ and } F_{TE} < C_{rf} mg \cdot \cos\left(\frac{\alpha\pi}{180^\circ}\right). \quad (3.4)$$

Aerodynamic drag is important, especially at high velocities. The aerodynamic drag depends on the air density  $\rho$ , the coefficient of drag  $C_d$ , the frontal area of the vehicle  $A$ , and the vehicle velocity  $v$  (relative to the air):

$$F_{AD} = \frac{1}{2} C_d \rho A v^2 \text{sgn}(v), \quad (3.5)$$

where

$$\begin{aligned} \text{sign}(v) &= +1 \text{ if } v > 0 \\ \text{sign}(v) &= -1 \text{ if } v < 0. \end{aligned}$$

The climbing resistance force due to the road grade depends on the mass of the vehicle  $m$ , road angle in degrees  $\alpha$ , and gravitational acceleration  $g$ . The equation for this force is

$$F_{CR} = -mg \cdot \sin\left(\frac{\alpha\pi}{180^\circ}\right). \quad (3.6)$$

The road load curves of a vehicle for varying road angles are shown in Figure 3.2, Tesla Roadster with its parameters listed in Table 3.1 was chosen for illustration. According to the literature, coefficients of rolling friction for tires are about 0.007 for dry road and 0.004 for wet road. It can be observed that the road load increases with the velocity and with the road angle.

Table 3.1. Parameters for the simulated vehicle [72]

Parameters	Value	Unit
Vehicle mass	1235	kg
Gravitational acceleration	9.81	m/s <sup>2</sup>
Rolling friction (dry road)	0.0075	-
Rolling friction (wet road)	0.004	-
Air density	1.225	kg/m <sup>3</sup>
Aerodynamic drag coefficient	0.35	-
Frontal area	1.93	m <sup>2</sup>
Tire diameter (21 in)	0.53	m

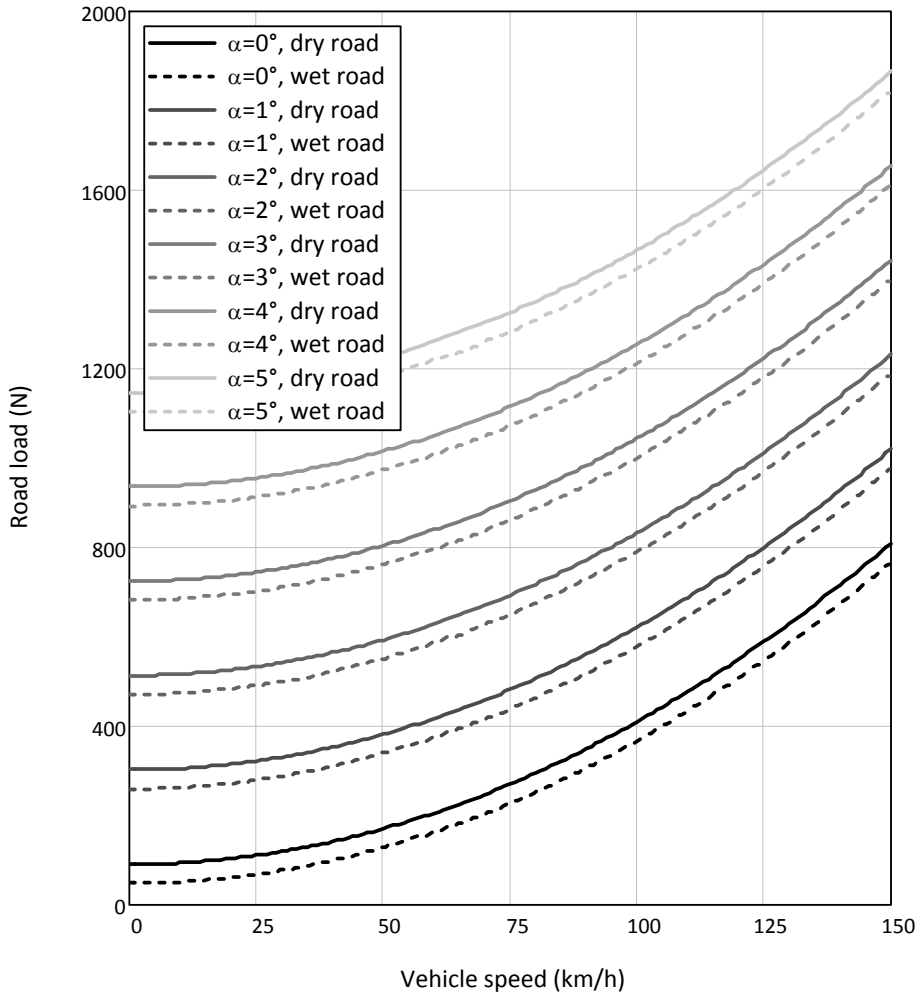


Figure 3.2. Road load characteristics for road slope angle  $\alpha=0^{\circ}-5^{\circ}$  and dry/wet road conditions

The acceleration force is the force needed to accelerate the vehicle, governed by Newton's second law. This force will provide the linear acceleration of the vehicle

$$F_{ACC} = ma = m \frac{dv}{dt}. \quad (3.7)$$

The total tractive effort is the sum of all the above forces:

$$F_{TE} = F_{RR} + F_{AD} + F_{CR} + F_{ACC}. \quad (3.8)$$

The vehicle's velocity is calculated by integrating the vehicle's acceleration with the starting value set to 0 km/h at  $t=0$  seconds. It is equal to

$$v = \frac{1}{m} \int_{t=0}^t (F_{TE} - F_{RR} - F_{AD} - F_{CR}) dt . \quad (3.9)$$

In an ICEV the vehicle propulsion force comes from the engine shaft torque and in a BEV from the traction motor shaft torque. Linear velocity of the vehicle should be referred to the motor (engine) shaft. Figure 3.3 shows the mechanical scheme of the motor-to-wheel transmission.  $T_{motor}$  is the torque developed by the propulsion motor,  $\omega_{motor}$  is the propulsion motor's angular velocity and  $GR_{TRANS}$  denotes the transmission gear ratio;  $T_{axle}$  and  $\omega_{axle}$  are wheel axel torque and angular velocity,  $GR_{DIFF}$  is the differential gear ratio;  $v$  is the vehicle speed (linear velocity).

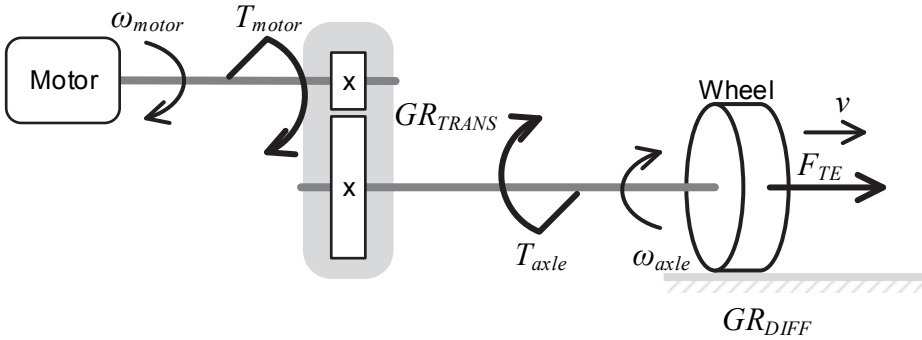


Figure 3.3. Mechanical scheme of motor-to-wheel transmission

From Figure 3.3 it follows that

$$GR_{TRANS} = \frac{\omega_{motor}}{\omega_{axle}} = \frac{T_{axle}}{T_{motor}} \quad (3.10)$$

and

$$GR_{DIFF} = \frac{\omega_{axle}}{v} = \frac{F_{TE}}{T_{axle}} \quad (3.11)$$

Equations (3.10) and (3.11) are related to the following:

$$T_{motor} = F_{TE} \cdot \frac{1}{GR_{TRANS}} \cdot \frac{1}{GR_{DIFF}} . \quad (3.12)$$

To simplify the model and prevent nonlinearity, the efficiency of the mechanical transmission is not considered (equal to 1).

Similarly, the frequency of rotation  $n_{motor}$  of the propulsion motor could be found:

$$n_{motor} = \frac{60}{2\pi} \cdot v \cdot GR_{TRANS} \cdot GR_{DIFF} \cdot \quad (3.13)$$

According to (3.11) and (3.12), the total tractive effort of the vehicle could be scaled to the propulsion motor. The motor load to the motor frequency rotation characteristics is shown in Figure 3.4, the road slope angle  $\alpha=0^\circ-5^\circ$  and dry/wet road conditions are presented. Characteristics Figure 3.4 in are valid for a steady-state driving mode, or cruising at a constant speed without acceleration.

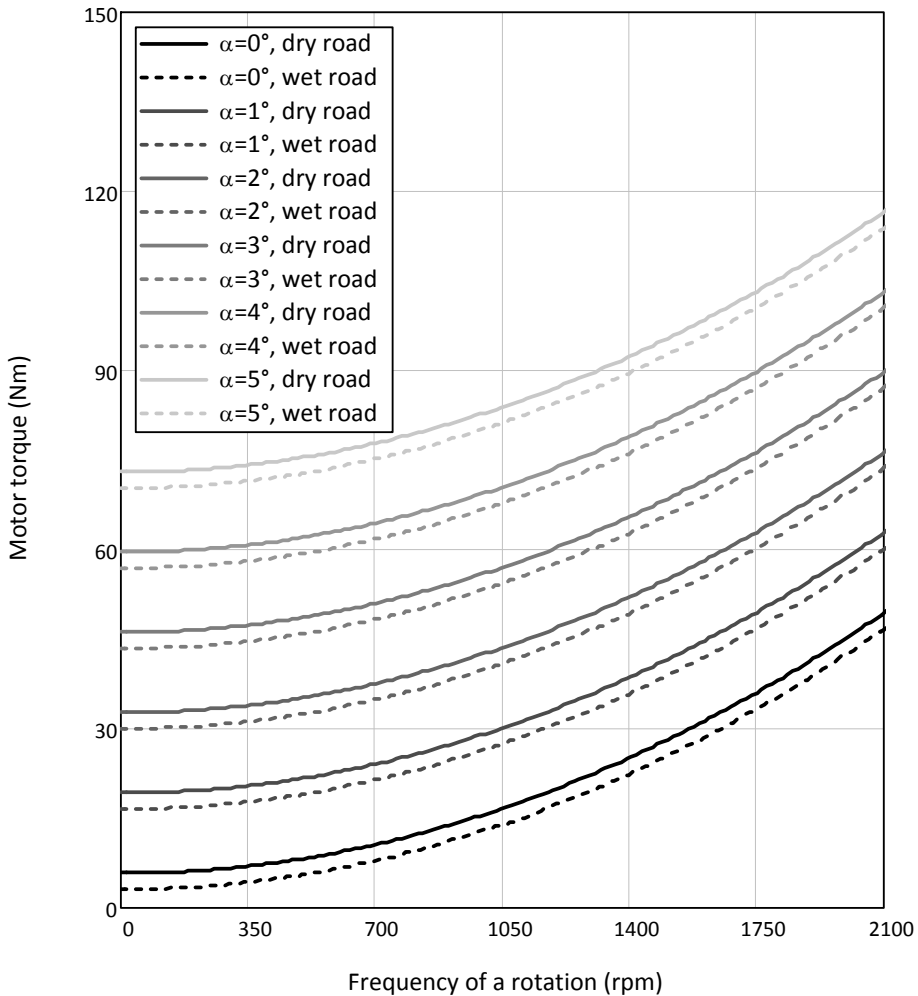


Figure 3.4. Propulsion motor load characteristics for the road slope angle  $\alpha=0^\circ-5^\circ$  and dry/wet road conditions

### ***Resume***

To be able to estimate the processes of the BEV propulsion drive it is very important to use a proper model of the propulsion drive load. The model of a BEV load is very complex as it contains many different components, and to prevent mistakes, each component needs to be modelled properly. In this section a road load model scaled to the propulsion motor of Tesla Roadster is presented. It was found that the load of the propulsion motor increases with the velocity, with acceleration and with the road angle.

Forces influencing the propulsion system of the BEV could be reduced to the propulsion motor shaft. It means that the propulsion drive of the BEV could be tested without complicated mechanical transmission and load forces and the torque could be replaced with the torque of the propulsion motor load.

### **3.2 Computer Model of the Propulsion Drive of BEV**

Many different ways are available to model a BEV. Mainly, all the models could be classified into three groups [73], [74]:

- Dynamic models based on the physical representation of different subsystems, their accuracy is depends on the description of different parts of the system;
- Static model takes into account steady-state processes of a BEV, i.e., it has no main time constant included in the model;
- The quasi-static model is a collaboration between the static and dynamic models; it is similar to the static model but it has the main time included.

The dynamic model gives good simulation accuracy. Proper simulation of power electronic devices with high switching frequencies is important. That makes the dynamic models more complicated for simulation and increases the simulating time. The main drawback of the static model is that no transient processes are included in the model. With a quasi-static model, the study of steady-state and transient modes is possible.

Abundant computer software is available today for computer modelling of the BEV systems. Such software as PSIM, PSCAD/EMTDC, MATLAB/Simulink, ANSYS Simplorer, Synopsys Saber, and Dymola could be used for dynamic models. These electronic circuit simulation software packages are designed for use in power electronics and electric motor drive simulations. Any electronic and equivalent circuit could be designed using those simulation packages. Many universities and research institutions have their own toolboxes for EV and HEV studies: SIMPLEV (DOE Idaho Laboratory), MARVEL and PSAT (Argonne National Laboratory), CarSim (AeroVironment Inc.), JANUS (Durham University), ADVISOR (DOE National Renewable Energy Laboratory), ELPH and V-ELPH (Texas A&M University), and Vehicle Mission Simulator (Software Engineering Professionals). Most of those software packages are MATLAB based toolboxes optimized and designed for EV/HEV studies.

### Load modelling

According to Figure 1.1, the load is not included in the propulsion motor drive system, but its effect could be taken into account in the simulation.

A part of the characteristic from Figure 3.4 was taken to imitate the propulsion motor load, according to Figure 3.5, the load of 15.7 Nm corresponds to the road slope angle  $\alpha=0^\circ$  and dry road conditions at the constant speed to the frequency of rotation of 1000 rpm (angular velocity 104.72 rad/s).

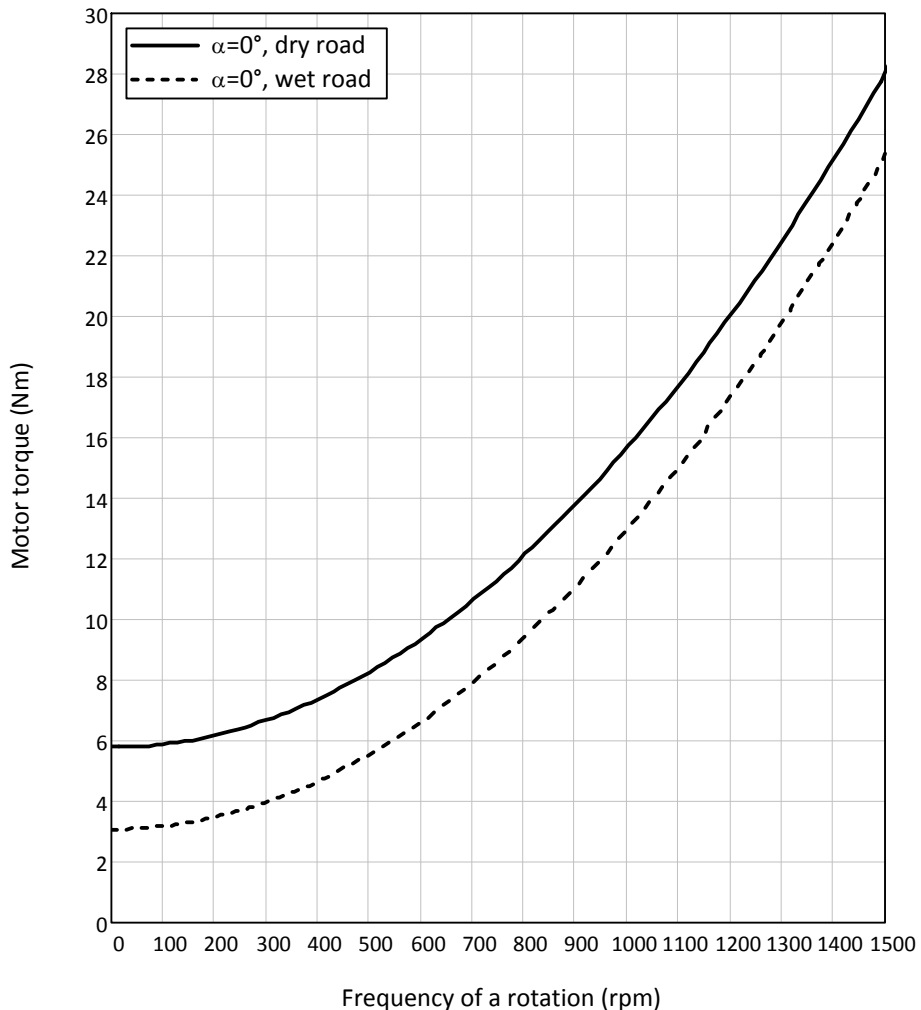


Figure 3.5. Propulsion motor load characteristics for the road slope angle  $\alpha=0^\circ$  and dry/wet road conditions

### ***ESS modelling***

According to Figure 1.1 the ESS of the BEV, like the load impact, is not included in the propulsion motor drive system, but its effect on the propulsion motor drive system should be taken into account. Section 2.4 presents the variety of ESS used in the BEV. Even the variety of BATs is so huge that it is impossible to use some single model for all ESS. The model of the ESS should take into account the charging/discharging characteristics, state of charge/discharge, environmental influence and other factors. The main attribute of the ESS is limited current (and as a result, limited torque) that should be taken into account during simulation.

### ***PSIM model of the propulsion motor drive***

The reason to choose the propulsion drive of the BEV based on an IM for this study was that it is more interesting and perspective, as mentioned in section 2.7. The computer model of the BEV propulsion motor drive created for the study assumes also that experimental data be confirmed for that case, creating a real motor model that can be used for further research is more reasonable. To test the motor of the propulsion drive, parameters of the IM from ABB Company M3AA 112m 3GAA 112022-ADC were chosen. MATLAB/Simulink, a more flexible and powerful software package, was chosen to create the propulsion motor drive model. Simulink model of M3AA 112m 3GAA 112022-ADC motor is presented in Figure 3.6.

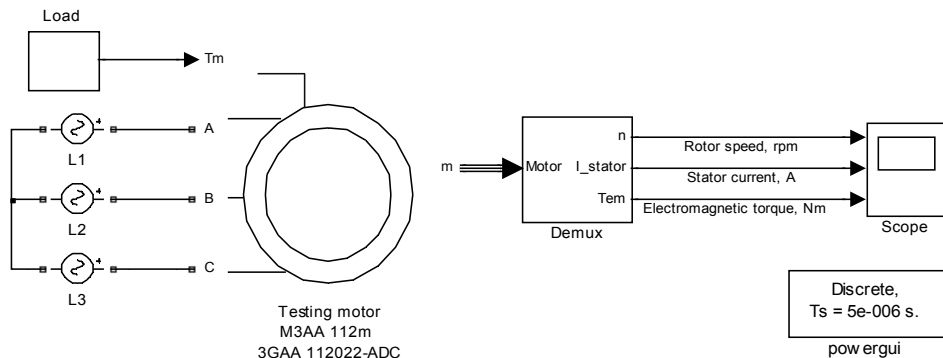


*Figure 3.6. MATLAB/Simulink model of the propulsion motor*

Transient mode of the Simulink motor model is shown in Figure 3.7. The results of the simulations are in agreement with the motor datasheet (rated current 9 A, rated torque 26.3 Nm, rated speed 1455 rpm).

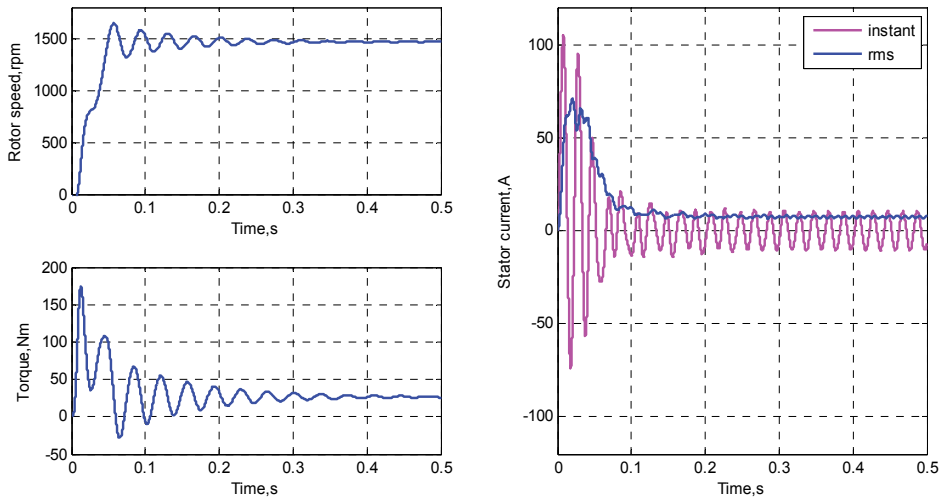


Figure 3.7. Speed-time, current-time and torque-time traces of MATLAB/Simulink model simulation of the propulsion drive in a transient mode

As mentioned before, the propulsion motor drive created for this research assumes also experimental data to be confirmed; to simplify the model, an induction motor drive block was taken. Figure 3.8 shows the Simulink propulsion motor drive model. A six-step inverter fed induction motor drive was taken to imitate the open-loop (SCALAR) control mode of the drive and direct torque and flux control (DTC) induction motor drive model to imitate the closed-loop system. The induction motor drive model provided with the SimPowerSystem™ library consists of a 3-phase diode rectifier, a 3-phase inverter and induction motor models. The induction motor drive block allows separate set-up of all parts of the model (motor, DC bus, controller), speed and torque references. Speed and torque reference blocks are presented in Appendix 1.

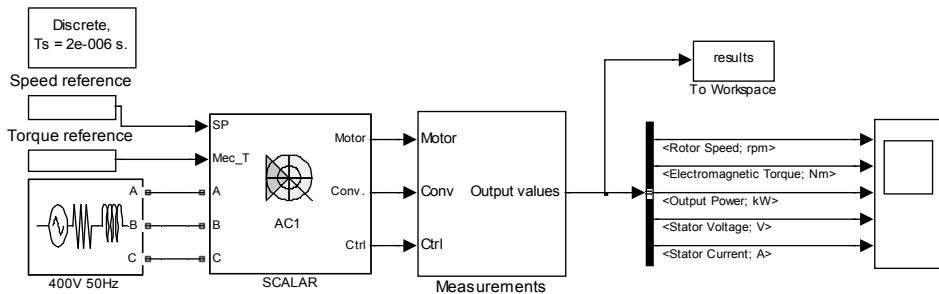


Figure 3.8. MATLAB/Simulink propulsion motor drive model

## ***Resume***

Steady-state and transient mode models of the propulsion motor drive system were created using MATLAB/Simulink simulation software packages. The model of the propulsion motor drive created assumes also the experimental data to be confirmed; the model induction motor drive block was taken to simulate the processes in the test bench described below. Two control mode models are proposed: open-loop and close-loop. Use of the load scaled to propulsion motor shaft allows simulation of real vehicle static loads and comparison of drive response on different loads.

### **3.3 A Test Bench to Study Propulsion Drives of BEV**

Today much attention is paid to the studies of BEVs and their test platforms. The test bench, combining advantages of software models and real equipment, contributes to the reduction of the number of vehicle test runs and safe maintenance. Reports of the test benches developed in different research centres cover energy management [75], optimal configuration [76]–[78], and combination of different energy sources of BEV [79], like the batteries [80], supercapacitor [15], [55], [56], [81]–[83] flywheels [79], and fuel cells [84].

Research problems solved for the BEV propulsion drives using the test benches are derived from the peculiarities of their performance, in particular from frequent accelerations and decelerations, multiple stops, and stochastic velocity changes, mechanical vibrations, and elastic deformations [85]. All these features require proper drive characteristics, like fast torque response, fault tolerance, and high efficiency at low maintenance and cost. These considerations imply that the design of the platform intended to study and monitor the BEV propulsion drive should be verified by forcing it to follow the test cycles that reproduce the actual operating conditions.

As the investigations were focused on the propulsion motor drive system of BEVs, the main objectives of the test bench developed and described in [PAPER-III]:

- to provide the research environment for analysis, investigation, and simulation of marketable BEV drive systems;
- to establish assessment and verification procedures for different motor, gear, and power converter types used for propulsion;
- to support commercial consulting, research and testing for enterprises;
- to promote student participation in research topics associated with electro mobility.

A test bench developed in the Laboratory of Electrical Drives at the TUT Department of Electrical Engineering is presented in [PAPER-I], [PAPER-II] and [PAPER-III]. The sketch of the test bench is presented in Figure 3.9.

According to [80], the test bench is based on the induction machines. Induction machines, especially squirrel cage motors, have high reliability and low manufacturing cost, but their efficiency and torque density are inadequate. As these demerits are unimportant for the test bench, this type of a machine was

used in the test platform. Unlike the synchronous and the DC motor, an IM has simple design and suits for both the open-loop and the close-loop exploration.

The test bench incorporates two motor drives. The testing system based on the ABB ACS800 electric drive consists of a squirrel cage IM, an active AC/DC power converter, a remote console, control, measurement, and cabling equipment. The testing drive is furnished with a foot pedal to imitate the real driver's habits in vehicle management. The testing motor M3AA 112M 3GAA 112022-ADC has the following parameters: rated speed of the motor – 1455 rpm, rated voltage – 400 V, frequency – 50 Hz, and rated power – 4 kW.

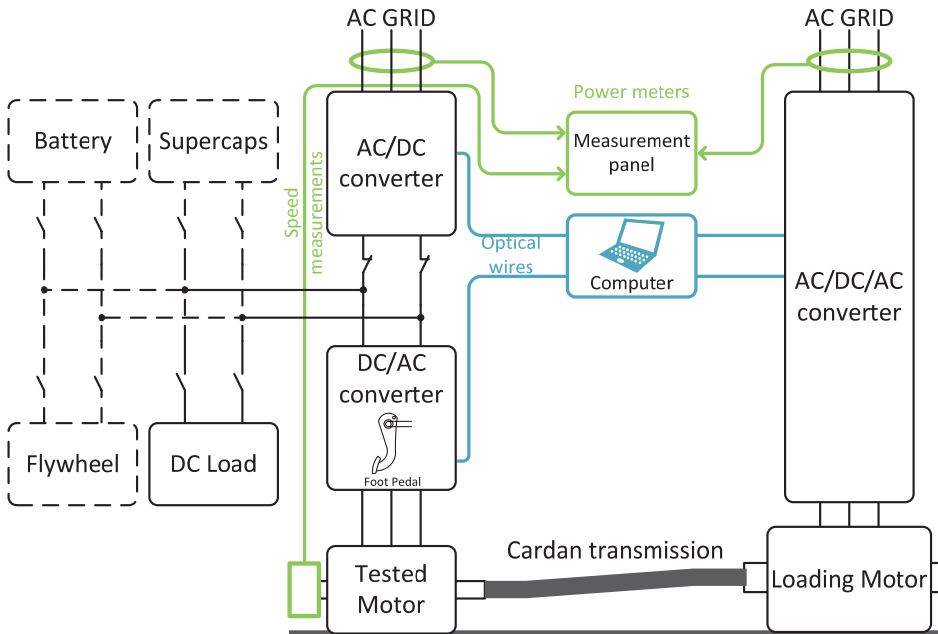


Figure 3.9. Basic circuit of the test bench

ABB ACS800 power converter is a middle-power class device with broad control possibilities. There are two main control modes of the drive, namely the Direct Torque Control (DTC) [86] and the Scalar control supporting the constant voltage-frequency ratio. The converter possesses several predefined macros with factory settings allowing flexible drive tuning for a user. Additionally, ABB ACS800 is equipped with the model-based measurement tools allowing the real-time parameter tracing. It includes the built-in logical controller for programming the converter outputs and inputs to fulfil the basic operations. In the developed test bench, this drive is employed in the scalar control mode to imitate the real driving needs of the BEV driver.

As distinct from [80] where the driven motor is connected to the utility supply through a voltage adjustment variator, in the proposed solution the loading machine is supplied with the DTC DC link converter. In this way, the testing drive operates in the speed control mode to follow the test cycles

whereas the loading drive performs in the torque control mode to follow the torque references. Both systems are power reversible.

The loading system built on the ABB ACS611 electric drive consists of an induction motor M3AA 132SB, AC/DC power converter with the diode front end, remote console, and measuring and cabling equipment. ABB ACS611 represents a variant of ABB ACS800 drive with a different firmware version and similar functionality. The DTC mode of the drive operation is suitable for the simulation of different loads of the real BEV. The loading motor M3AA132SB 3GAA 138110-ADC has the following parameters: the rated speed of the motor – 2820 rpm, rated voltage – 400 V, frequency – 50 Hz, and power – 4.7 kW.

To imitate the mechanical chain of a BEV, the belts with electromagnetic clutches were used in [78] that join the motor with the transmission shaft. In [80] the traction motor was connected to the wheels via a step-down gear stage. On the contrary, in the proposed solution, a direct coupling through the long metal shaft is implemented, as recommended in [87]. The transmission has a possibility to change the slope angle, thus simulating the cardan with alternating transmission rigidity and moment of inertia. The testing and loading motors are placed on the uniform base to provide their joint operation.

Remaining installation equipment is mounted within a specially manufactured cabinet where interconnections are provided through the cabling equipment. The remote control buttons and measurement devices are located on the front panel of the cabinet. Two power meters Merlin Gerlin Power Logic PM500 acquire full information about the input power variables of each drive, such as voltage and current values, active, reactive and apparent powers, power factor, and total harmonic distortion. For speed measurements, the Leine&Linde 861007455 encoder of 9–30 VDC supply voltage and 2048 pulses per revolution is fitted on the motor shaft. To measure device connection, the 4 mm laboratory plugs are available. For quick shutdown of the laboratory setup, the emergency shutdown button is placed on the front panel of the cabinet.

Both drives are connected to the computer through a set of optical wires. The ABB toolbox DriveWindow provides the remote control of the tested and the loading drives, their tuning, monitoring, graphical trending, and registration of the drive parameters. The output data from the DriveWindow software can be presented and saved in graphical and numerical forms for the following analysis.

### ***Study of Propulsion Drive Performance in Steady-state mode using the Test Bench***

To validate equipment installation and tuning of the test bench, measurements were performed. The testing drive can be calibrated to obtain the speed-torque characteristics similar to those shown in Figure 3.10. The test bench enables smooth load variation of the testing drive in four quadrants. It means that all the possible running and braking modes can be explored here.

Wide range of road conditions (dry, wet, icy surfaces, etc.) can be simulated on the test bench, by adjusting the torque. Different slip values including the vehicle locking that is similar to the braking process of a vehicle whose wheel can rotate freely or be locked. IM characteristics are asymmetrical, therefore different voltages and frequencies for motor exciting can be studied.

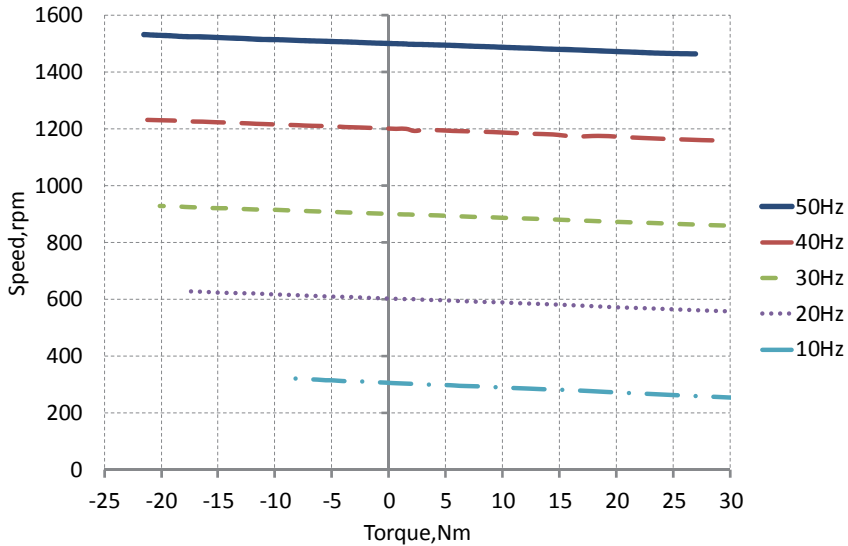


Figure 3.10. Speed-torque characteristics of the tested induction motor obtained from the test bench

The diagram in Figure 3.11 represents an active power dependence on the load within a broad speed range. The measurements can be taken in the first and second quadrants of the power-torque plane. To study the testing drive at different speeds, it is supplied with variable voltages and frequencies in the scalar mode. To explore the motor performance at different loads, the loading drive operates in the DTC mode with smooth transition between the forward and the reverse torque values. The speed of the motor rotation is measured with the speed sensor from the measurement panel of the test bench. This study enables us to register the energy flow in the motoring and regenerative braking modes for all four quadrants where the testing motor could operate. An active DC load allows the active energy flow to be registered during the regenerative braking.

Many studies concentrate on propulsion efficiency. The main goal is to reduce the losses of the drive and as a result, maximize the efficiency. The test bench enables us to plot the ratio of the shaft power to the consumed power that represents efficiency diagrams for some part of the propulsion system, for all four quadrants of the drive performance and to conduct their full-scale analysis. Figure 3.12 shows the diagram of the ratio of the shaft power to the consumed power of the testing drive that resulted from the analysis of the measurements. The traces in the first quadrant were derived as the ratio of the shaft power and

the active power consumed by the testing drive. The loading drive output power is taken as a shaft power, whereas the testing drive input power measured by the input power meters is considered as the consumed value. For the second quadrant of the diagram in Figure 3.12, an active power consumed by the DC load is taken as an output power, whereas the loading drive output power is considered as an input power of the drive.

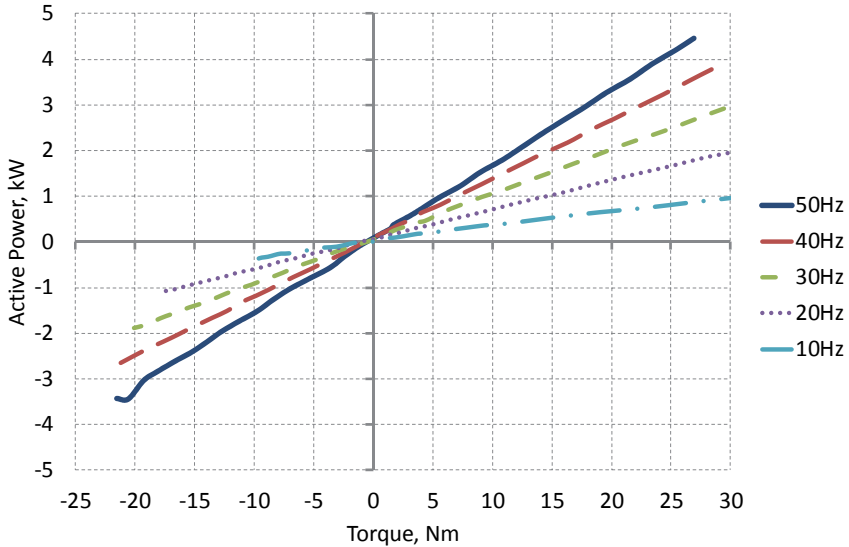


Figure 3.11. Active power diagram of the testing induction motor obtained from the test bench

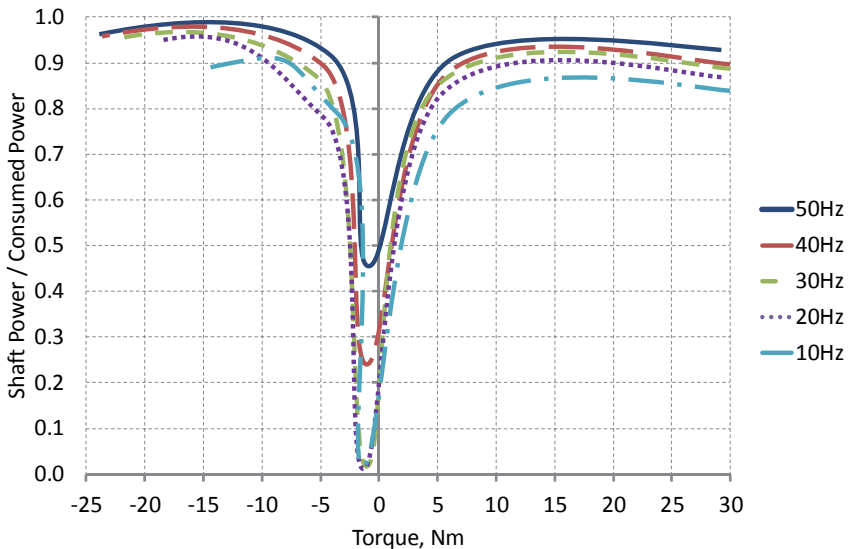


Figure 3.12. Ratio of the shaft power to the consumed power of the testing induction motor obtained from the test bench

### ***Study of Propulsion Drive Performance in Transient Mode using the Test Bench***

To explore transient modes, the standard urban driving cycle ECE-R15 is commonly taken, which represents an alternating speed of the BEV in the predefined time intervals. To set the required speed set-points, an adaptive programming of the built-in controller is executed. The sample speed set-point diagram adopted for the test bench is shown by the dashed lines in Figure 3.13. The ABB ACS800 controller has 15 functional blocks that can be programmed with 25 different arithmetical and logical functions. The diagram in Figure 3.13 was plotted by the DriveWindow toolbox at different constant loads, from 0 to 21 Nm, to the same speed reference cycle.

The set of speed timing traces in Figure 3.13 shows that the measured values of speed correspond to the speed set-point values. Some inaccuracies in the corners could be explained by the normal open-loop system operation. Inaccuracy during the constant-speed motion could be explained by the sliding of the induction motor.

The timing diagram in Figure 3.14 shows the active power distribution during the driving cycle at different loads. The timing diagram in Figure 3.15 displays the motor torque alternation during the driving cycle at changing loads. The highest torque spikes are observed in the initial points of the drive acceleration. Also, as the test bench can operate in regenerative braking mode, the definite level of spikes occurs in this mode, only a part of energy can be regenerated during braking.

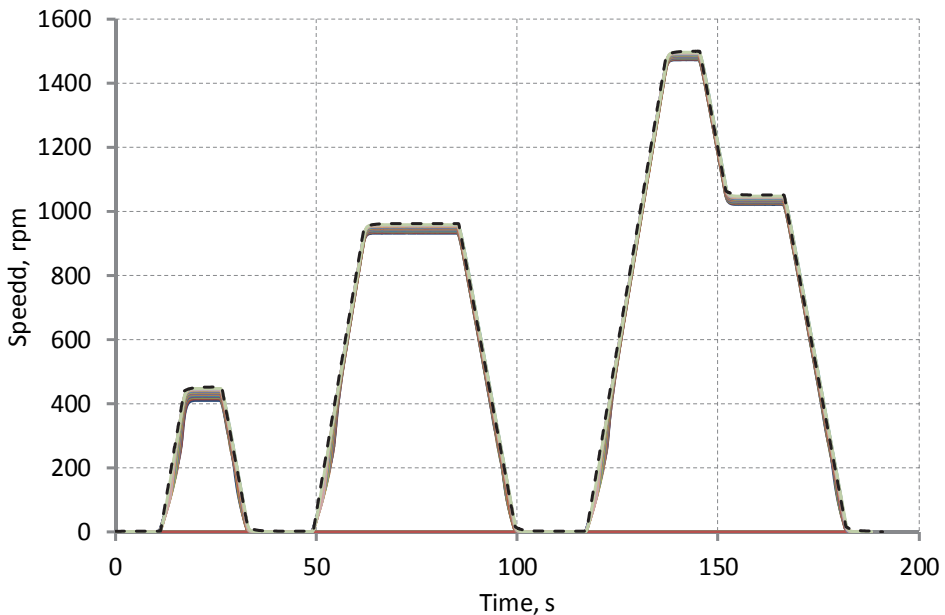


*Figure 3.13. Sample speed timing diagram of the tested drive applying the ECE-R15 driving cycle*

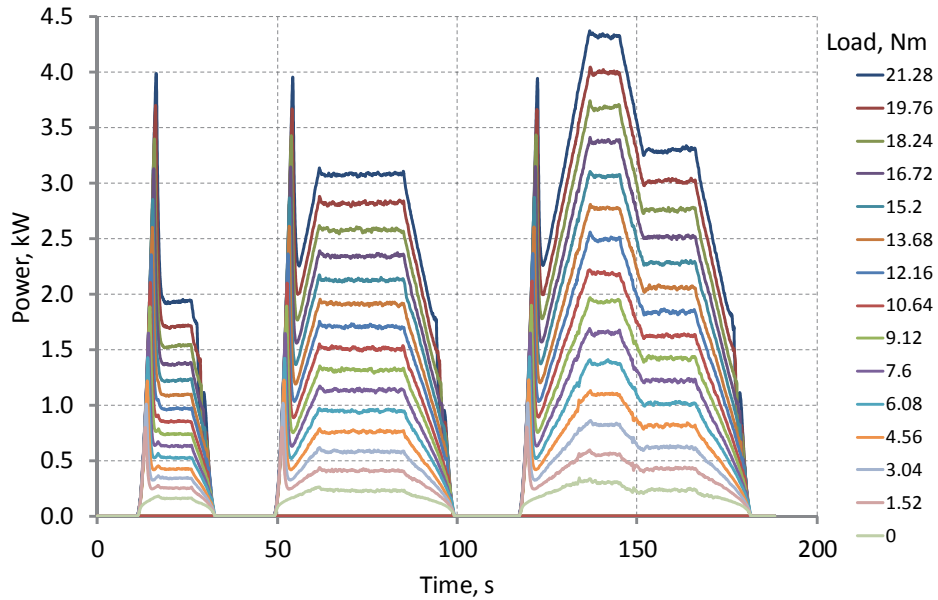


Figure 3.14. Active power timing diagram of the tested drive obtained from the test bench

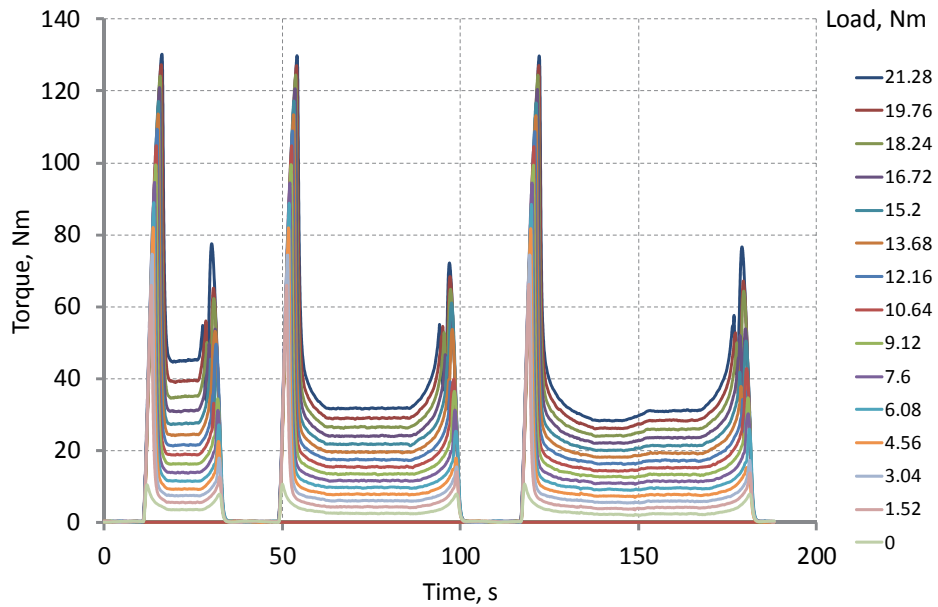


Figure 3.15. Motor torque timing diagram of the tested drive obtained from the test bench

### **Using of the Test Bench in Educational Proposes**

Based on the test bench developed for research purposes, a laboratory course for graduate students was prepared. The graduate students could acquire and

improve their skills in field of electrical drives, by study mechanical and power characteristics, different drive control methods, programming and tuning of the drive, vehicle imitation tests, etc. A laboratory practice exercise book was published [BOOK-I]. These regulations are intended for use as a tutorial aid for laboratory works under the Advanced Course of Electrical Drives (AAV0040) at TUT. A student is expected to have acquired knowledge of the basic course of electrical drives, electrical motors, electronic components, standard electrical wiring, and electrical schematic symbols.

### ***Resume***

After reviewing the test benches available for the propulsion drive of the BEV, a test bench was set up and tuned in the TUT Laboratory of Electrical Drives. The test bench allows steady-state and transient mode imitation of the propulsion drive of the BEV.

Using the test bench, the testing motor could be scaled to the IMs used by a real vehicle, for example, Tesla Motors using 3-phase 4-pole IM for their vehicles Tesla Model S (peak motor parameters for vehicle with 60 kWh energy storage: 225 kW, 430 Nm; 85 kWh: 310 kW, 600 Nm), Tesla Roadster (peak motor parameters for vehicle v. 1.5 and v. 2.0: 185 kW, 270 Nm; v. 2.5 non-sport: 215 kW, 370 Nm; v. 2.5 sport: 215 kW, 400 Nm).

The loading drive of the test bench allows imitating different load modes using the DTC, which corresponds to the Model of the vehicle's propulsion drive load in section 3.1. By scaling the propulsion motor load to the shaft, different areas on the load-speed diagram in Figure 3.4-3.5 could be studied in more detail.

## **3.4 Summary of Chapter 3**

Since a vehicle is a very complicated device, to provide maximal comfort and safety for the driver, the final design of the vehicle must be optimized and simplified. For more detailed study of separate parts of the complex vehicle and to be able to estimate the processes of the BEV propulsion drive, it is very important to have a proper model of the propulsion motor drive. The chapter describes three models: a load model of the propulsion drive, a computer model of the propulsion drive system and an experimental setup. All the models are scaled to a real vehicle.

The model of the BEV propulsion motor drive load is very complex and contains many different components. In the first section, a road load model scaled to the propulsion motor of Tesla Roadster is presented. The scaled model takes into account road slip, road slipping condition (dry or wet road), air drag and acceleration load. BEV load is scaled to the propulsion motor shaft that simplifies the testing of the system.

Proper computer model is very important to prevent mistakes and avoid mechanical damage of the system. Steady-state and transient mode models of the propulsion motor drive system were created using MATLAB/Simulink simulation software packages eDrive and PSIM. Computer model of the

propulsion motor drive system is described in the second section of the chapter. Scaled to the propulsion motor's shaft load, the model is applied as a load to the computer model.

Following the study of the driven load, an experimental test bench was created in the TUT Laboratory of Electrical Drives. A test bench was set up and tuned according to the results of the first two sections of the chapter and it is described in the third section. The test bench allows steady-state and transient mode imitation of the propulsion motor drive system of the BEV. The loading drive of the test bench allows imitating different load modes according to the road load model.

## 4 STUDY OF ELECTRIC PROPULSION MOTOR DRIVES

### 4.1 Vehicle Testing Cycles

Driving cycles produced by different countries and organizations are used to assess the performance of vehicles, such as pollutant emissions, fuel consumption and traffic impact. Different cycles are required for different types of vehicles. In this chapter light vehicle (<3500 kg) cycles are represented.

There are two main categories of test cycles: legislative cycles employed in type-approval tests for vehicle emission certification and non-legislative cycles mainly used in research [88]. New European Driving Cycle (NEDC) is commonly used in Europe, JC08 used in Japan and FTP-75 in the United States. World Forum for the Harmonization of Vehicle Regulations of the United Nations Economic Commission for Europe is making efforts to develop a world-wide harmonized light duty driving test cycle (WLTC), to represent typical driving characteristics around the world. The vehicle testing cycles are presented in Figure 4.1.

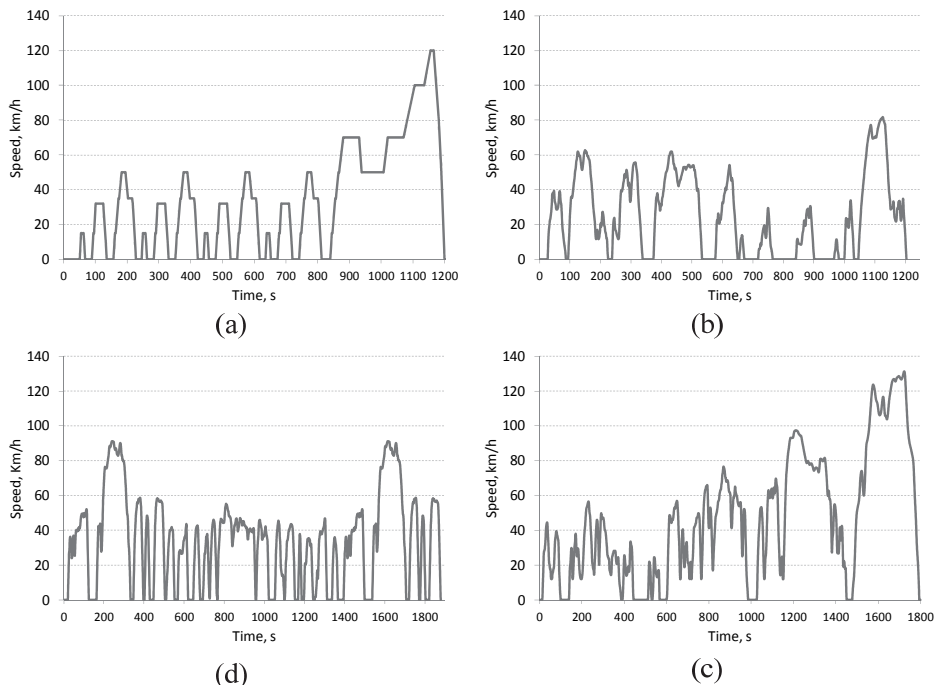


Figure 4.1. Vehicle testing cycles: a)NEDC; b)JC08; c)FTP-75; d)WLTC class 3, ver 5

#### ***New European Driving Cycle (NEDC)***

NEDC consists from two parts: four repeats of urban driving cycles (ECE-R15) and one Extra Urban Driving Cycle (EUDC). The ECE-R15, also known

as UDC, was devised to represent city driving conditions in European capitals (e.g. in Paris or Rome). It is characterized by low vehicle speed, low engine load, and low exhaust gas temperature. It has three segments with standardized speed and acceleration levels, with maximum speed of 50 km/h. The EUDC segment has been added to account for more aggressive, high speed driving modes. The maximum speed of the EUDC cycle is 120 km/h (90 km/h for low-powered vehicles). NEDC does not represent real driving behavior of a vehicle in actual traffic, thus it does not necessarily reflect pollutant emissions and fuel consumption [88]. NEDC is presented in Figure 4.1.a

### ***Japanese Driving Cycle JC08***

The JC08 test cycle represents driving in congested city traffic, including idling periods and frequently alternating acceleration and deceleration. Measurements should be made twice, with a cold start and with a warm start. JC08 has an average speed 24.4 km/h, with a maximum of 81.6 km/h. The Japanese test cycle represents real driving behavior but only in congested city traffic situations and does not cover other driving conditions and road types [88]. JC08 is presented in Figure 4.1.b.

### ***US Driving Cycle FTP-75***

FTP-75 (Federal Test Procedure) is used in US for emission certification and fuel economy testing of light-duty vehicles. The test cycle consists of three segments: cold state phase, stabilized phase and hot start phase. JC08 has an average speed 34.1 km/h, with a maximum of 91.25 km/h. FTP-75 covers a wider range of driving conditions than JC08 or NEDC, however it is still not complete enough to cover all possible driving situations [88]. FTP-75 is presented in Figure 4.1.c

### ***World-wide Harmonized Light Duty Driving Test Cycle (WLTC)***

WLTC is a chassis dynamometer test cycle for the determination of emissions and fuel consumption from light-duty vehicles. This test is expected to replace the NEDC procedure for type approval testing of light-duty vehicles. The WLTP includes three different test cycles applicable to vehicle categories of different power-to-mass ratios (PMR= rated power, W / curb mass, kg): class 1:  $PMR \leq 22$ ; class 2:  $22 < PMR \leq 34$ ; class 3:  $PMR > 34$ . With the highest PMR ratio, class 3 is representative of vehicles driven in Europe and Japan. WLTC class 3 cycle (Version 5) is presented in Figure 4.1.d

### ***Resume***

Table 2.1 compares such light vehicle driving cycle values as distance, total duration and idle time, average and maximum speeds, and Relative Positive Acceleration (RPA). RPA is the sum of the multiplication of the speed on acceleration and the time cut for positive accelerations, divided by the cycle distance. It can be interpreted as specific acceleration work. RPA is a good descriptor for the cycle dynamics, thus WLTC has the highest and NEDC has

the lowest dynamics. The WLTC has lower stop percentages and higher speeds than the other cycles; the JC08 is the other extreme (highest stop percentages and lowest speeds).

Table 4.1. Comparison of vehicle testing cycles [88], [89]

Characteristics	NEDC	JC08	FTP-75	WLTC, class 3,v 5	Unit
Distance	11.013	8.172	17.780	23.266	km
Total time	1180	1204	1876	1800	s
Idle (standing) time	267	357	367	242	s
Stop percentage	22.6	29.6	19.6	13.4	%
Average speed (incl. stops)	33.6	24.4	34.1	46.5	km/h
Average driving speed (excl. stops)	44.7	34.7	42.4	53.8	km/h
Maximum speed	120	81.6	91.25	131.3	km/h
Maximum acceleration	1.042	1.53	1.48	1.58	m/s <sup>2</sup>
Relative Positive Acceleration	0.1114	0.1707	0.1704	0.1524	$\frac{\text{kW}\cdot\text{s}}{\text{kg}\cdot\text{km}}$

Each of these driving cycles has its advantages and disadvantages. Driving cycles are used to assess the vehicle performance, but the tuning of the propulsion system is not taken into account. For proper tuning of the vehicle propulsion system those test cycles are too long, which complicates research. The NEDC driving cycle for the tuning of the propulsion drive system shows some disadvantages. The tuning of the propulsion drive is possible only from the side of speed reference control. NEDC has many constant speed cuts that is very rare for urban driving, but it is more suitable for highway cruising. NEDC can be used for steady-state mode tuning of the propulsion drive system.

JC08 and FTP/75 have some advantages over NEDC, they have less steady-state mode cuts during the test cycles, which makes them more suitable for transient mode tuning. That means the transient processes could be described more carefully and the drive load forces could be taken into account by using the system dynamic torque  $T_{dyn}$ :

$$T_{dyn} = J \frac{d\omega}{dt}, \quad (4.1)$$

where  $J$  is the moment of inertia of the drive system and  $\frac{d\omega}{dt}$  is an acceleration.

JC08 represents real driving behavior but only in congested city traffic situations and does not cover other driving conditions and road types. FTP-75 covers a wider range of driving conditions than JC08, however it is still not complete enough to cover all possible driving situations [88].

WLTC has been created to represent typical driving characteristics around the world and overcome drawbacks and disadvantages of other testing cycles. Despite all its benefits, WLTC is still under development and it is not covering the tuning requirements of the propulsion drive.

## **4.2 Library of Samples to Study BEV Drive Behavior**

To qualify the HEV/EV drives, different indicators have been proposed. In terms of controllability, a drive must have acceptable performance with regard to both the steady-state operation and the transient responses [90]. The steady-state operation is concerned with the accuracy of control and how closely the vehicle follows slow excursions of the control signal.

Important steady-state estimation is the rate of the system response to rapid input and load changes [85]. In power converters, the overload capacity is restricted by their heat dissipation features. Typically, for the semiconductor devices it is relatively small, but for the electric machines this value is significant enough. The rated overload capacity of motors represents the ratio of their maximal and rated torques indicated in the datasheets whereas the practically reachable value depends on the actual control possibilities of the particular drive design. The torque rise time of the open-loop systems is about 10 ms whereas this parameter for the closed-loop drives is within 1 ms. The speed rise time is usually by an order greater. When determining the transient responses, the physical properties of the drive subsystems are of primary importance.

A speed range is another important index showing the ratio of the maximal motor speed to its minimally accessible level upon the full area of disturbances [91]. In particular, to measure the speed adjustment range, the drift of the load torque should be within the expected maximal and minimal levels.

Speed regulation is also a specific feature of the drive operation. It deals with the fractional reduction of speed upon the variable load torque [92]. Nearby the zero speed regulation can be realized by the use of frequency-controlled synchronous motors or with the help of induction motors in the closed-loop control systems with a tachometric negative feedback. Loss of efficiency or power/weight ratio could be a consequence of rigorous specification for speed regulation.

The ECE-15R driving cycle in the test bench tuning (Figure 3.13 - 3.15) for the tuning of the propulsion drive system shows some disadvantages. The ECE-15R is too long and has many steady-state cuts. The tuning of the drive is possible only from the side of speed reference control, but the different driving conditions there should also be taken into account. For that reason the testing cycle could be simplified and applied on both sides of the propulsion drive, the speed-reference and/or the load-reference.

### ***Testing Software for BEV Performance Study***

To estimate the abovementioned indicators, specific test samples were designed. The testing samples library to study BEV performance is presented in

[PAPER-IV]. The library can be adopted to simulate multiple mechanics, thus allowing the study of the different parameters and load conditions for testing and tuning of the open-loop and closed-loop propulsion drive systems. Figure 4.2 shows the developed test samples.

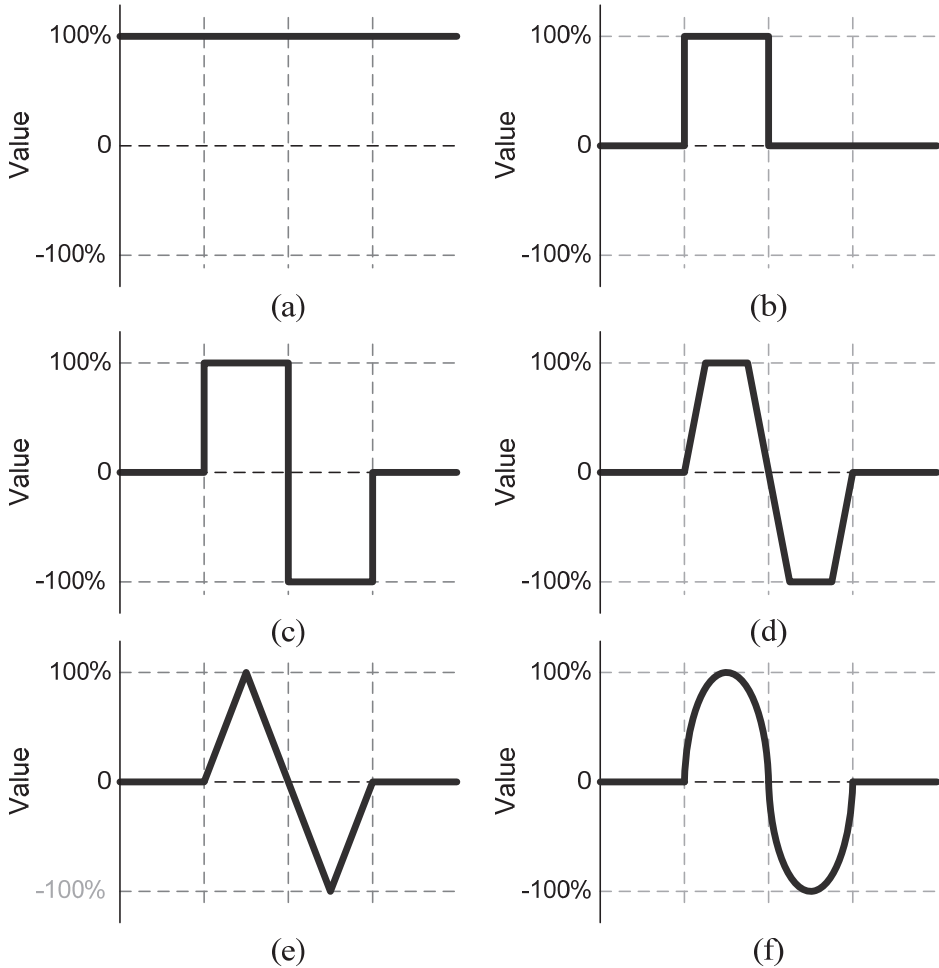


Figure 4.2. Test samples: a) constant; b) pulse; c) meander; d) triangle; e) trapeze; f) sinusoidal

Test samples could be adopted as both the references and the loading signals of the BEV propulsion motor drive.

A constant set-point (as shown in Figure 4.2.a) is simulated by the step signal  $y^*$  of the required level  $k$ :

$$y^* = k . \quad (4.2)$$

This speed-reference imitates a constant-speed vehicle motion, particularly the stable cruising control mode. The same load reference imitates constant-load vehicle motion during the highway cruising.

A rectangle pulse reference sample (Figure 4.2.b) is represented by the permanent input  $k$  within the time slot  $t \in \{0; t_1\}$ ,  $t_1 < \tau$ , where  $\tau$  is the signal period. Within the remaining part of the period a delay is assumed:

$$\begin{cases} y^* = k, & t \in \{0; t_1\} \\ y^* = 0, & t \in \{t_1; \tau\} \end{cases} \quad (4.3)$$

This speed-reference sample is used to imitate the speed up and break modes of the vehicle travelling at self-adjusted acceleration and deceleration. In this way, some typical parking regimes are provided. Such load-reference samples are common for acceleration and deceleration at constant  $\frac{d\varpi}{td}$ .

A meander reference sample (Figure 4.2.c) corresponds to some specific parking regimes, where the drive requires fast reverse; it is simulated by the permanent signal  $k$  within the time slot  $t_1 < \tau$ . Meander load-reference sample is typical of some variable speed driving modes. Within the remaining part of the period the set-point changes its sign:

$$\begin{cases} y^* = k, & t \in \{0; t_1\} \\ y^* = -k, & t \in \{t_1; \tau\} \end{cases} \quad (4.4)$$

In the triangle reference sample (Figure 4.2.d), the set-point temporary rises within the first quarter of the period. Next, it drops until the last quarter of the period. Finally, it rises again:

$$\begin{cases} y^* = kt, & t \in \left\{0; \frac{\tau}{4}\right\} \\ y^* = y_{\frac{\tau}{4}}^* - k\left(t - \frac{\tau}{4}\right), & t \in \left\{\frac{\tau}{4}; \frac{3\tau}{4}\right\} \\ y^* = -y_{\frac{\tau}{4}}^* + k\left(t - \frac{3\tau}{4}\right), & t \in \left\{\frac{3\tau}{4}; \tau\right\} \end{cases} \quad (4.5)$$

This speed-reference sample simulates different driving modes: uphill and downhill vehicle operation; overtaking; or even city cruising between the traffic lights. This load-reference sample imitates the vehicle load during overtaking, with changeable  $\frac{d\varpi}{td}$ .

A trapezoidal reference cycle (Figure 4.2.e) is a composition of the triangle and meander reference cycles:

$$\begin{cases} y^* = kt, t \in \{0; t_1\} \\ y^* = y_{t_1}^*, t \in \{t_1; t_2\} \\ y^* = y_{t_1}^* - k(t_3 - t_2), t \in \{t_2; t_3\} \\ y^* = -y_{t_3}^*, t \in \{t_3; t_4\} \\ y^* = -y_{t_3}^* + k(\tau - t_4), t \in \{t_4; \tau\} \end{cases} \quad (4.6)$$

This speed-reference sample imitates the most conventional city cruising, particularly between the traffic lights.

A sinusoidal reference cycle (Figure 4.2.e) of an amplitude  $k_1$  changes relatively the constant level  $k$  at the required frequency  $\omega=2\pi/\tau$  as follows:

$$y^* = k + k_1 \sin(\omega t), t \in \{0; \tau\}. \quad (4.7)$$

Using this signal, accurate travelling up the gradient and taking a turn can be effectively simulated from the speed-reference and load-reference tests.

### ***Test samples programming with ABB adaptive programming***

To implement the laws (4.2)–(4.7), the ABB adaptive programming methodology and the ABB DriveAP toolkit were used [93]–[95].

Conventionally, users can control the drive operation using different parameters. Each parameter has a fixed set of choices or a setting range. Parameterization provides enough fuzzy control, but the number of choices is limited, thus restricting user’s control possibilities. ABB adaptive programming enlarges the control range without an application of any special programming language. This is a suitable build-in instrument to complete programs from the function blocks, the number of blocks is limited by 15.

A user builds the program linking the function blocks called Block Parameter Sets. These blocks are also used to read values from the drive application programs and to transfer data to the drive application programs. Each function block includes five parameters: function block type, three inputs and output. Figure 4.3 shows an example of the adaptive program. For programming the rectangle pulse sample (as shown in Figure 4.2.a) three Block Parameter Sets are required: two timers and one that sets the absolute value of the output signal. Input/output signal is connected to each block by giving the address of the opposite signal.

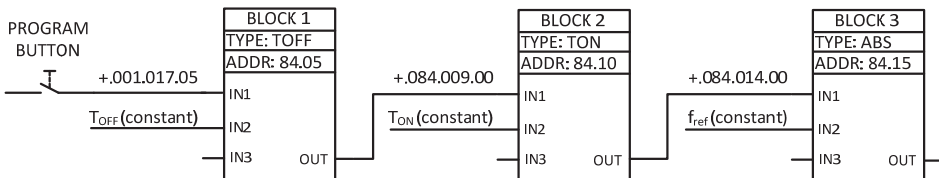


Figure 4.3. Adaptive program of a rectangle pulse

All five testing samples were programmed by using adaptive programming in the same way as in the example with rectangle pulse above. Moreover, more complicated programs, like driving cycle ECE-R15, could be created by using this methodology. All the programs described created with the ABB DriveAP toolkit are provided in Appendix 1.

### **Resume**

Analysis of the vehicle testing cycles shows that they are unsuitable for propulsion drive tuning, which is confirmed by the verification on the test bench. Different driving conditions should also be taken into account.

An effective methodology for research, assessment and tuning of the BEV propulsion drives was proposed to explore the drive responses under changeable control and disturbance signals. Toolbox library of six testing samples describes almost all driving conditions of the vehicle and could be applied for propulsion system tuning.

Testing samples library is implemented by using the ABB adaptive programming methodology and the ABB DriveAP toolkit.

### **4.3 Tuning of propulsion motor drive**

To tune the electrical propulsion motor drive, the parameters of the speed control regulator are chosen to ensure stability of the prescribed motor speed and independence of the load. A block diagram of the propulsion motor drive system is presented in Figure 4.4. The power converter is described by the transfer function  $W_C(s)$ , motor  $W_M(s)$ , feedback speed sensor  $W_F(s)$ , and the speed regulator  $W_R(s)$ . Speed set-point  $\omega^*$ , actual speed  $\omega$  and control signal  $\delta$  represent signal processing.

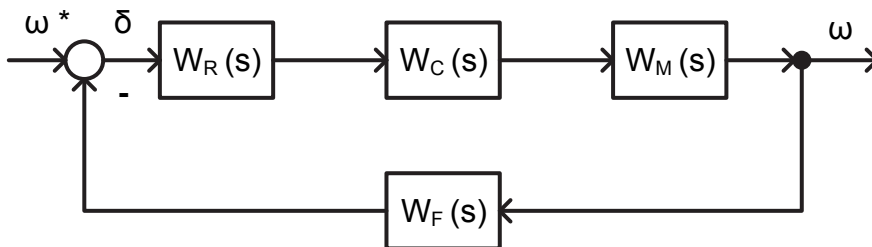


*Figure 4.4. Block diagram of propulsion motor drive system*

The PI-regulator was chosen for speed regulation, while vehicle transient processes are long-term processes and differential gain is not reasonable in that case. For the speed regulator tuning, the propulsion motor drive response to disturbance is taken. The model of the propulsion motor drive system described in section 3.2 is running at constant speed 1000 rpm and constant load that corresponds to 15.2 Nm, after 3 s running, the load increases by 50% up to the value 22.7 Nm.

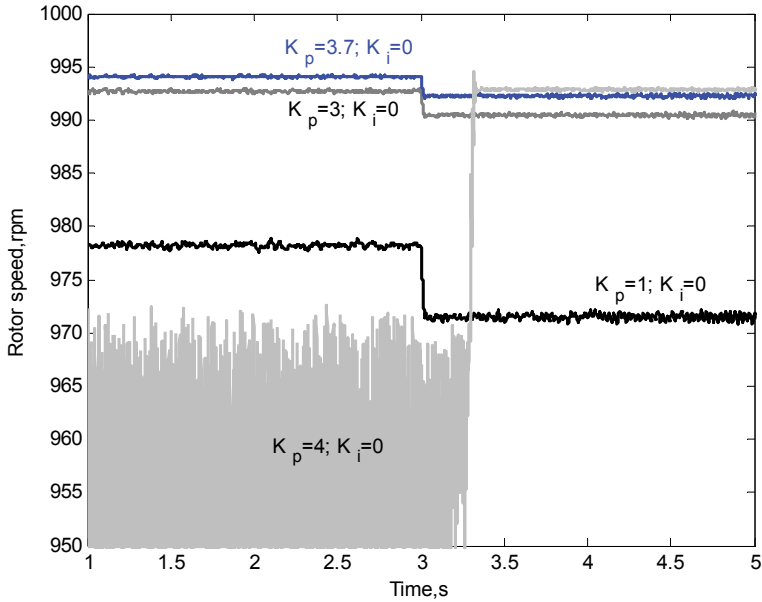


Figure 4.5. System speed responses at variations of the proportional coefficient  $K_p$

Figure 4.5 shows the speed responses of the propulsion motor drive system model at variations of the proportional coefficient  $K_p$ . As can be seen, the best performance is at the proportional coefficient equal to 3.7, after which the system becomes unstable.

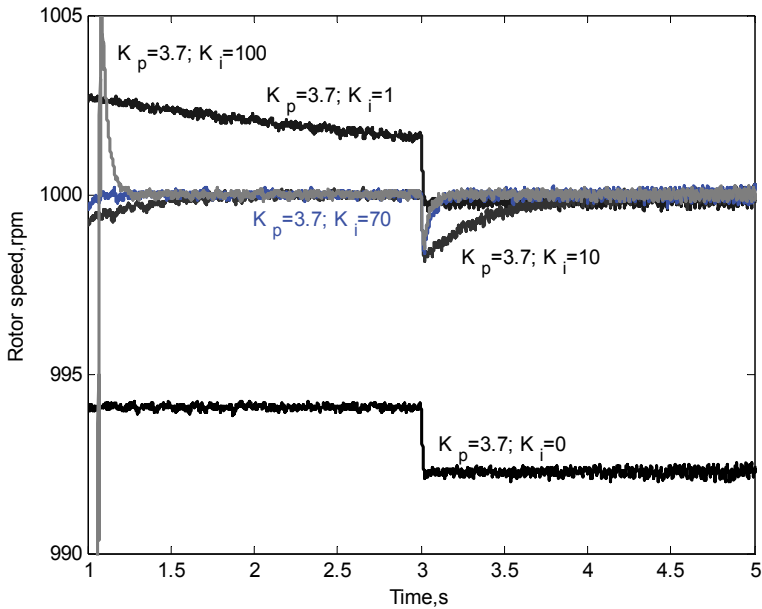


Figure 4.6 System speed responses at variations of proportional coefficient  $K_i$

Figure 4.6 shows the system speed responses at variations of the integral coefficient  $K_i$ . As can be seen, the best performance is at the integral coefficient equal to 70, below that value the transient process of speed sedation is too long and the value system becomes unstable. After speed regulator tuning, the minimum motor speed is 998.4 rpm, which means that the maximum speed error is 1.6 rpm, the transient speed settling time is 0.12 s and there is no static speed error presented.

After the tuning of the propulsion motor drive system, chosen regulator settings could be tested on a MATLAB model (Section 3.2) and the experimental test bench (Section 3.3).

#### **4.4 Study of the Propulsion Drive Regarding Speed Reference**

This section describes the application of the sample library (section 4.2) to the test bench (section 3.3). All the tests were conducted in both the sensorless closed-loop (DTC) and the open-loop (SCALAR) control mode of testing.

The trials were initially performed in the closed-loop system under the proportional gain equal to 3.7 and the integral gain equal to 70 without the derivative gain. The 25 ms time constant of the speed active filter was assigned. Then, the drive was tested at the SCALAR control mode with compensated slip (speed correction under testing load was made manually).

The first part of the tests were made at an initial speed around 1000 rpm, according to the scaling factor (Figure 3.5), the load of the loading drive was chosen equal to 15.7 Nm. The second part of tests were made at around the initial speed of zero, according to the scaling factor (Figure 3.5), the load of the loading drive was chosen equal to 5.8 Nm.

For each test sample, a specific driving mode was adopted that describes the similar speed response. A time interval chosen for test samples is short for some real driving modes, but in terms of the tuning of the propulsion motor drive it is important to have the same time intervals, to compare different tests. The test samples presented in Figure 4.2 could be adapted to some typical driving modes behavior of the vehicle. Driving modes are presented below.

##### ***Aggressive driving***

The way of the driving in which the driver deliberately behaves in such a way as to increase the risk of a road accident. This driving regime is followed by frequent and quick speed change around some driving speed that starts from some initial driving speed. Laws (4.3) and (4.4) pulse and meander test samples applied under some base speed imitate aggressive driving regimes.

##### ***Overtaking***

Under overtaking driving regime the driving speed is usually increased, for overcoming onward vehicle or hindrance. Manoeuvre starts from initial driving speed and the after end of manoeuvre the speed is returned back to the driving speed. Laws (4.5) and (4.6) triangle and trapeze test samples applied under some base speed imitate overtaking regimes.

### ***Taking a turn***

During the accurate turning the speed of the vehicle bands and its shape can be described as a polynomial of the third degree [96]. The regime imitating it could be simplified to sinusoidal waveform. Law (4.7) sinus test sample applied under some base speed imitates the turning regime.

### ***Parking regimes***

During parking the vehicle accelerates very fast to some value of speed and similarly breaks fast to zero, this speed value should not be very high in order to provide better control of the vehicle. Very frequently direction change is typical for parking, front and back movement. Parking load of the vehicle is the reactive load, it means that resistance forces are always opposite to the traction effort, and do not depend on the direction. In summary, the parking regime could be imitated by accelerating the propulsion motor drive to small speed with respect to the reactive load in one direction (forward) and the same acceleration (backward) with an opposite load, but the loads would be the same in both movements, as well as speeds. According to law (4.3) pulse test sample applied to zero speed imitates a typical parking regime.

### ***City cruising***

Regular city cruising between traffic lights is represented by triangle and trapeze speed-reference signals. Vehicle is usually accelerating up to permitted speed after the traffic light, cruising with constant speed and decelerating on the next traffic light. In case the distance between traffic lights is too short, there is no constant speed cruising presented. In city cruising mode it is important to understand that a vehicle needs to accelerate from the standing position and brakes to full stop.

Laws from (4.4) to (4.7) meander, triangle, trapeze and sinusoidal test samples applied above zero speed imitate city cruising regimes.

Similarly to the parking mode, typical city cruising load in the reactive load does not depend on the direction. In that case the test samples could be simplified to the half-cycle test sample, in order to provide a wider picture for the propulsion motor drive tuning the test samples wave under the zero speed.

### ***Resume***

The tests made could be divided into two groups: those made around the initial speed and other ones above zero. Therefore, in the tuning procedure of the speed response on the testing samples tuning around the initial speed and tuning above zero could be distinguished.

Visual results of tuning are presented in the figures in Appendix 3. As it can be seen from the traces, a closed-loop system (DTC) is properly tuned for the speed reference response. An open-loop system has a static error and transient processes are smoothed because of the inertia of the system. All the testing cycles were properly executed. As a result, good controllability of the propulsion drive of the BEV could be achieved by proper tuning.

Table 4.2. Study of the Propulsion Drive Regarding Speed Reference

		Test bench			MATLAB/Simulink model		
		SCALAR			SCALAR		
		Max, %	Static, %	Transient time, s	Max, %	Static, %	Transient time, s
Speed reference at 0 rpm	Pulse	-	19.81	1.30	-	-	-
	Meander	-	-	-	-	-	-
	Triangle	-	12.98	0.00	-	-	-
	Trapeze	-	9.70	0.00	-	-	-
	Sinusoidal	-	14.12	0.00	-	-	-
		DTC			DTC		
		Max, %	Static, %	Transient time, s	Max, %	Static, %	Transient time, s
	Pulse	6.41	0.00	0.80	0.70	0.00	0.09
	Meander	-	-	-	-	-	-
	Triangle	18.81	0.00	0.00	0.00	0.00	0.00
	Trapeze	14.41	0.00	0.00	0.64	0.00	0.05
Sinusoidal	14.94	0.00	0.00	0.00	0.00	0.00	
Speed reference at 1000 rpm		Test bench			MATLAB/Simulink model		
		SCALAR			SCALAR		
		Max, %	Static, %	Transient time, s	Max, %	Static, %	Transient time, s
	Pulse	-	2.19	0.60	-	1.94	0.18
	Meander	-	1.67	0.50	-	1.52	0.25
	Triangle	-	2.11	0.00	-	2.19	0.00
	Trapeze	-	2.17	0.00	-	1.52	0.25
	Sinusoidal	-	2.09	0.00	-	1.85	0.00
		DTC			DTC		
		Max, %	Static, %	Transient time, s	Max, %	Static, %	Transient time, s
	Pulse	3.02	0.00	0.50	0.51	0.00	0.80
Meander	2.07	0.00	0.40	0.17	0.00	0.20	
Triangle	0.00	0.00	0.00	0.00	0.00	0.00	
Trapeze	0.72	0.00	0.10	0.04	0.00	0.00	
Sinusoidal	0.00	0.00	0.00	0.00	0.00	0.00	

Table 4.2 compares the results of the response analysis. Speed error max shows the maximal difference in percentage between the speed reference and the real speed response. Static speed error demonstrates the average difference in percentage between the speed reference and the real speed response values after the transient period. Transient time shows the transient process time in seconds (s).

As can be seen from the result errors, the propulsion motor drive shows better performance under the DTC control mode. Under the SCALAR control mode, a static error exists, the IM slip should be taken into account. Certainly no overlap is present during the SCALAR control mode, but transient processes take long. At lower speeds the motor drive in the DTC control mode has a higher error than in the operation closer to the rated speed. Under the SCALAR control mode, the drive could not operate properly, the tests observed from the test bench were limited by current (as a consequence by the torque). Results observed from MATLAB/Simulink simulation have no current limit, therefore torque value is extremely high (see Appendix 3).

Analysis of the speed responses under the desired test cycles shows that in the majority of typical driving situations, closed-loop control is preferable. At proper tuning, minimal steady-state errors occur, thus providing better controllability, faster rate of the system response, broader speed range, and higher speed regulation.

#### **4.5 Study of the Propulsion Drive Regarding Load**

As pointed out in section 3.1, the propulsion motor load changes with velocity, acceleration and road conditions (road angle and tire-to-road friction). All loads could be simplified and reduced to the testing samples developed and described in section 4.2. The section analyses the use of test samples as load reference to the testing drive rotated at constant speed (cruising mode of BEV) under open-loop and closed-loop control modes.

##### ***Constant acceleration and deceleration loads***

According to (3.7), acceleration force will be constant during direct change of the driving speed ( $\frac{dv}{td} = const$ ), as well as at dynamic torque (4.1) with

constant angular acceleration ( $\frac{d\varpi}{td} = const$ ), which means that the motor load under that load could be described by law (4.3) pulse test sample. With respect to the direction of the force pulse, the test sample could be applied as positive or negative disturbance.

##### ***Passing wet or icy surfaces***

During crossing the interferences on the road, like puddles or areas partially covered with ice or sand, the load could suddenly be changed for a short time.

Table 4.3. Study of the Propulsion Drive Regarding Load Reference

		Test bench			MATLAB/Simulink model		
		SCALAR			SCALAR		
		Max, %	Static, %	Transient time, s	Max, %	Static, %	Transient time, s
Load reference at 100 rpm	Pulse	-	-	-	-	-	-
	Meander	-	-	-	-	-	-
	Triangle	-	-	-	-	-	-
	Trapeze	-	-	-	-	-	-
	Sinusoidal	-	-	-	-	-	-
		DTC			DTC		
		Max, %	Static, %	Transient time, s	Max, %	Static, %	Transient time, s
	Pulse	10.49	-0.15	-	0.93	0.00	0.09
	Meander	15.90	-1.02	-	1.09	0.00	0.13
	Triangle	7.88	0.24	-	0.20	0.00	0.00
	Trapeze	9.93	-0.47	-	0.20	0.00	0.00
Sinusoidal	9.55	0.56	-	0.25	0.00	0.00	
Load reference at 1000 rpm		Test bench			MATLAB/Simulink model		
		SCALAR			SCALAR		
		Max, %	Static, %	Transient time, s	Max, %	Static, %	Transient time, s
	Pulse	-	1.42	0.90	-	1.25	0.26
	Meander	-	1.03	0.90	-	1.25	0.35
	Triangle	-	1.21	-	-	1.25	0.00
	Trapeze	-	1.20	-	-	1.25	0.00
	Sinusoidal	-	1.19	-	-	1.26	0.00
		DTC			DTC		
		Max, %	Static, %	Transient time, s	Max, %	Static, %	Transient time, s
	Pulse	0.81	0.02	0.60	0.10	0.00	0.90
Meander	1.06	0.01	0.70	0.20	0.00	0.90	
Triangle	0.53	0.01	0.00	0.03	0.00	0.00	
Trapeze	1.13	0.01	0.00	0.03	0.00	0.00	
Sinusoidal	0.57	0.02	0.00	0.03	0.00	0.00	

Some of such load influence could be described by law (4.4) meander test sample.

### ***Overtaking***

Under overtaking, the loads on the propulsion motor drive are very similar to the speed reference signal. According to (3.7), acceleration force will be variable during direct change of the driving speed ( $\frac{dv}{td} = \text{var}$ ), as well as at dynamic torque (4.1) with constant angular acceleration ( $\frac{d\varpi}{td} = \text{var}$ ), which means that laws (4.5) and (4.6) applied to triangle and trapeze test samples could also imitate overtaking loads.

### ***Turning loads***

During the accurate turning, the load changes similarly to the speed, thus law (4.7) sinus test sample imitates also the load under turning.

### ***Resume***

Table 4.3 and figures in Appendix 3 show the results of the drive speed responses at different loads in the reference testing sample cycles under DTC and SCALAR control modes. As shown by the traces, open-loop system has some delay and it makes the speed response at different loads smoother, while the closed-ended system has some speed spikes. Table 4.3 shows the same parameters of the testing drive as in Table 4.2. As the analyses reveal, under variable load mode, closed-loop control mode (DTC) shows better performance.

The values of the speed response in the open-loop system under low speed could not be taken into account, for the reason similar to that in speed reference tests, i.e. the system is overloaded.

## **4.6 Dynamic load for electric motor drive testing on the test bench**

From equation (3.8) it can be seen that in the tractive effort, resistance components on rolling (3.3) and climbing (3.6) do not depend on the speed, but rather on the aerodynamic drag (3.5) together with the acceleration force (3.7) varieties under speed changing. It means that together with speed reference, the load should be changed as well. Dynamic load tests could provide more realistic load of the propulsion motor drive. The dynamic load relation to the speed reference could be described as follows:

$$F_{TE}(v) = C^*_1 \cdot v^2 + C^*_2 + C^*_3 \cdot a, \quad (4.8)$$

where,  $C^*_1$ ,  $C^*_2$  and  $C^*_3$  are dynamic load coefficients related to the linear vehicle speed,  $v$  is the vehicle linear speed and  $a$  is the vehicle acceleration.

Dynamic load coefficients could be found as:

$$C^*_1 = \frac{F_{AD}}{v^2} = \frac{1}{2} C_d \rho A, \quad (4.9)$$

$$C^*_2 = F_{RR} + F_{CR} \text{ and} \quad (4.10)$$

$$C^*_3 = m. \quad (4.11)$$

According to equations (3.12) and (3.13), the dynamic load coefficients should be reduced to the traction motor shaft:

$$T_{motor}(n_{motor}) = C_1 \cdot n_{motor}^2 + C_2 + C_3 \cdot \frac{dn_{motor}}{dt}, \quad (4.12)$$

where  $C_1$ ,  $C_2$  and  $C_3$  are dynamic load coefficients related to the traction motor shaft,  $n$  is the rotation frequency and  $\frac{dn_{motor}}{dt}$  is the angular acceleration

( $\frac{dn_{motor}}{dt} = r \cdot a$ , with the wheel radius  $r$ ). According to the previous equations, dynamic load coefficients could be found as:

$$C_1 = C^*_1 \cdot \left(\frac{2\pi}{60}\right)^2 \cdot \left(\frac{1}{GR_{TRANS}} \cdot \frac{1}{GR_{DIFF}}\right)^3, \quad (4.13)$$

$$C_2 = C^*_2 \cdot \frac{1}{GR_{TRANS}} \cdot \frac{1}{GR_{DIFF}} \text{ and} \quad (4.14)$$

$$C_3 = J_{eq} \cdot \frac{1}{GR_{TRANS}} \cdot \frac{1}{GR_{DIFF}}. \quad (4.15)$$

$J_{eq}$  is the equivalent inertia moment of the system reduced to the propulsion motor shaft that could be found from the following:

$$J_{eq} \cdot \omega_{motor}^2 = W_{k,vehicle} + W_{k,trans} + W_{k,motor}, \quad (4.16)$$

where  $\omega_{motor}$  is the angular speed,  $W_k$  is the respective kinetic energy stored in the moving vehicle ( $W_{k,vehicle}$ ), vehicle's transmission ( $W_{k,trans}$ ) and motor ( $W_{k,motor}$ ). The kinetic energy stored in the moving vehicle ( $W_{k,vehicle}$ ) could be found as:

$$W_{k,vehicle} = \frac{m \cdot v_{vehicle}^2}{2}. \quad (4.17)$$

To account for the rotational kinetic energy, the total kinetic energy is assumed 1.05 times the linear kinetic energy (for Tesla Roadster) [72]. The inertia moment of the motor ( $J_{motor}$ ) is given in the data sheet and the kinetic energy could be found as follows:

$$W_{k,motor} = \frac{J_{motor} \cdot \omega_{motor}^2}{2} . \quad (4.18)$$

The linear movement ( $v_{vehicle}$ ) speed could be recalculated to the motor's angular speed ( $\omega_{motor}$ ):

$$v_{vehicle} = r \cdot \omega_{motor} . \quad (4.19)$$

From (4.16)-(4.19) it follows:

$$J_{eq} = 1.05 \cdot m \cdot r^2 \cdot \left( \frac{1}{3.6^2} \right) . \quad (4.20)$$

According to data from Table 3.1, dynamic load coefficients for the imitation of Tesla Roadster road load related to the traction motor shaft are  $C_1 = 1.171 \cdot 10^{-6}$ ;  $C_2 = 5.785$ ;  $C_3 = 0.447$ .

Obtained coefficients were applied to the MATLAB/Simulink model (Section 3.2) and the test bench (Section 3.3). MATLAB/Simulink model of the dynamic load presents a speed feedback that has an effect on the input torque. The MATLAB/Simulink subsystem for the dynamic load simulation is presented in Figure 4.7. The figure shows the calculation of the dynamic load torque reference by using the input speed signal and the coefficients (4.13)-(4.14).

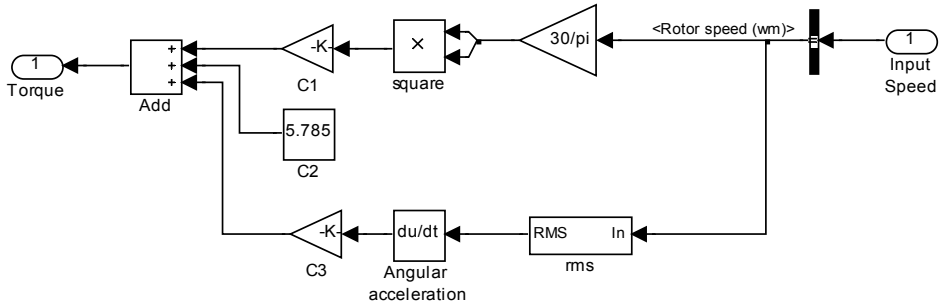


Figure 4.7. MATLAB/Simulink subsystem for dynamic load realisation

While the experimental test bench has two frequency converters that contain a build-in controller for programming speed and torque reference signals (Section 3.3), an adaptive program for the dynamic load was created. The adaptive program is provided in Appendix 2. The ABB ACS frequency converter allows measurements of drive speed and acceleration, whereas these two signals could be used as input signals for the adaptive program. The output signal of the adaptive program is an input reference torque signal for the loading drive.

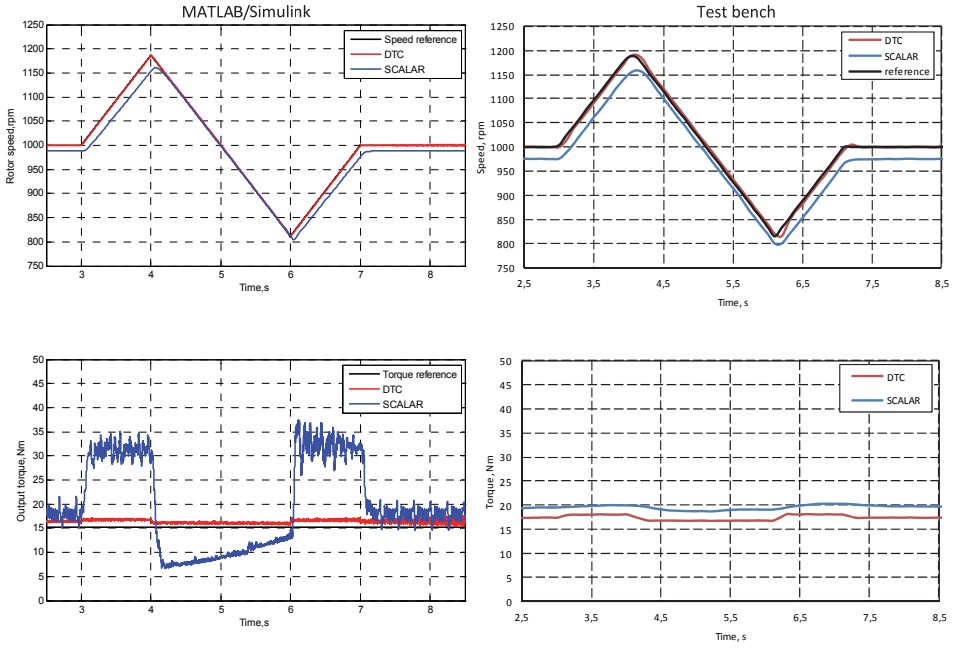


Figure 4.8. Torque response on the speed triangle reference under different control modes

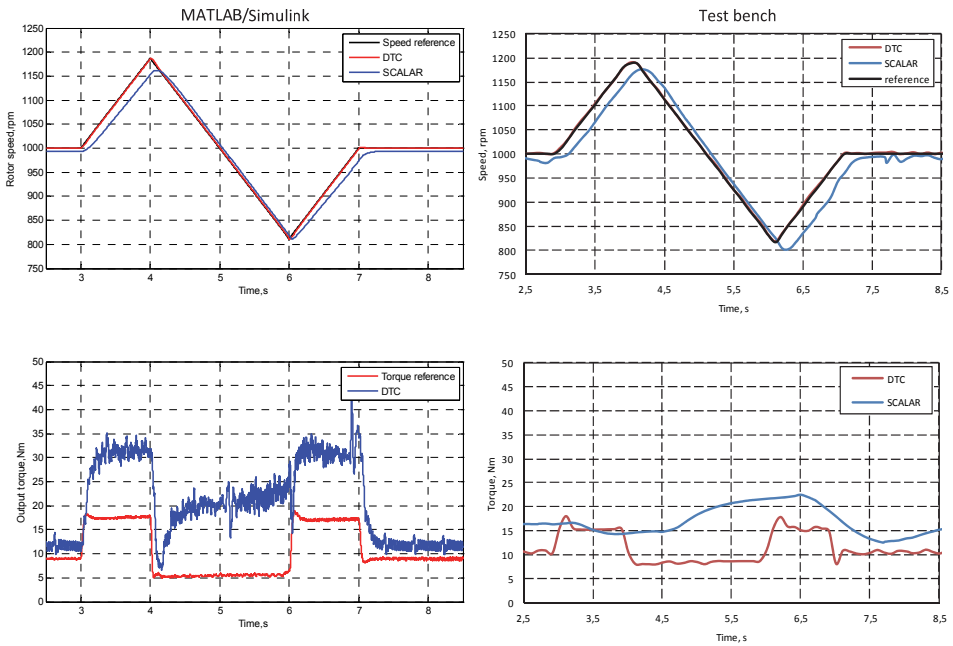


Figure 4.9. Torque response (dynamic load) on the speed triangle reference under different control modes

Speed and torque traces presented in Figure 4.8 show the torque response of the MATLAB/Simulink model and the test bench experiments under the testing sample of the speed triangle reference applied on 1000 rpm. Figure 4.9 shows the same speed reference testing sample applied with a dynamic load. As can be seen from the traces, the experimental motor drive load under the dynamic load is higher under acceleration and lower under deceleration, which means that it depends on the reference speed that is very similar to a real vehicle road load.

Results from the MATLAB/Simulink model and the test bench for different testing samples are presented in Appendix 3.

### ***Resume***

A dynamic load close to reality is proposed in this section. The methodology for coefficient determination is presented and verified with the MATLAB/Simulink model and the test bench. Simulation and experimental results show that additional forces occurring during the acceleration and deceleration of the vehicle are taken into account while the results observed are more realistic.

## **4.7 Summary of Chapter 4**

The testing cycles existing were studied and compared. Studies show that the testing cycles of today's vehicles could be used for estimating energy consumption rather than for tuning of the propulsion motor drive.

An effective methodology for research, assessment and tuning of the BEV drives was proposed to explore the drive responses under changeable control and disturbance signals. Using the laboratory test bench, multiple conventional modes of the vehicle motion were studied.

Analysis of test results shows that the closed-loop control system (DTC) is preferable for speed variable working modes. It shows a smaller speed response error and better energy performance. Under changeable load conditions, the open-loop control system (SCALAR) could be recommended. Speed response is more accurate and energy consumption is lower under the SCALAR control mode of the propulsion motor drive.

The developed methodology can be recommended to adjust the electric drives for different kinds of testing equipment, including the synchronous, induction, and direct current machines. Experimental validation of the approach described has demonstrated broad possibilities for the steady-state and transient modes of vehicle quality evaluation. It suits for recommendations to be made with regard to the tuning of the drive regulators, control looping, sensor allocation, and feedback arrangements.

## 5 FUTURE WORK. EXTENDED APPLICATION OF THE BEV PROPULSION DRIVE SYSTEM

### 5.1 STATCOM as a Part of BEV Propulsion Drive System

Today's BEV charging devices are unidirectional, which means that they allow the power flow from the grid to the vehicle battery. Many research institutions are making efforts to apply bidirectional charging devices with the battery to the grid power flow [97]–[100]. Some solutions have an additional battery, or some another energy source included directly in the charging stations [101]–[103]. An additional energy storage extends the features of charging systems, for example, a battery energy storage system included in the charging system has the following features: modularity, environmentally benign, high efficiency and quick response [104].

Using specific control algorithms, manufacturers of the charging devices are trying to keep the power factor during the charging as high as possible [105], but some of the test results show that during different charging modes the power factor could vary. Timing diagram in Figure 5.1 shows that the power factor varies during fast and medium charging modes of Nissan Leaf and using the fast DC charging station ABB Terra SC 4EPY410036R1. The charging test was made in the TUT Laboratory of Electric Drives.

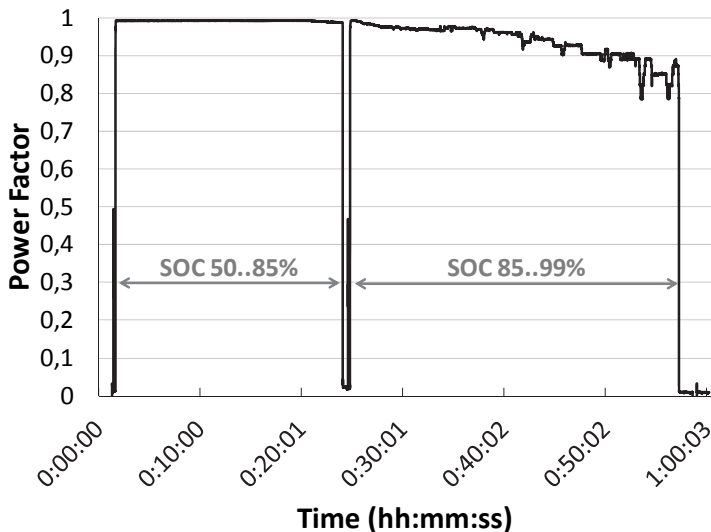


Figure 5.1. Power factor varies during different charging modes of Nissan Leaf

During fast charging (state of charge (SOC) from 50 to 85%), time slice 0 to 25 min, charging current was on the level of 29 A and the power factor almost 1. But under medium charging (SOC from 85 to 99%), time slice 25 min

to 1 h, charging current was decreasing to zero and the power factor was already less than 1. An active power was in the range of 20 kW during fast charging, decreasing to zero during medium charging. The value of reactive power flow during the whole charging (fast and medium) was 2.3-2.5 kvar.

The BEV connected to the grid during charging consumes not only active power from the grid but also reactive power that affects the quality of grids power. As the experimental results show, some power factor correction is required during the charging mode of the BEV. In case several vehicles are connected, the effect on the grid could be even worse. If there are several BEV connected to the grid at the same time, they have different SOCs, which means that they could be used in different modes. In that case, one of the BEV connected to the grid can analyse the power quality of the grid, by measuring the grid's parameters and could provide power factor correction, if required.

The concept of using part of the propulsion system as STATCOM was presented in [PAPER-IV], [PAPER-VI] and [PAPER-VII]. A STATCOM is a flexible AC transmission system controller based on a self-commutated solid-state VSI that is used to provide reactive power/voltage control and transient stability enhancement.

A possible solution is presented in Figure 5.2. One side of the winding of the traction motor ( $u1-v1-w1$ ) is connected to the voltage source inverter VSI. A VSI is connected to the battery storage system BAT via the filtering capacitor C and the buck-boost converter. The other side of the stator winding ( $u2-v2-w2$ ) is connected to two contactors. The first contactor KM1 is required to provide Y connection for the stator winding of the traction motor, when the BEV operates in the traction mode. Another contactor KM2 is required to connect the vehicle to the grid, when it operates in the plug-in mode. In that case the stator winding of the traction motor is used as a coupling reactor of STATCOM.

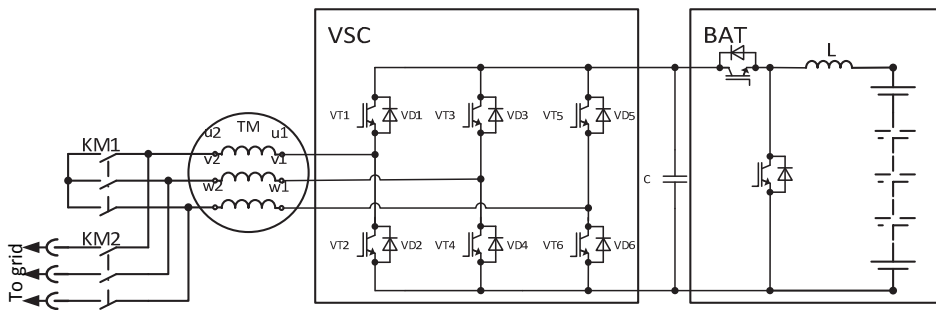


Figure 5.2. Possible STATCOM implementation

### Resume

Analysis of vehicle charging shows that during the charging the power factor is decreasing while the SOC reaches its maximum value. It means that reactive currents reach the grid from the side of the charging system. To achieve better

performance of the grid, the reactive power (and the power factor as its indicator) need to be compensated.

In the solution suggested in this section part of the propulsion motor drive of the plugged-in BEV was used as a STATCOM device. As a result, some benefits and new features could be introduced.

## 5.2 PSIM Model of Topology

### *STATCOM Topology*

STATCOM has many interesting features, such as high speed of response (sub-cycle), versatile controlling and operational characteristics, ability to implement controllers of low/medium/high MVA ratings, low-space requirement, higher stability margins [106].

STATCOM is based on the principle that a self-commutating inverter can be connected between three-phase AC power lines and controlled to draw mainly reactive current from the transmission lines. The current can be controlled to be either capacitive or inductive and is almost unaffected by the line voltage [107]. There are some different circuit configuration designs for STATCOM, but they generally have the same application principles. The STATCOM is based on a solid-state VSI, implemented with an inverter and connected in a shunt with the power system through a coupling reactor [PAPER-VI]. The series reactor is connected in order to provide harmonic minimization and depending on the power of the device can be the heaviest part of the STATCOM. With the battery to DC link capacitor connection the STATCOM acquires an ability for active and reactive powers compensation. STATCOM provides much better performance of reactive compensation over the conventional Static var Compensator (SVC). With STATCOM, a number of valuable benefits can be attained in power systems, such as [107], [108]:

- interface with a real power source;
- higher response to system changes;
- dynamic voltage control, increased power transmission capability, and stability of long power corridors;
- facilitating connection of renewable generation by maintaining grid stability, fulfilling grid codes, and facilitating the building of high speed rail;
- maintaining power quality in grids dominated by heavy industrial loads such as steel plants and large mining complexes;
- enabling the implementation of Smart Grids.

The operation modes of STATCOM are presented in Figure 5.3. As shown in Figure 5.3.a, the voltage magnitude of STATCOM  $U_{\text{STATCOM}}$  is equal to the magnitude  $U_{\text{grid}}$  of the grid voltage and the device operates in no-load operation mode. STATCOM operates in a capacitive operation mode (Figure 5.3.b) when the voltage magnitude  $U_{\text{STATCOM}}$  is higher  $U_{\text{grid}}$  and the current through the coupling reactor  $I_{\text{xl}}$  becomes leading. If the current  $I_{\text{xl}}$  lags, the  $U_{\text{grid}}$  is higher than the  $U_{\text{STATCOM}}$ , and the device would operate opposite to the previous mode

as a reactor with controllable inductive reactance. In that case, the STATCOM operates in an inductive operation mode (Figure 5.3.c).

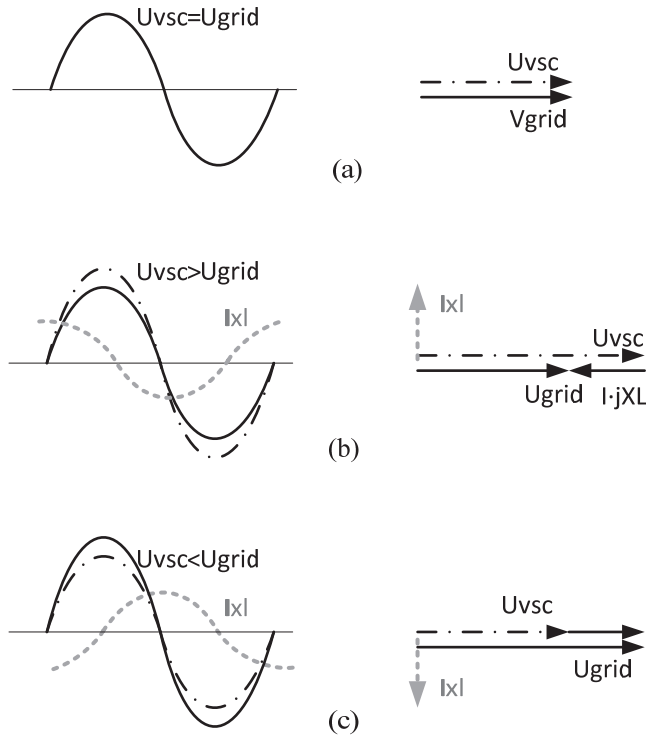


Figure 5.3. Operation modes of STATCOM

Mathematically the active power  $P$  of the STATCOM can be predicted by equation (5.1) and the reactive power  $Q$  according to (5.2):

$$P = \frac{U_{STATCOM} \cdot U_{grid}}{X_L} \sin \gamma, \quad (5.1)$$

$$Q = \frac{U_{STATCOM} \cdot U_{grid}}{X_L} \cos \gamma - \frac{U_{grid}^2}{X_L}, \quad (5.2)$$

where  $X_L$  is the reactance of the coupling reactor;  $\gamma$  is the phase difference between the voltages. As can be seen from equations (5.1) and (5.2), changing the voltage magnitude with a voltage source converter allows using STATCOM in different operation modes.

#### ***PSIM model of STATCOM implementation in Propulsion Drive System***

The topology was proved with simulation results using the PSIM software tools. PSIM is modern simulation software for power electronics, motor drive, and transient mode systems. Principal diagram is shown in Figure 5.4. To simplify the model, instead of a battery pack a series connected frequency

converter, the 3-phase AC source was taken as an energy source. Similarly, the 3-phase AC source and 3-phase resistance were taken as the grid model.

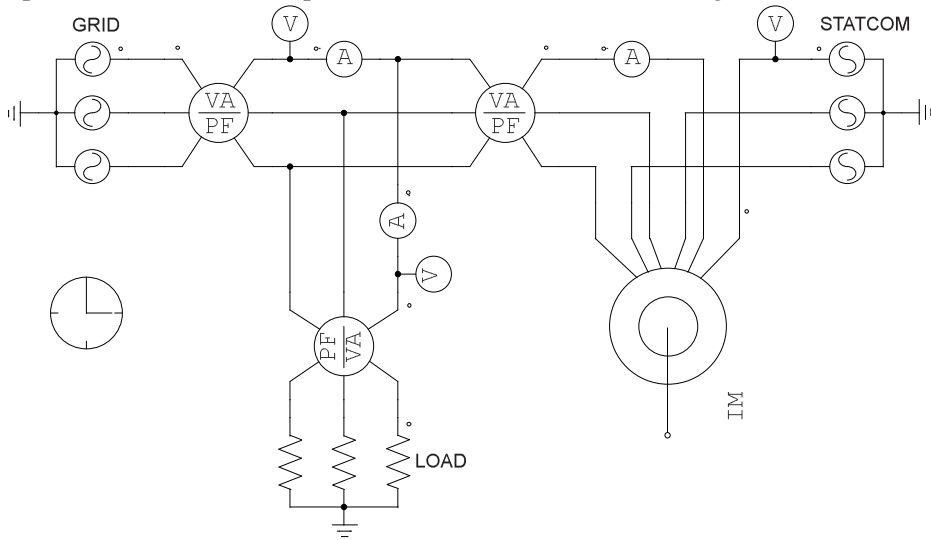


Figure 5.4. Principle diagram of the PSIM model

Results of the simulation in Figure 5.5. Figure 5.5.a show the mode where the grid voltage is equal to STATCOM output voltage, whereas no phase shift between the grid and the load currents exist. Figure 5.5.b shows the mode where the grid voltage is over STATCOM output voltage, as the traces reveal, even the reduced voltage of 20 V gives the phase shift on the grid site for  $17^\circ$ .

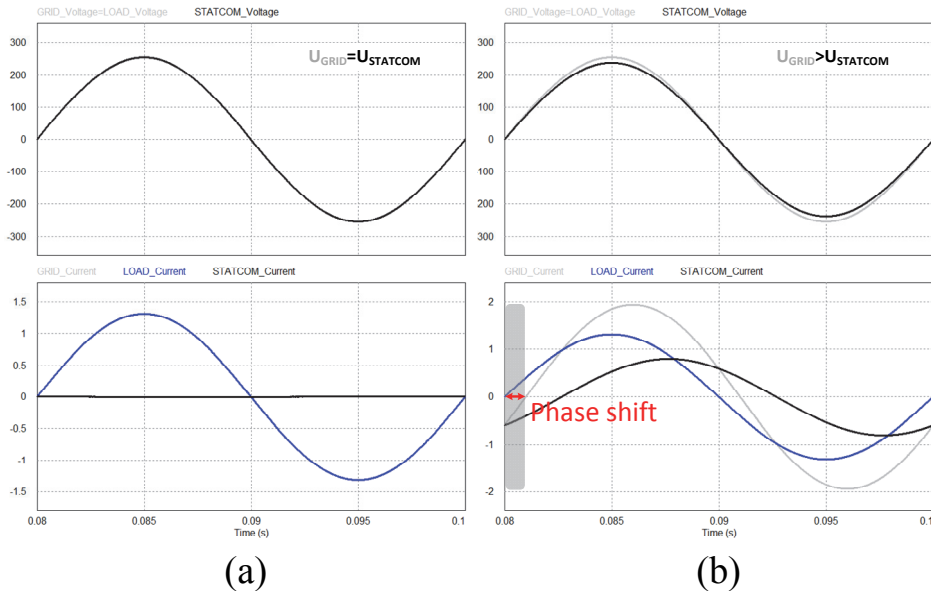


Figure 5.5. Simulation results with compensated (a) and uncompensated (b) power factor

## Resume

The principles and features of a STATCOM device were described. The topology presented provides an additional energy source connected in parallel to the existed system grid-to-load. The main benefits of the presented topology are its simplicity of connection and control.

The PSIM model of the STATCOM was created for research that assumes also confirmation of the experimental data, however, developing a model of a real motor that can be used for further research is more reasonable. Parameters of SIEMENS 3Mot 1LA7090-4AA10-Z IM were chosen as simulated IM.

The verification of the developed PSIM model of the STATCOM confirmed that the device could be used for the power factor correction by controlling the voltage of STATCOM, the phase shift between the current and the voltage of the device could be achieved.

## 5.3 Experimental Verification of Topology Application

To verify the simulation results the experimental setup of STATCOM implementation into the BEV propulsion drive system was created. The principal diagram of the experimental setup is shown in Figure 5.6.

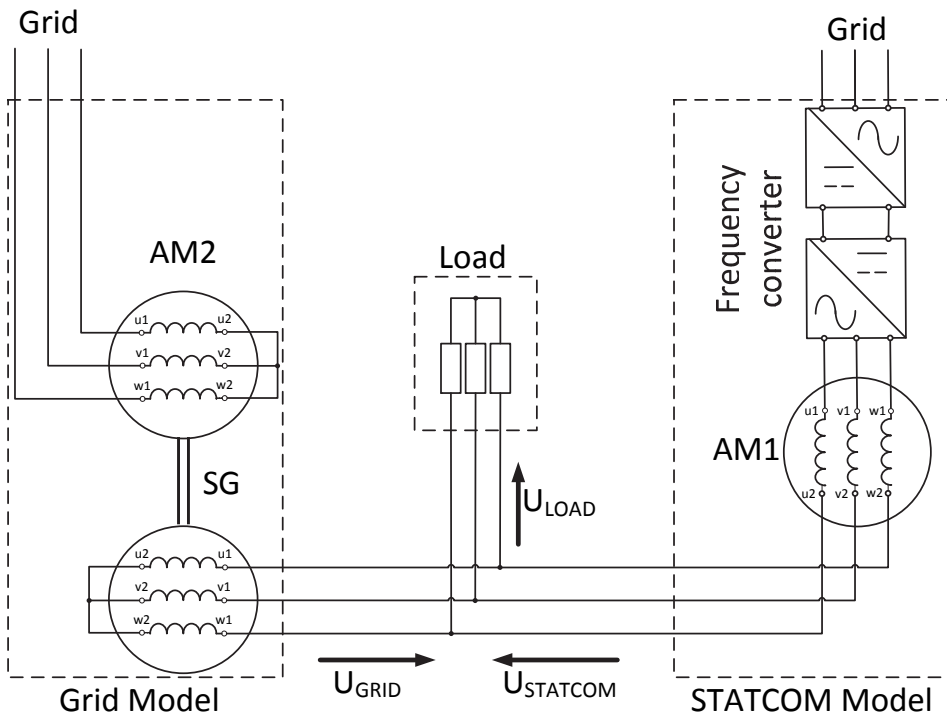


Figure 5.6. Principle diagram of the experimental setup

A 3-phase frequency converter with a stator winding of IM (AM1) connected in series was taken, in that case the DC link of the frequency

converter was used instead of the battery of the propulsion drive. A Siemens Micromaster 440 1 AC, 0.12 to 3 kW (0.16 to 4 HP) frequency converter was used. The stator windings of the IM used as series inductors separate the two voltage sources and also filter the switching ripple in the inverter current [109]. The IM SIEMENS 3Mot 1LA7090-4AA10-Z has the following parameters: the rated speed of the motor – 1415 rpm, rated voltage – 400 V, frequency – 50 Hz, current – 2.55 A, and power – 1.1 kW. Frequency converter together with IM stator windings representing a STATCOM model.

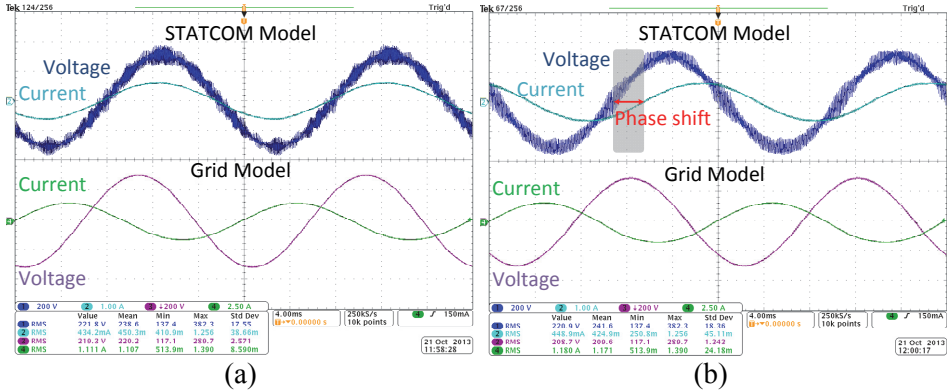


Figure 5.7. Experimental test results with compensated (a) and uncompensated (b) power factor

The 3-phase synchronous generator (SG) and 3-phase star-connected resistance were imitating the real grid and the grid load. SG with a mechanical connection to the induction motor (AM2) where used to create a torque for SG and synchronize two AC systems (grid and STATCOM). The induction motor italtec TTS Typ 033.75-401 has the following parameters: the rated speed of the motor – 1500 rpm, rated voltage – 400 V, frequency – 50 Hz, current –1.52 A, excitation voltage – 220 VDC, excitation current max 0.6 A and power – 0.81 kW/1 kVA. As AM2 and AM1 are the same, AM1 was used.

The 3-phase active load box was taken as the testing load, with the rated value of 192.8 Ω.

Both parts of the experimental setup have a possibility to control the rms value of the output voltage and could be synchronized in the common AC-link.

During the tests the frequency converter was connected to the load, then the synchronous generator was started as the motor for frequency synchronization and the excitation winding was fed to turn the machine into the generator mode with the synchronized frequency. While two equal energy sources were used, the synchronous generator was chosen as the voltage control device. As it can be seen from the experimental test results in Figure 5.7, the phase shift of one of the energy source current could be controlled with a voltage variation of the other. Depending on the load the power factor could be shifted on both sides (inductive or capacitive load modes).

### ***Resume***

The experiments of the BEV traction drive connected to the grid part were verified. Two independent energy sources were connected in parallel to the same load. Voltage control of one of the part of the them brings the current shifting to the other. The possibility of the power factor correction was proved. The results of the experimentation are in agreement with the simulation preconditions shown previously in Figure 5.5.

## **5.4 Summary of Chapter 5**

With high attention to the plug-in BEVs, their influence on the existing utility grid is a topic of current interest. The chapter presents a possibility to improve vehicle propulsion motor drive systems. A simple and quick solution for power factor control is proposed. Relevant schematic was proved theoretically, with a PSIM model and practically, with an experimental setup. Both proofs show that the voltage value control has an effect on the load's power factor. The power factor could be corrected in both directions (inductive and capacitance loads).

The scheme suggested has all the advantages of STATCOM apparatus, meaning that in addition to the power factor correction, asymmetrical load balancing, voltage control, active harmonics filtration and flicker mitigation could be performed. Economic benefits and reductions in weight can be achieved by the use of the windings of the propulsion motor instead of separate inductors. The existing BEV with IM or SM could be updated. Moreover, an on-board solution is presented, which means that no additional devices are required.

## References

- [1] C. Mi, M. A. Masrur, and D. W. Gao, *Hybrid Electric Vehicles: Principles and Applications with Practical Perspectives*, 1st ed. Publication A John Wiley & Sons, Ed. United Kingdom: A John Wiley & Sons, Ltd., 2011, p. 448.
- [2] N. A. Owen, O. R. Inderwildi, and D. A. King, "The status of conventional world oil reserves—Hype or cause for concern?," *Energy Policy*, vol. 38, no. 8, pp. 4743–4749, 2010.
- [3] F. Magnussen, "On design and analysis of synchronous permanent magnet machines for field-weakening operation in hybrid electric vehicles," *Elektrotekniska system*, 2004.
- [4] O. D. Momoh and M. O. Omoigui, "An overview of hybrid electric vehicle technology," in *2009 IEEE Vehicle Power and Propulsion Conference*, 2009, pp. 1286–1292.
- [5] M. Ehsani, Y. Gao, and A. Emadi, *Modern Electric, Hybrid Electric, and Fuel Cell Vehicles: Fundamentals, Theory, and Design, Second Edition (Power Electronics and Applications Series)*, Second Edi. CRC Press, 2009, p. 557.
- [6] J. Fenton and R. Hodkinson, *Lightweight Electric/Hybrid Vehicle Design*. Oxford, UK: Butterworth-Heinemann Linacre House, Jordan Hill, Oxford OX2 8DP 225 Wildwood Avenue, Woburn, MA 01801-2, 2001, p. 288.
- [7] L. Kullingsjö and S. Karlsson, "The possibility for energy regeneration by electrification in Swedish car driving," in *EVS27 International Battery, Hybrid and Fuel Cell Electric Vehicle Symposium*, 2013, pp. 1–7.
- [8] A. Burke, "Hybrid/Electric Vehicle Design Options and Evaluations," in *International Congress & Exposition*, 1992.
- [9] S. Grammatico, A. Balluchi, and E. Cosoli, "A series-parallel hybrid electric powertrain for industrial vehicles," in *2010 IEEE Vehicle Power and Propulsion Conference*, 2010, pp. 1–6.
- [10] B.-H. Lee, S.-I. Kim, J.-J. Lee, J.-P. Hong, and C.-S. Park, "Design of an interior permanent magnet synchronous in-wheel for electric vehicles," in *Electrical Machines and Systems (ICEMS), 2010 International Conference on*, 2010, pp. 1226–1229.
- [11] F. Caricchi, F. Crescimbeni, F. Mezzetti, and E. Santini, "Multistage axial-flux PM machine for wheel direct drive," *IEEE Trans. Ind. Appl.*, vol. 32, no. 4, pp. 882–888, 1996.
- [12] A. K. Verma, B. Singh, and D. T. Shahani, "Grid to vehicle and vehicle to grid energy transfer using single-phase bidirectional AC-DC converter and bidirectional DC-DC converter," in *2011 International Conference on Energy, Automation and Signal*, 2011, pp. 1–5.
- [13] I. Husain, *Electric and Hybrid Vehicles*. CRC PRESS Boca Raton London New York Washington, D.C, 2011, p. 523.
- [14] Y. Gao and M. Ehsani, "Systematic design of fuel cell powered hybrid vehicle drive train," in *IEMDC 2001. IEEE International Electric Machines and Drives Conference (Cat. No.01EX485)*, 2001, pp. 604–611.
- [15] E. Schaltz, A. Khaligh, and P. O. Rasmussen, "Influence of Battery/Ultracapacitor Energy-Storage Sizing on Battery Lifetime in a Fuel Cell Hybrid Electric Vehicle," *IEEE Trans. Veh. Technol.*, vol. 58, no. 8, pp. 3882–3891, Oct. 2009.
- [16] J. Bernard, S. Delprat, F. N. Buchi, and T. M. Guerra, "Fuel-Cell Hybrid Powertrain: Toward Minimization of Hydrogen Consumption," *IEEE Trans. Veh. Technol.*, vol. 58, no. 7, pp. 3168–3176, Sep. 2009.
- [17] Y. Wu and H. Gao, "Optimization of Fuel Cell and Supercapacitor for Fuel-Cell Electric Vehicles," *IEEE Trans. Veh. Technol.*, vol. 55, no. 6, pp. 1748–1755, Nov. 2006.
- [18] G. Romeo, F. Borello, and E. Cestino, "Design of inter-city transport aircraft powered by fuel cell & flight test of zero emission 2-seater aircraft powered by fuel cells," in *2012 Electrical Systems for Aircraft, Railway and Ship Propulsion*, 2012, pp. 1–7.

- [19] J. Shin, B. Song, S. Lee, S. Shin, Y. Kim, G. Jung, and S. Jeon, "Contactless power transfer systems for On-Line Electric Vehicle (OLEV)," in *2012 IEEE International Electric Vehicle Conference*, 2012, pp. 1–4.
- [20] B. Song, J. Shin, S. Lee, S. Shin, Y. Kim, S. Jeon, and G. Jung, "Design of a high power transfer pickup for on-line electric vehicle (OLEV)," in *2012 IEEE International Electric Vehicle Conference*, 2012, pp. 1–4.
- [21] Y. J. Jang, Y. D. Ko, and S. Jeong, "Optimal design of the wireless charging electric vehicle," in *2012 IEEE International Electric Vehicle Conference*, 2012, pp. 1–5.
- [22] Y. D. Ko and Y. J. Jang, "The Optimal System Design of the Online Electric Vehicle Utilizing Wireless Power Transmission Technology," *IEEE Trans. Intell. Transp. Syst.*, vol. 14, no. 3, pp. 1255–1265, Sep. 2013.
- [23] R. Gilbert and A. Perl, "Grid-connected vehicles as the core of future land-based transport systems," *Energy Policy*, vol. 35, no. 5, pp. 3053–3060, 2007.
- [24] A. Kara, K. Mardikyan, and S. Baran, "Application of regenerative braking energy to Istanbul metro operation system," in *2012 Electrical Systems for Aircraft, Railway and Ship Propulsion*, 2012, pp. 1–3.
- [25] L. Latkovskis and V. Bra is, "Simulation of the Regenerative Energy Storage with Supercapacitors in Tatra T3A Type Trams," in *Tenth International Conference on Computer Modeling and Simulation (uksim 2008)*, 2008, pp. 398–403.
- [26] L. Streit and P. Drabek, "Simulation and emulation of tram with onboard supercapacitors on Pilsen tram line," in *2013 International Conference on Clean Electrical Power (ICCEP)*, 2013, pp. 703–706.
- [27] A. Muetze, Y. C. Tan, and B. Y. A. Muetze, "Electric bicycles - A performance evaluation," *IEEE Ind. Appl. Mag.*, vol. 13, no. 4, pp. 12–21, Jul. 2007.
- [28] M. Ehsani and S. Gay, "Characterization of electric motor drives for traction applications," in *IECON'03. 29th Annual Conference of the IEEE Industrial Electronics Society (IEEE Cat. No.03CH37468)*, vol. 1, pp. 891–896.
- [29] W. Wang, Q. Wang, Y. Yu, X. Zeng, and N. Zou, "Study on the Operation Region of Induction Traction Motor for Electric Vehicle," in *2009 International Conference on Measuring Technology and Mechatronics Automation*, 2009, vol. 2, pp. 699–703.
- [30] W. Fei, P. C. K. Luk, and K. Jinupun, "A new axial flux permanent magnet Segmented-Armature-Torus machine for in-wheel direct drive applications," in *2008 IEEE Power Electronics Specialists Conference*, 2008, pp. 2197–2202.
- [31] W. Fei, P. C.-K. Luk, J. Shen, and Y. Wang, "A novel outer-rotor permanent-magnet flux-switching machine for urban electric vehicle propulsion," 2009, pp. 1–6.
- [32] W. Kim and K. Yi, "Coordinated Control of Tractive and Braking Forces Using High Slip for Improved Turning Performance of an Electric Vehicle Equipped with In-Wheel Motors," in *2012 IEEE 75th Vehicular Technology Conference (VTC Spring)*, 2012, pp. 1–5.
- [33] J. Puranen, "INDUCTION MOTOR VERSUS PERMANENT MAGNET SYNCHRONOUS MOTOR IN MOTION CONTROL APPLICATIONS: A COMPARATIVE STUDY," Lappeenranta University of Technology, 2006.
- [34] J. G. Hayes, R. P. R. de Oliveira, S. Vaughan, and M. G. Egan, "Simplified electric vehicle power train models and range estimation," in *2011 IEEE Vehicle Power and Propulsion Conference*, 2011, pp. 1–5.
- [35] A. Al-Busaidi and V. Pickert, "Comparative Study of Rectifier Circuits for Series Hybrid Electric Vehicles," in *Hybrid and Eco-Friendly Vehicle Conference, 2008. IET HEVC 2008*, 2008, pp. 1–6.
- [36] Zhiqiao Wu and Gui-Jia Su, "High-performance permanent magnet machine drive for electric vehicle applications using a current source inverter," in *2008 34th Annual Conference of IEEE Industrial Electronics*, 2008, pp. 2812–2817.

- [37] M. Al Sakka, J. Van Mierlo, H. Gualous, and U. Brussel, "DC / DC Converters for Electric Vehicles," in *Electric Vehicles - Modelling and Simulations*, vol. c, Dr. Seref Soyulu, Ed. InTech, 2011, p. 466.
- [38] F. Farret and M. Simões, "Integration of Alternative Sources of Energy," in *Integration of Alternative Sources of Energy*, 1st ed., Wiley-IEEE Press, 2006, pp. 301 – 332.
- [39] L. Giorgi and F. Leccese, "Fuel Cells: Technologies and Applications," *Open Fuel Cells J.*, vol. 6, pp. 1–20, 2013.
- [40] A. Andrijanovits, H. Hoimoja, and D. Vinnikov, "Comparative Review of Long-Term Energy Storage Technologies for Renewable Energy Systems," *Electron. Electr. Eng.*, vol. 118, no. 2, pp. 21–26, Feb. 2012.
- [41] D. Berndt, "A look back at forty years of lead-acid-battery development; A survey especially regarding stationary applications," in *INTELEC 05 - Twenty-Seventh International Telecommunications Conference*, 2005, pp. 269–275.
- [42] N. Omar, P. Van den Bossche, G. Mulder, M. Daowd, J. M. Timmermans, J. Van Mierlo, and S. Pauwels, "Assessment of performance of lithium iron phosphate oxide, nickel manganese cobalt oxide and nickel cobalt aluminum oxide based cells for using in plug-in battery electric vehicle applications," in *2011 IEEE Vehicle Power and Propulsion Conference*, 2011, pp. 1–7.
- [43] J. Garche, S. Smedley, and X. G. Zhang, "Secondary Batteries - Metal-Air systems: Zinc–Air: Hydraulic Recharge," in *Encyclopedia of Electrochemical Power Sources*, 2009, pp. 393–403.
- [44] T. Crompton, "Metal-air cells," in *Battery Reference Book*, 2000, pp. 1–8.
- [45] S. Yang and H. Knickle, "Design and analysis of aluminum/air battery system for electric vehicles," *J. Power Sources*, vol. 112, no. 1, pp. 162–173, 2002.
- [46] T. Khoo, P. C. Howlett, M. Tsagouria, D. R. MacFarlane, and M. Forsyth, "The potential for ionic liquid electrolytes to stabilise the magnesium interface for magnesium/air batteries," *Electrochim. Acta*, vol. 58, pp. 583–588, 2011.
- [47] K. Rajashekara, "Present Status and Future Trends in Electric Vehicle Propulsion Technologies," *IEEE J. Emerg. Sel. Top. Power Electron.*, vol. 1, no. 1, pp. 3–10, Mar. 2013.
- [48] S. J. Gerssen-Gondelach and A. P. C. Faaij, "Performance of batteries for electric vehicles on short and longer term," *J. Power Sources*, vol. 212, pp. 111–129, 2012.
- [49] A. Parasuraman, T. M. Lim, C. Menictas, and M. Skyllas-Kazacos, "Review of material research and development for vanadium redox flow battery applications," *Electrochim. Acta*, vol. 101, pp. 27–40, 2013.
- [50] K. van Berkel, T. Hofman, B. Vroemen, and M. Steinbuch, "Optimal energy management for a flywheel-based hybrid vehicle," in *American Control Conference (ACC), 2011*, 2011, pp. 5255–5260.
- [51] A. Buchroithner, I. Andrasec, and M. Bader, "Optimal system design and ideal application of flywheel energy storage systems for vehicles," in *2012 IEEE International Energy Conference and Exhibition (ENERGYCON)*, 2012, pp. 991–996.
- [52] R. G. Lawrence, K. L. Craven, and G. D. Nichols, "Flywheel UPS," *IEEE Ind. Appl. Mag.*, vol. 9, no. 3, pp. 44–50, May 2003.
- [53] F. A. Limited, "Flybrid® Flywheel Tech," 2014. [Online]. Available: <http://www.flybridsystems.com/flywheeltech.html>. [Accessed: 12-Mar-2014].
- [54] F. O. W. C. Limited, "Energy Recovery Systems (ERS)," 2014. [Online]. Available: [http://www.formula1.com/inside\\_f1/understanding\\_the\\_sport/8763.html](http://www.formula1.com/inside_f1/understanding_the_sport/8763.html). [Accessed: 12-Mar-2014].
- [55] S. Lu, S. Member, K. A. Corzine, S. Member, and M. Ferdowsi, "A New Battery / Ultracapacitor Energy Storage System Design and Its Motor Drive Integration for Hybrid Electric Vehicles," *Veh. Technol. IEEE Trans.*, vol. 56, no. 4, pp. 1516–1523, 2007.
- [56] H. Yoo, S. Member, S. Sul, Y. Park, and J. Jeong, "System Integration and Power-Flow Management for a Series Hybrid Electric Vehicle Using Supercapacitors and Batteries," *IEEE Trans. Ind. Appl.*, vol. 44, no. 1, pp. 108–114, 2008.

- [57] A. Jaafar, C. R. Akli, B. Sareni, X. Roboam, and A. Jeunesse, "Sizing and Energy Management of a Hybrid Locomotive Based on Flywheel and Accumulators," *IEEE Trans. Veh. Technol.*, vol. 58, no. 8, pp. 3947–3958, Oct. 2009.
- [58] A. Jaafar, B. Sareni, X. Roboam, and M. Thiounn-Guermeur, "Sizing of a hybrid locomotive based on accumulators and ultracapacitors," *2010 IEEE Veh. Power Propuls. Conf.*, pp. 1–6, Sep. 2010.
- [59] M. H. Ali and R. A. Dougal, "An Overview of SMES Applications in Power and Energy Systems," *IEEE Trans. Sustain. Energy*, vol. 1, no. 1, pp. 38–47, Apr. 2010.
- [60] L. Trevisani, A. Morandi, F. Negrini, P. L. Ribani, and M. Fabbri, "Cryogenic Fuel-Cooled SMES for Hybrid Vehicle Application," *IEEE Trans. Appl. Supercond.*, vol. 19, no. 3, pp. 2008–2011, Jun. 2009.
- [61] D. Wu, K. T. Chau, S. Member, C. Liu, S. Gao, and F. Li, "Transient Stability Analysis of SMES for Smart Grid With Vehicle-to-Grid Operation," *Appl. Supercond. IEEE Trans.*, vol. 22, no. 3, 2012.
- [62] K. T. Chau, "SMES Control for Power Grid Integrating Renewable Generation and Electric Vehicles," *IEEE Trans. Appl. Supercond.*, vol. 22, no. 3, pp. 5701804–5701804, Jun. 2012.
- [63] Z. Gizinski, M. Gasiewski, I. Mascibrodzki, M. Zych, K. Zymmer, and M. Zulawnik, "Hybrid - type system of power supply for a trolleybus with an asynchronous motor," in *2008 13th International Power Electronics and Motion Control Conference*, 2008, pp. 1562–1567.
- [64] S. F. Tie and C. W. Tan, "A review of energy sources and energy management system in electric vehicles," *Renew. Sustain. Energy Rev.*, vol. 20, pp. 82–102, 2013.
- [65] D. of Defense, "Electrical Energy Storage System by SMES Method for Ultra-High Power and Energy Density," 2011. [Online]. Available: <http://www.sbir.gov/node/361161>. [Accessed: 12-Mar-2014].
- [66] G. Simbolotti and R. Kempener, "Electricity storage, Technology Brief," 2012.
- [67] K. Bradbury, "Energy Storage Technology Review, tutorial." Kyle Bradbury, Durham, North Carolina, USA, 2010.
- [68] M. Yilmaz and P. T. Krein, "Review of charging power levels and infrastructure for plug-in electric and hybrid vehicles," in *2012 IEEE International Electric Vehicle Conference*, 2012, pp. 1–8.
- [69] H. H. Wu, A. Gilchrist, K. Sealy, P. Israelsen, and J. Muhs, "A review on inductive charging for electric vehicles," in *2011 IEEE International Electric Machines & Drives Conference (IEMDC)*, 2011, pp. 143–147.
- [70] A. Neves, D. M. Sousa, A. Roque, and J. M. Terras, "Analysis of an inductive charging system for a commercial electric vehicle." pp. 1–10, 2011.
- [71] J. Laugis, T. Lehtla, J. Joller, A. Rosin, D. Vinnikov, and M. Lehtla, *Light rail vehicle drives and control (in estonian)*, 1st ed. Tallinn, Estonia: Tallinn University of Technology, Department of Electrical Drives and Power Electronics, 2008, p. 200.
- [72] R. Van Haaren, "Assessment of Electric Cars ' Range Requirements and Usage Patterns based on Driving Behavior recorded in the National Household Travel Survey of 2009," New York, USA, 2012.
- [73] T. Letrouve, A. Bouscayrol, W. Lhomme, N. Dollinger, and F. M. Calvairac, "Different models of a traction drive for an electric vehicle simulation," in *2010 IEEE Vehicle Power and Propulsion Conference*, 2010, pp. 1–6.
- [74] Siavash Zoroofi, "Modeling and Simulation of Vehicular Power Systems," CHALMERS UNIVERSITY OF TECHNOLOGY, 2008.
- [75] Liu Jun, Wang Li-fang, Yang Jian, and Liu Gui-dong, "Research of a novel flexible load for electric vehicle test bench," in *2010 International Conference on Computer and Communication Technologies in Agriculture Engineering*, 2010, vol. 1, pp. 223–226.
- [76] F. Marra, D. Sacchetti, A. B. Pedersen, P. B. Andersen, and E. Larsen, "Implementation of an Electric Vehicle test bed controlled by a Virtual Power Plant for contributing to regulating power reserves," in *2012 IEEE Power and Energy Society General Meeting*, 2012, pp. 1–7.

- [77] I. Alcalá, A. Claudio, and G. Guerrero, "Test bench to emulate an electric vehicle through equivalent inertia and machine dc," in *2008 11th IEEE International Power Electronics Congress*, 2008, pp. 198–203.
- [78] Zhao Hui, Li Cheng, and Zhang Guojiang, "Design of a versatile test bench for hybrid electric vehicles," in *2008 IEEE Vehicle Power and Propulsion Conference*, 2008, pp. 1–4.
- [79] C. Lungoci, D. Bouquain, A. Miraoui, and E. Helerea, "Modular test bench for a hybrid electric vehicle with multiples energy sources," in *2008 11th International Conference on Optimization of Electrical and Electronic Equipment*, 2008, pp. 299–306.
- [80] P. Khatun, C. M. Bingham, N. Schofield, and P. H. Mellor, "An experimental laboratory bench setup to study electric vehicle antilock braking/ traction systems and their control," in *Proceedings IEEE 56th Vehicular Technology Conference*, 2002, vol. 3, pp. 1490–1494.
- [81] Y. Cheng, V. M. Joeri, and P. Lataire, "Research and test platform for hybrid electric vehicle with the super capacitor based energy storage," in *2007 European Conference on Power Electronics and Applications*, 2007, pp. 1–10.
- [82] P. Drabek, L. Streit, and M. Los, "The energy storage system with supercapacitor," in *Proceedings of 14th International Power Electronics and Motion Control Conference EPE-PEMC 2010*, 2010, pp. T9–39–T9–43.
- [83] D. Iannuzzi, "Improvement of the energy recovery of traction electrical drives using supercapacitors," in *2008 13th International Power Electronics and Motion Control Conference*, 2008, pp. 1469–1474.
- [84] P. Thounthong, "Control of a Three-Level Boost Converter Based on a Differential Flatness Approach for Fuel Cell Vehicle Applications," *IEEE Trans. Veh. Technol.*, vol. 61, no. 3, pp. 1467–1472, Mar. 2012.
- [85] V. Vodovozov, Z. Raud, and T. Lehtla, "A Toolbox to Design Inverters for Automotive Applications," in *11th World Conference on Applications of Electrical Engineering AEE 2012*, 2012, pp. 190–195.
- [86] ABB, *Technical Guide No. 1: Direct Torque Control*, 1st ed. Helsinki, Finland: ABB Inc., 2002.
- [87] Kempten University of Applied Sciences, "Institut für Angewandte Batterieforschung (IABF)." [Online]. Available: <http://www.hochschule-kempton.de/forschung/forschungszentrum-allgaeu-fza/institut-fuer-elektrische-energiesysteme-iees/institutsbeschreibung.html>. [Accessed: 28-Dec-2013].
- [88] M. Tutuianu, A. Marotta, H. Steven, E. Ericsson, T. Haniu, N. Ichikawa, and H. Ishii, "Development of a World-wide Worldwide harmonized Light duty driving Test Cycle ( WLTC ), Technical Report, DHC subgroup."
- [89] T. J. Barlow, S. Latham, I. S. McCrae, and P. G. Boulter, "A reference book of driving cycles for use in the measurement of road vehicle emissions."
- [90] V. Vodovozov, *Electric Drive Systems and Operation*. London, UK: Bookboon, 2012, p. 102.
- [91] V. Vodovozov and Z. Raud, "A toolbox to design and study mechatronic systems," in *Proceedings of the IASTED International Conference on Modelling, Identification and Control*, 2010, pp. 276–283.
- [92] V. Vodovozov, *Electric Drive Dimensioning and Tuning*. London, UK: Bookboon, 2012, p. 103.
- [93] ABB, *ACS800 Firmware Manual. Standard Application Program 7.x*. ABB Inc., 2005, p. 264.
- [94] ABB Drives, *Application Guide: Adaptive Program*. Helsinki, Finland: ABB Oy, 2005, p. 44.
- [95] ABB Drives, *User's Manual DriveAP*. Helsinki, Finland: ABB Oy, 2010, p. 32.
- [96] A. Wolfermann, W. K. M. Alhajyaseen, and H. Nakamura, "Modeling Speed Profiles of Turning Vehicles at Signalized Intersections," in *3rd International Conference on Road Safety and Simulation*, 2011, pp. 1–17.
- [97] M. Mägi, "Utilization of Electric Vehicles Connected to Distribution Substations for Peak Shaving of Utility Network Loads," *Sci. J. Riga Tech. Univ. - Electr. Control Commun. Eng.*, vol. 2, no. 1, pp. 47–54, Apr. 2013.

- [98] J. Escoda, J. Fontanilles, D. Biel, V. Repecho, and R. Cardoner, "G2V and V2G operation 20 kW Battery Charger," in *EVS27 International Battery, Hybrid and Fuel Cell Electric Vehicle Symposium*, 2013, pp. 1–5.
- [99] T. S. Ustun, C. R. Ozansoy, and A. Zayegh, "Implementing Vehicle-to-Grid (V2G) Technology With IEC 61850-7-420," *IEEE Trans. Smart Grid*, vol. 4, no. 2, pp. 1180–1187, Jun. 2013.
- [100] X. Yan, B. Zhang, X. Xiao, H. Zhao, and L. Yang, "A bidirectional power converter for electric vehicles in V2G systems," in *2013 International Electric Machines & Drives Conference*, 2013, pp. 254–259.
- [101] B. C. Liu, K. T. Chau, D. Wu, S. Gao, and C. Liu, "Opportunities and Challenges of Vehicle-to-Home , Vehicle-to-Grid Technologies," *Proc. IEEE*, vol. 101, no. 11, pp. 2409–2427, Nov. 2013.
- [102] T. Korotko, M. Magi, K. Peterson, R. Teemets, and E. Pettai, "Analysis and development of protection and control functions for Li-Ion based prosumers provided by low voltage part of distribution substation," in *2013 International Conference-Workshop Compatibility And Power Electronics*, 2013, pp. 19–24.
- [103] M. Becherif, M. Y. Ayad, D. Hissel, and R. Mkahl, "Design and sizing of a stand-alone recharging point for battery electrical vehicles using photovoltaic energy," in *2011 IEEE Vehicle Power and Propulsion Conference*, 2011, pp. 1–6.
- [104] C.-F. Lu, "Dynamic modelling of battery energy storage system and application to power system stability," *IEE Proc. - Gener. Transm. Distrib.*, vol. 142, no. 4, p. 429, Jul. 1995.
- [105] "ABB: Electric Vehicle Charging Infrastructure Terra multi-standard DC charging station 53," 2014.
- [106] K. Al-Haddad, R. Saha, A. Chandra, and B. Singh, "Static synchronous compensators (STATCOM): a review," in *IET Power Electronics*, 2009, vol. 2, no. 4, pp. 297–324.
- [107] A. Karami, M. Rashidinejad, A. A. Gharaveisi, and S. Bahonar, "Optimal location of STATCOM for voltage security enhancement via artificial intelligent," in ... *Technology, 2006. ICIT ...*, 2006, no. 2, pp. 2704–2708.
- [108] R. Grünbaum and L. Andreasson, "STATCOM for Improved Grid Stability and Power Transmission Capability." ABB AB - FACTS, SE-721 64, Västerås, Sweden.
- [109] P. S. S. Sensarma, K. R. R. Padiyar, and V. Ramanarayanan, "A STATCOM for composite power line conditioning," in *Proceedings of IEEE International Conference on Industrial Technology 2000 (IEEE Cat. No.00TH8482)*, vol. 2, pp. 542–547.

## List of Author's Publications

The present doctoral thesis is based on the following publications that are referred to in the text by Roman numbers.

- [PAPER-I] **Rassõlkin, A.;** Vodovozov, V. (2013). A Test Bench to Study Propulsion Drives of Electric Vehicles. 2013 International Conference-Workshop Compatibility and Power Electronics (CPE 2013) Ljubljana (Slovenia), IEEE, pp. 275 – 279.
- [PAPER-II] **Rassõlkin, A.;** Vodovozov, V. (2013). Test Bench with Supercapacitor Storage to Study Propulsion Drives. Journal: "Energy Saving. Power Engineering. Energy Audit. 114 (8,2)", Ukraine, pp. 65 - 70.
- [PAPER-III] **Rassõlkin, A.;** Vodovozov, V. (2013). Experimental Setup to Explore the Drives of Battery Electric Vehicles. The 27th International Electric Vehicle Symposium & Exhibition (EVS27), Barcelona (Spain), 17-20.11.2013, (Eds.) Fira Barcelona.
- [PAPER-IV] **Rassõlkin, A.;** Liivik, L.; Vodovozov, V.; Raud, Z. (2014). A Library of Samples for E-Vehicle Propulsion Drive Tuning. The Scientific Journal of Riga Technical University: Electrical, Control and Communication Engineering, vol 5, Riga, Latvia, 2014, pp. 27 - 33.
- [PAPER-V] **Rassõlkin, A.;** Hõimoja, H. (2012). Switching Locomotive as a Part of Smart Electrical Grid. The 8th Power Plant and Power System Control Symposium (PPPSC'8), Toulouse (France), 02-05.09.2012. (Eds.) Fadel, M.; Caux, S. IFAC, pp. 606 - 609.
- [PAPER-VI] **Rassõlkin, A.;** Hõimoja, H. (2012). Power Quality Application of Hybrid Drivetrain. The 12th International Conference on Electrical Systems for Aircraft, Railway and Ship Propulsion (ESARS'12), Bologna (Italy), 16.10-18.10.2012. IEEE.
- [PAPER-VII] **Rassõlkin, A.;** Kallaste, A.; Hõimoja, H. (2014) Power Factor correction with Vehicle-to-Grid STATCOM implementation, Electric Power Quality and Supply Reliability 2014 (PQ 2014), Rakvere (Estonia), 11-13.06.2014
- [BOOK-I] Vodovozov, V.; **Rassõlkin, A.** (2013). Laboratory works: Advanced Course of Electrical Drives, 1st ed. Tallinn, Estonia: Department of Electrical Engineering, Tallinn University of Technology, 2013, p. 31.

### ***Author's Own Contribution***

This section describes the author's contribution to the papers listed in the thesis as author's publications.

- [PAPER-I] Anton Rassõlkin is the main author of the paper, responsible for the data collection, calculations and modeling. He had a major role in writing. He presented the paper at 8th International Conference-Workshop Compatibility and Power Electronics (CPE2013), Ljubljana, Slovenia.
- [PAPER-II] Anton Rassõlkin is the main author of the paper, responsible for the literature review, data collection, calculations and modeling. He had a major role in writing. He presented the paper at International Conference „Silovaja Elektronika i Energo-effektivnostj 2013 CEE'2013", Alushta, Ukraine.
- [PAPER-III] Anton Rassõlkin is the main author of the paper, responsible for the literature review and data collection. He had a major role in writing. He presented the paper at 27th International Electric Vehicle Symposium & Exhibition, Barcelona, Spain.
- [PAPER-IV] Anton Rassõlkin is the main author of the paper, responsible for the literature overview, data collection and calculations. He had a major role in writing.
- [PAPER-V] Anton Rassõlkin is the main author of the paper, responsible for the literature review, data collection, calculations and modeling. He had a major role in writing. He presented the paper at 8th Power Plant and Power System Control Symposium (PPSC'8), Toulouse, France.
- [PAPER-VI] Anton Rassõlkin is the main author of the paper, responsible for the literature review, data collection, calculations and modeling. He had a major role in writing. He presented the paper at 12th Systems for Aircraft, Railway and Ship Propulsion (ESARS'12), Bologna, Italy.
- [PAPER-VII] Anton Rassõlkin is the main author of the paper, responsible for the literature review, data collection, calculations and modeling. He had a major role in writing. He presented the paper at 9th Electric Power Quality and Supply Reliability (PQ 2014), Rakvere, Estonia
- [BOOK-II] Anton Rassõlkin is the co-author of the laboratory practice exercise book.

## **Abstract**

### **Research and Development of Trial Instrumentation for Electric Propulsion Motor Drives**

As the world population is growing, transportation needs are increasing, which means that more vehicles are required. Vehicles with ICE and those that burn fossil fuels increase the carbon dioxide CO<sub>2</sub> emission in the Earth's atmosphere that causes the greenhouse effect and climate change. The electric vehicles claim to replace today's vehicles with internal combustion engines. An electric vehicle is a rather complex system for accurate mathematical description, monitoring, and validation. However, today much attention is paid to the studies of different parts of electric vehicles. Laboratory studies with test benches, combining advantages of software models and real equipment, contribute to the reduction of the number of vehicle test runs and safe maintenance. By using a variety of different test benches, separate parts of an electric vehicle could be studied and improved.

The aim of the doctoral thesis is to study the basic components of the electric propulsion motor drive technologies and propulsion drive segments. Focus is on the study of electric drive propulsion systems of hybrid and electrical vehicles. Studies include the following topologies: electric motors, power electronic devices, energy storage applications for propulsion drive systems, as well as regenerative braking and charging systems.

Special attention is paid to electric vehicle modelling. There are three models described in the thesis: load model of the propulsion drive, computer model of the propulsion drive system and the experimental setup. All the models are scaled to the real vehicle. The modelling methodology could be used to model propulsion motor drive systems of different vehicles.

The existing vehicle testing cycles were studied and compared. An effective methodology for research, assessment and tuning of the propulsion electric motor drives was proposed to explore the drive responses under changeable control and disturbance signals. Using the laboratory test bench, multiple conventional modes of the vehicle motion were studied. The developed methodology can be recommended for adjusting the electric drives for different kinds of testing equipment, including the synchronous, induction, and direct current machines. Experimental validation of the described approach has demonstrated broad possibilities for the steady-state and transient modes of the evaluation of vehicle quality. It suits for recommendations to be made with regard to the tuning of the drive regulators, control looping, sensor allocation, and feedback arrangements.

Plugging the electrical vehicle to the existing electrical grid and its influence on the grid is a topic of current interest. The thesis presents a possibility to improve vehicle propulsion motor drive systems for controlling the power factor of the grid. The simple and quick solution is proved theoretically, with a

PSIM model and practically, with an experimental setup. The scheme suggested has all the advantages of STATCOM apparatus, meaning that in addition to the power factor correction, asymmetrical load balancing, voltage control, active harmonics filtration and flicker mitigation could be performed. Economic benefits and reductions in weight could be achieved by the use of the windings of the propulsion motor instead of separate inductors. The existing hybrid and electrical vehicles with induction or synchronous propulsion motors could be updated.

## Kokkuvõte

### **Elekterveoajamite katsetuste metoodika loomine, rakendamine ja edasiarendused**

Koos rahvaarvuga kasvavad ka transpordimahud, mis tähendab järjest lisanduvaid sõidukeid. Sisepõlemismootoriga ja fossiilseid kütuseid kasutavad sõidukid suurendavad süsinikdioksiidi CO<sub>2</sub> sisaldust Maa atmosfääris, mis omakorda põhjustab kasvuhooneefekti ja kliimamuutusi. Elektriautodes nähakse lahendust, mis asendab tänapäeval veel valdavad sisepõlemismootoriga sõidukid. Elektrisõiduk tervikuna on täpseks matemaatiliseks kirjeldamiseks, jälgimiseks ja tulemuste valideerimiseks küllaltki keerukas süsteem. Samas on tänapäeval suur tähelepanu pööratud seadmete erinevate osade uurimisele ja arendamisele. Katsestendidel läbiviidavad laboratoorsed uuringud ühendavad arvutimudeli ja reaalse seadme eelised ning aitavad vähendada ka tegelike proovisõitude ja turvatestide arvu. Erinevate katsestendide kasutamine annab võimaluse uurida ja arendada elektersõiduki osi eraldi.

Doktoritöö põhieesmärk on uurida elekterveoajami põhikomponentide tehnilisi lahendusi ja veoajami tüüpsõlmi. Doktoritöös keskendutakse elektri- ja hübriidautode elekterveoajami uurimisele. Uuringud hõlmavad järgmisi alamvaldkondi: elektrimootorid, jõumuundurid, veoajami elektrisalvestid, kuid ka rekuperatiivpidurdust ja laadimismooduseid.

Erilist tähelepanu on pööratud elektersõidukite modelleerimisele. Doktoritöös on kirjeldatud kolme mudelit: veoajami koormusmudel, veoajami arvutimudel ja eksperimentaalne katsestend. Kõiki mudeleid on võrreldud reaalse sõidukiga. Modelleerimise metoodikat on võimalik kasutada ka teiste elekterveoajamitega sõidukite uurimiseks.

Olemasolevate sõidukite katsesükleid uuriti ja võrreldi omavahel. Elekterveoajamite uurimiseks, kvalitatiivseks hindamiseks ja häälestamiseks pakuti efektiivne metoodika, et vaadelda jõuajami reaktsiooni juhtsignaalide muutumisel ja väliskeskkonna häiringute puhul. Tavalisi sõidukitalitlusi on uuritud katsestendiga. Väljatöötatud metoodikat võib soovitada erinevate elektriajami katseseadmete (sh sünkroon-, asünkroon- ja alalisvoolumasinad) reguleerimiseks. Kirjeldatud katsetuste metoodika eksperimentaalne valideerimine annab palju võimalusi elektersõiduki püsi- ja siirdetalitluse kvaliteedi hindamiseks. Metoodika annab soovitusi ajami seadistamiseks, juhtahelate projekteerimiseks, andurite paigaldamiseks ning tagasisideahelate koostamiseks.

Elektersõiduki ühendamine elektrivõrguga ja selle mõju süsteemile on eraldiseisev peatükk. Doktoritöö esitleb veoajami ühendamise metoodikat elektrivõrgu võimsusteguri parandamiseks. Lihtne ja kiire lahendus on tõestatud teoreetiliselt arvutimudeliga ja praktiliselt katsestendi abil. Pakutud skeemil on olemas kõik staatilise reaktiivvõimsuse kompensatori eelised, mis tähendab, et seda saab kasutada mitte ainult võimsusteguri parandamiseks, vaid ka

faasikoormuste tasakaalustamiseks, pinge reguleerimiseks, harmooniliste aktiivfiltrina ja väreluse vähendamiseks. Majanduslik kasu ning väiksem kaal on võimalik saavutada veomootorite staatorimähise kasutamisega induktiivpoolide asemel. Olemasolevaid asünkroon- või sünkroonveomootoriga hübriid- ja elektersõidukeid on eeltoodud funktsionaalsuse lisamiseks võimalik kaasajastada.

## Elulookirjeldus

### 1. Isikuandmed

Ees- ja perekonnanimi	Anton Rassõlkin
Sünniaeg ja -koht	28.09.1985, Tallinn
Kodakondsus	Eesti
E-posti aadress	anton.rassolkin@ttu.ee

### 2. Hariduskäik

Õppeasutus (nimetus lõpetamise ajal)	Lõpetamise aeg	Haridus (eriala/kraad)
Tallinna Tehnikaülikool	2010	Elektriamid ja jõuelektronika/ Tehnikateaduse magister
Gießen-Friedbergi Rakendus kõrgkool	2010	Automaatika/ Diplomeeritud insener
Tallinna Tehnikaülikool	2008	Elektriamid ja jõuelektronika/ Tehnikateaduste bakalaureus
Tallinna Polütehnikum	2005	Elektriseadmed ja -süsteemid/ Erikeskharidus
Tallinna Paekaare Gümnaasium	2001	Põhiharidus

### 3. Keelteoskus (alg-, kesk- või kõrgtase)

Keel	Tase
Vene keel	Kõrgtase
Eesti keel	Kõrgtase
Inglise keel	Kõrgtase
Saksa keel	Kõrgtase

### 4. Teenistuskäik

Töötamise aeg	Tööandja nimetus	Ametikoht
2012 - ...	Tallinna Tehnikaülikool; Energeetikateaduskond, Elektrotehnika instituut	Insener
2010 - ...	Tallinna Polütehnikum; Energeetika ja automaatika osakond	Kutseõpetaja

2009	Rittal GmbH & Co. KG, Herborn, Saksamaa	Praktikant
2008	AS ESTEL, Tallinn, Eesti	Elektriinsener
2007	ABB GmbH, Cottbus, Saksamaa	Praktikant
2007	Metos AS, Tallinn, Eesti	Elektrimontöör
2004-2006	ABB AS MPST, Keila, Eesti	Elektrimontöör

#### 5. Teaduspreemiad ja -tunnustused

- 2012 Kõige aktiivsem osaleja 12. rahvusvahelisel sümposiumil "Topical Problems in the Field of Electrical and Power Engineering", Kuressaare, Eesti
- 2012 Parim ettekanne sektsioonis "Elektrotehnika II" 12. rahvusvahelisel sümposiumil "Topical Problems in the Field of Electrical and Power Engineering", Kuressaare, Eesti
- 2012 Kristjan Jaagu stipendium
- 2008 Erasmuse välisõppe stipendium
- 2007 Leonardo da Vinci välispraktika stipendium

#### 6. Teadustöö põhisuunad

Loodusteadused ja -tehnika, Energeetikaalased uuringud, Energeetika

#### 7. Jooksvad projektid

- Aktiivsete elektrijaotusvõrkude muundurite topoloogiad ja juhtimis-meetodid
- Elektersõidukite kiirloomiseks kasutatavate uudsete kahesuunaliste muunduritopoloogiatega ja juhtimisalgoritmide uurimine ja väljatöötamine
- Kvaasi-impedantsallikaga alalis- ja vahelduvpingemuundurid

#### 8. Juhendatud väitekirjad

- 2013 Aare Rõõmussaar, magistrikraad. Ülikondensaatorite õppepaneeli väljatöötamine, Tallinna Tehnikaülikool

# Curriculum Vitae

## 1. Personal data

Name	Anton Rassõlkin
Date and place of birth	28.09.1985, Tallinn, Estonia
E-mail	anton.rassolkin@ttu.ee

## 2. Education

Educational institution	Graduation year	Education (field of study/degree)
Tallinn University of Technology	2010	Electric drives and power electronics / Master of Science
University of Applied science Giessen-Friedberg	2010	Automation Diploma-Engineer
Tallinn University of Technology	2008	Electric drives and power electronics / Bachelor of Science
Tallinn Polytechnic School	2005	Electrical Equipment and Systems / Vocational education
Secondary School Paekaare	2001	Basic

## 3. Language competence/skills (fluent; average, basic skills)

Language	Level
Russian	Fluent
Estonian	Fluent
English	Fluent
German	Fluent

## 4. Professional Employment

Period	Organisation	Position
2012 - ...	Tallinn University of Technology, Faculty of Power Engineering, Department of Electrical Engineering	Staff member
2010 - ...	Tallinn Polytechnic School; Department of Energy and Automation	Vocational teacher

2009	Rittal GmbH & Co. KG, Herborn, Germany	Trainee
2008	AS ESTEL, Tallinn, Estonia	Electrical engineer
2007	ABB GmbH, Cottbus, Germany	Trainee
2007	Metos AS, Tallinn, Estonia	Circuit installer
2004-2006	ABB AS MPST, Keila, Estonia	Circuit installer

## 5. Honours & Awards

- 2012 Most active Participant at 12th International Symposium "Topical Problems in the Field of Electrical and Power Engineering", Kuressaare, Estonia
- 2012 Best Presenter Award in Electrical Engineering II at 12th International Symposium "Topical Problems in the Field of Electrical and Power Engineering", Kuressaare, Estonia
- 2012 Kristijan Jaak foundation scholarship
- 2008 Erasmus scholarship for foreign studies
- 2007 Leonardo da Vinci scholarship for foreign scholarship

## 6. Field of research

Natural Sciences and Engineering, Energetic Research, Energy research

## 7. Current grants & projects

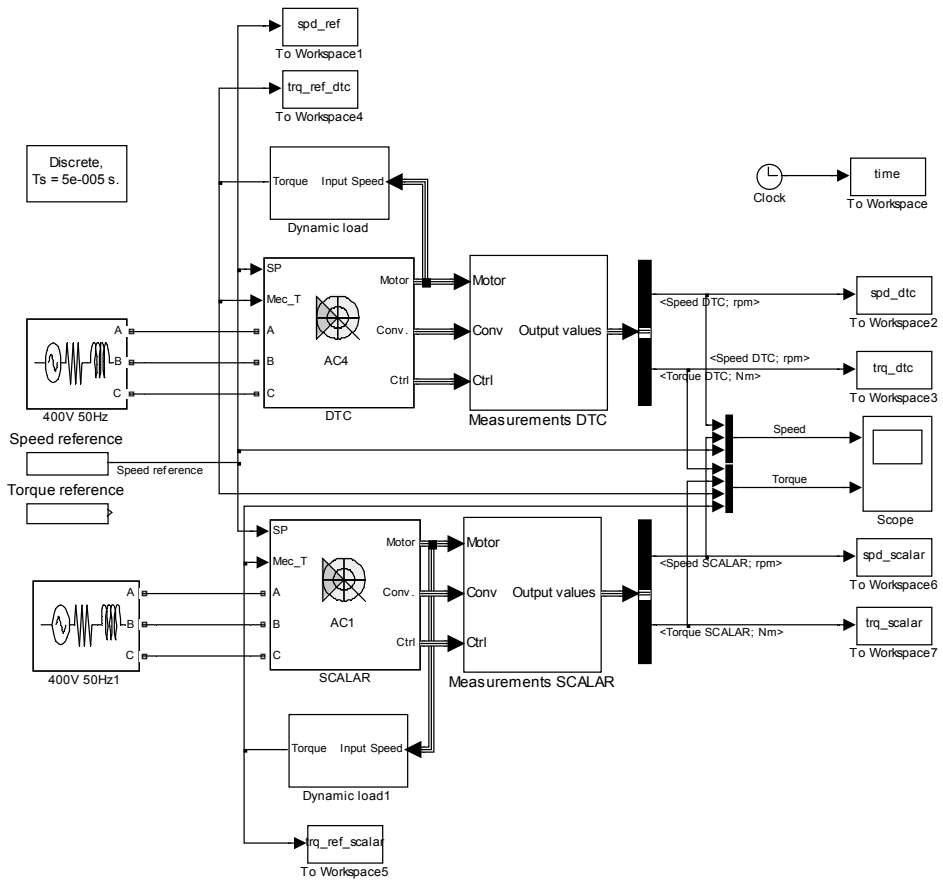
- New Converter Topologies and Control Methods for Electronic Power Distribution Networks
- Research and development of new converter topologies and control methods for fast charging of electric vehicles
- Quasi-Impedance Source DC/DC and AC/AC Converters

## 8. Dissertations supervised

- 2013 Aare Rõõmussaar, Master's Degree. Development of an Ultracapacitor Training Panel, Tallinn University of Technology

## **Appendix 1. MATLAB/Simulink model of test bench**

Appendix 1. 1. Test bench SCALAR and DTC control mode MATLAB/Simulink model.....	104
---	-----



Appendix 1. 1. Test bench SCALAR and DTC control mode MATLAB/Simulink model

## **Appendix 2. Adaptive programs**

Testing sample: Pulse .....	106
Testing sample: Meander .....	107
Testing sample: Triangle .....	108
Testing sample: Trapeze .....	109
Testing sample: Sinusoidal .....	110
ECE-R15 Urban Driving Cycle .....	111
Adaptive program of dynamic load .....	112

86.01 = 6000
86.02 = 3000
86.03 = 2000
86.04 = 1000
86.05 = 32832
86.06 = 0
86.07 = 0
86.08 = 0
86.09 = 0
86.10 = 0
86.11 = MESSAGE1
86.12 = MESSAGE2
86.13 = MESSAGE3
86.14 = MESSAGE4
86.15 = MESSAGE5
1.17.6



EXT1 STRT/STPDIR	1004
EXT 1 STRT PTR	1004
EXT2 STRT/STPDIR	1002
EXT 2 STRT PTR	1005
EXTTEXT2 SELECT	1102
EXT 1/2 SEL PTR	1109
EXT REFT SELECT	1109 X
EXT 1 REF PTR	1110 -84.24
EXT REFS SELECT	1108
EXT 2 REF PTR	1111 -84.24
RELAY RO OUT	1401
RELAY RO PTR	1418
RELAY RO2 OUT	1409
RELAY RO2 PTR	1417
RELAY RO3 OUT	1409
RELAY RO3 PTR	1418
DIC MOD1 RO*	1410
RO PTR4	1410
DIC MOD1 RO2	1411
RO PTR5	1420
DIC MOD2 RO*	1412
RO PTR6	1421
DIC MOD2 RO2	1413
RO PTR7	1422
DIC MOD3 RO*	1414
RO PTR8	1423
DIC MOD3 RO2	1415
RO PTR9	1424
ANALOGUE OUTPUT1	1501
ACT PTR	1511
ANALOGUE OUTPUT2	1506
ACT PTR	1512
RUN ENABLE	1601
RUN ENA PTR	1606
FAULT RESET SEL	1604
FAULT RESET PTR	1611
MIN TORQ SEL	2013
TORQ MIN PTR	2018
MAX TORQ SEL	2014
TORQ MAX PTR	2019
ACC/DEC SEL	2201
ACC PTR	2208
DEC PTR	2209
NOT MOD COMPENSA	3507
NOT MOD COMP PTR	3508
ACTUAL INPLT SEL	4027
ACTUAL PTR	4025
TRIM REF SEL	4016
TRIM REF PTR	4028
FLUX REF PTR	2609
MSW 511 PTR	9218
MSW 514 PTR	9219

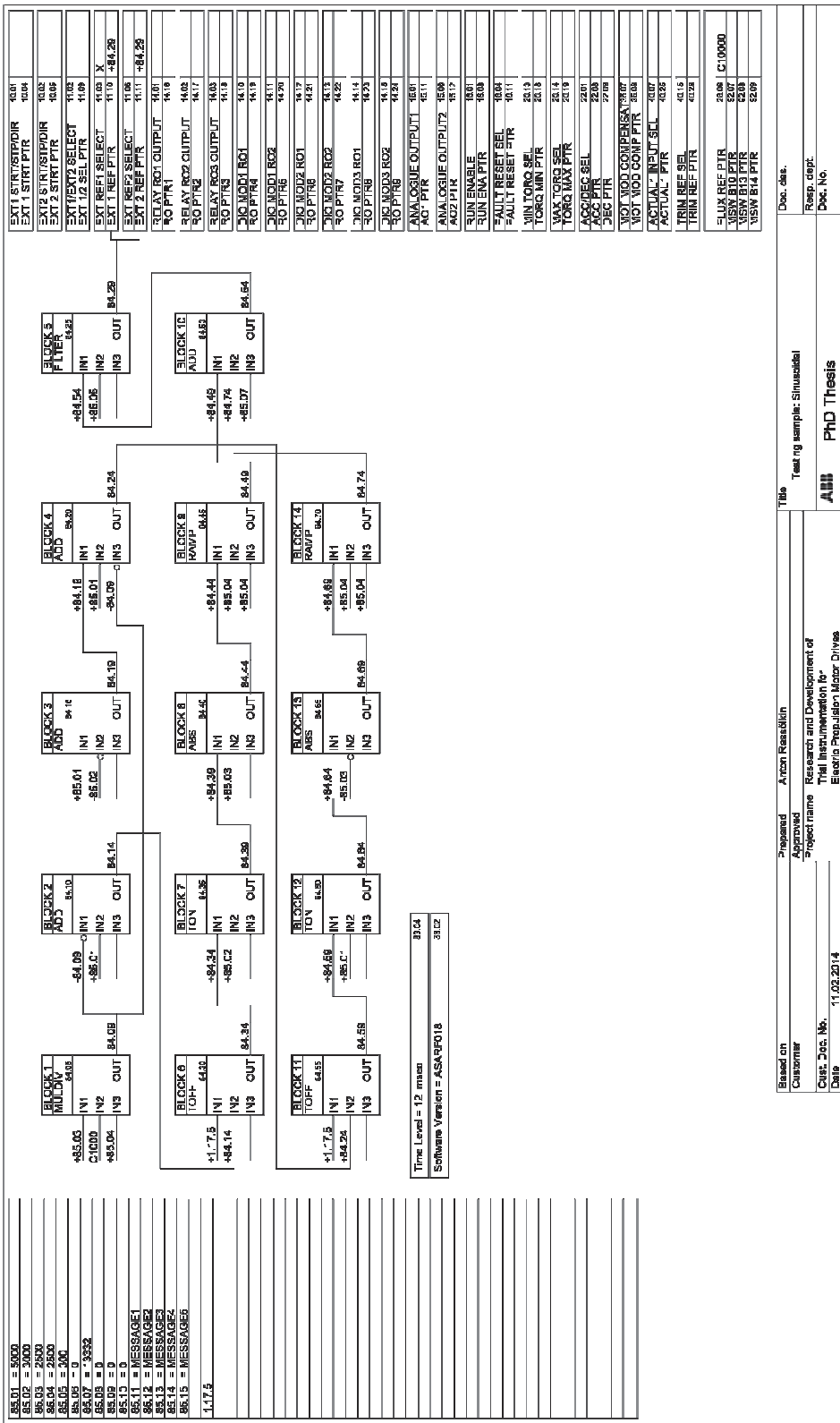
Time Level = 12 msec  
 31.04  
 32.02  
 Software Version = ASARFD16

Based on Customer	Prepared by	Ambar Rassaikin	Title	Doc. dis.
	Approved		Testing sample: Pulse	
Project name	Research and Development of Trial Instrumentation for Electric Propulsion Motor Drives			
Cust. Doc. No.	11.02.2014	<b>A111</b>	<b>PHD Thesis</b>	
Date				









Time Level = 12 msec  
 Software Version = ASAR010

EXT1 STRT REF PTR	601	604
EXT1 STRT PTR	603	606
EXT2 STRT REF PTR	605	608
EXT2 STRT PTR	607	610
EXT1/2 SELECT	609	
EXT1/2 SEL PTR	611	
EXT REF1 SELECT	613	X
EXT REF1 PTR	615	618, 621, 28
EXT REF2 SELECT	617	
EXT REF2 PTR	619	622, 28
RELAY ROT OUTPUT	621	624, 28
RELAY ROT PTR	623	
RELAY ROT OUTPUT	625	
RELAY ROT PTR	627	
RELAY ROT OUTPUT	629	
RELAY ROT PTR	631	
RELAY ROT OUTPUT	633	
RELAY ROT PTR	635	
RELAY ROT OUTPUT	637	
RELAY ROT PTR	639	
RELAY ROT OUTPUT	641	
RELAY ROT PTR	643	
RELAY ROT OUTPUT	645	
RELAY ROT PTR	647	
RELAY ROT OUTPUT	649	
RELAY ROT PTR	651	
RELAY ROT OUTPUT	653	
RELAY ROT PTR	655	
RELAY ROT OUTPUT	657	
RELAY ROT PTR	659	
RELAY ROT OUTPUT	661	
RELAY ROT PTR	663	
RELAY ROT OUTPUT	665	
RELAY ROT PTR	667	
RELAY ROT OUTPUT	669	
RELAY ROT PTR	671	
RELAY ROT OUTPUT	673	
RELAY ROT PTR	675	
RELAY ROT OUTPUT	677	
RELAY ROT PTR	679	
RELAY ROT OUTPUT	681	
RELAY ROT PTR	683	
RELAY ROT OUTPUT	685	
RELAY ROT PTR	687	
RELAY ROT OUTPUT	689	
RELAY ROT PTR	691	
RELAY ROT OUTPUT	693	
RELAY ROT PTR	695	
RELAY ROT OUTPUT	697	
RELAY ROT PTR	699	
RELAY ROT OUTPUT	701	
RELAY ROT PTR	703	
RELAY ROT OUTPUT	705	
RELAY ROT PTR	707	
RELAY ROT OUTPUT	709	
RELAY ROT PTR	711	
RELAY ROT OUTPUT	713	
RELAY ROT PTR	715	
RELAY ROT OUTPUT	717	
RELAY ROT PTR	719	
RELAY ROT OUTPUT	721	
RELAY ROT PTR	723	
RELAY ROT OUTPUT	725	
RELAY ROT PTR	727	
RELAY ROT OUTPUT	729	
RELAY ROT PTR	731	
RELAY ROT OUTPUT	733	
RELAY ROT PTR	735	
RELAY ROT OUTPUT	737	
RELAY ROT PTR	739	
RELAY ROT OUTPUT	741	
RELAY ROT PTR	743	
RELAY ROT OUTPUT	745	
RELAY ROT PTR	747	
RELAY ROT OUTPUT	749	
RELAY ROT PTR	751	
RELAY ROT OUTPUT	753	
RELAY ROT PTR	755	
RELAY ROT OUTPUT	757	
RELAY ROT PTR	759	
RELAY ROT OUTPUT	761	
RELAY ROT PTR	763	
RELAY ROT OUTPUT	765	
RELAY ROT PTR	767	
RELAY ROT OUTPUT	769	
RELAY ROT PTR	771	
RELAY ROT OUTPUT	773	
RELAY ROT PTR	775	
RELAY ROT OUTPUT	777	
RELAY ROT PTR	779	
RELAY ROT OUTPUT	781	
RELAY ROT PTR	783	
RELAY ROT OUTPUT	785	
RELAY ROT PTR	787	
RELAY ROT OUTPUT	789	
RELAY ROT PTR	791	
RELAY ROT OUTPUT	793	
RELAY ROT PTR	795	
RELAY ROT OUTPUT	797	
RELAY ROT PTR	799	
RELAY ROT OUTPUT	801	
RELAY ROT PTR	803	
RELAY ROT OUTPUT	805	
RELAY ROT PTR	807	
RELAY ROT OUTPUT	809	
RELAY ROT PTR	811	
RELAY ROT OUTPUT	813	
RELAY ROT PTR	815	
RELAY ROT OUTPUT	817	
RELAY ROT PTR	819	
RELAY ROT OUTPUT	821	
RELAY ROT PTR	823	
RELAY ROT OUTPUT	825	
RELAY ROT PTR	827	
RELAY ROT OUTPUT	829	
RELAY ROT PTR	831	
RELAY ROT OUTPUT	833	
RELAY ROT PTR	835	
RELAY ROT OUTPUT	837	
RELAY ROT PTR	839	
RELAY ROT OUTPUT	841	
RELAY ROT PTR	843	
RELAY ROT OUTPUT	845	
RELAY ROT PTR	847	
RELAY ROT OUTPUT	849	
RELAY ROT PTR	851	
RELAY ROT OUTPUT	853	
RELAY ROT PTR	855	
RELAY ROT OUTPUT	857	
RELAY ROT PTR	859	
RELAY ROT OUTPUT	861	
RELAY ROT PTR	863	
RELAY ROT OUTPUT	865	
RELAY ROT PTR	867	
RELAY ROT OUTPUT	869	
RELAY ROT PTR	871	
RELAY ROT OUTPUT	873	
RELAY ROT PTR	875	
RELAY ROT OUTPUT	877	
RELAY ROT PTR	879	
RELAY ROT OUTPUT	881	
RELAY ROT PTR	883	
RELAY ROT OUTPUT	885	
RELAY ROT PTR	887	
RELAY ROT OUTPUT	889	
RELAY ROT PTR	891	
RELAY ROT OUTPUT	893	
RELAY ROT PTR	895	
RELAY ROT OUTPUT	897	
RELAY ROT PTR	899	
RELAY ROT OUTPUT	901	
RELAY ROT PTR	903	
RELAY ROT OUTPUT	905	
RELAY ROT PTR	907	
RELAY ROT OUTPUT	909	
RELAY ROT PTR	911	
RELAY ROT OUTPUT	913	
RELAY ROT PTR	915	
RELAY ROT OUTPUT	917	
RELAY ROT PTR	919	
RELAY ROT OUTPUT	921	
RELAY ROT PTR	923	
RELAY ROT OUTPUT	925	
RELAY ROT PTR	927	
RELAY ROT OUTPUT	929	
RELAY ROT PTR	931	
RELAY ROT OUTPUT	933	
RELAY ROT PTR	935	
RELAY ROT OUTPUT	937	
RELAY ROT PTR	939	
RELAY ROT OUTPUT	941	
RELAY ROT PTR	943	
RELAY ROT OUTPUT	945	
RELAY ROT PTR	947	
RELAY ROT OUTPUT	949	
RELAY ROT PTR	951	
RELAY ROT OUTPUT	953	
RELAY ROT PTR	955	
RELAY ROT OUTPUT	957	
RELAY ROT PTR	959	
RELAY ROT OUTPUT	961	
RELAY ROT PTR	963	
RELAY ROT OUTPUT	965	
RELAY ROT PTR	967	
RELAY ROT OUTPUT	969	
RELAY ROT PTR	971	
RELAY ROT OUTPUT	973	
RELAY ROT PTR	975	
RELAY ROT OUTPUT	977	
RELAY ROT PTR	979	
RELAY ROT OUTPUT	981	
RELAY ROT PTR	983	
RELAY ROT OUTPUT	985	
RELAY ROT PTR	987	
RELAY ROT OUTPUT	989	
RELAY ROT PTR	991	
RELAY ROT OUTPUT	993	
RELAY ROT PTR	995	
RELAY ROT OUTPUT	997	
RELAY ROT PTR	999	
RELAY ROT OUTPUT	1001	

Doc. des. \_\_\_\_\_  
 Resp. dept. \_\_\_\_\_  
 Doc. No. \_\_\_\_\_

Test ing sample: Shuuzidai

Prepared \_\_\_\_\_  
 Approved \_\_\_\_\_  
 Customer \_\_\_\_\_  
 Project name \_\_\_\_\_  
 Date \_\_\_\_\_

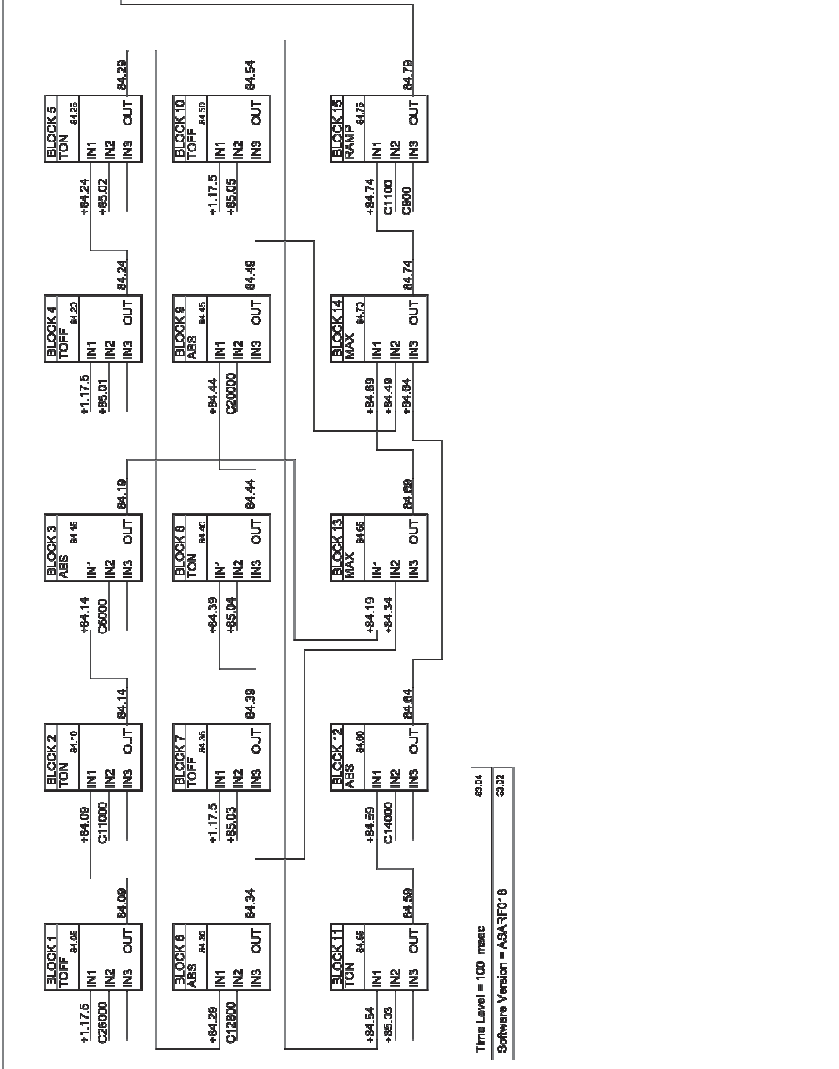
Research and Development of  
 Thin Insulation for  
 Electric Power Distribution

1111 PhD Thesis

Based on \_\_\_\_\_  
 Customer \_\_\_\_\_  
 Date \_\_\_\_\_

11.02.2014

85.01 = 85000	EX1 STRT1PDIR	10.01
85.02 = 80000	EX1 STRT1PTR	10.04
85.03 = 495000	EX2 STRT2PDIR	10.08
85.04 = 495000	EX2 STRT2PTR	10.16
85.05 = 0	EX1/2 SEL	11.08
85.06 = 0	EX1/2 SEL PTR	11.04
85.07 = 0	EX1 REF1 SELECT	11.08 X
85.08 = 0	EX1 REF1 PTR	11.01 401.79
85.09 = 0	EX1 REF2 SELECT	11.08
85.10 = 0	EX1 REF2 PTR	11.01
85.11 = MESSAGE1	RELAY R01 OUTPUT	14.01
85.12 = MESSAGE2	RO PTR1	14.16
85.13 = MESSAGE3	RELAY R02 OUTPUT	14.01
85.14 = MESSAGE4	RO PTR2	14.16
85.15 = MESSAGE5	RELAY R03 OUTPUT	14.01
1.17.5	RO PTR3	14.16
	DIO MOD1 R01	14.16
	RO P1M1	14.16
	DIO MOD1 R02	14.16
	RO P1M2	14.16
	DIO MOD2 R01	14.16
	RO P1M3	14.16
	DIO MOD2 R02	14.16
	RO P1M4	14.16
	DIO MOD3 R01	14.16
	RO P1M5	14.16
	DIO MOD3 R02	14.16
	RO P1M6	14.16
	ANALOGUE OUTPUT1	16.01
	ANAL1 PTR	16.11
	ANAL1 GROUP OUTPUT2	16.08
	ANAL2 PTR	16.11
	ANAL2 GROUP	16.08
	ANAL3 PTR	16.11
	ANAL3 GROUP	16.08
	FAULT RESET SEL	16.08
	FAULT RESET PTR	16.11
	MIN TO Q SEL	20.16
	TORQ MIN PTR	20.16
	MAX TORQ SEL	20.16
	TORQ MAX PTR	20.16
	ACC DEC SEL	22.08
	DEC PTR	22.08
	WOT WOD COMPENSATION	30.16
	WOT WOD COMP PTR	30.16
	ACTUAL IN/OUT SEL	40.16
	ACTUAL IN/OUT PTR	40.16
	TRIM REF SEL	42.16
	TRIM REF PTR	42.16
	FLUX REF PTR	20.08 C10000
	MSW B10 PTR	60.07 13.14.9
	MSW B13 PTR	62.08
	MSW B14 PTR	62.08



85.01 = 85000	EX1 STRT1PDIR	10.01
85.02 = 80000	EX1 STRT1PTR	10.04
85.03 = 495000	EX2 STRT2PDIR	10.08
85.04 = 495000	EX2 STRT2PTR	10.16
85.05 = 0	EX1/2 SEL	11.08
85.06 = 0	EX1/2 SEL PTR	11.04
85.07 = 0	EX1 REF1 SELECT	11.08 X
85.08 = 0	EX1 REF1 PTR	11.01 401.79
85.09 = 0	EX1 REF2 SELECT	11.08
85.10 = 0	EX1 REF2 PTR	11.01
85.11 = MESSAGE1	RELAY R01 OUTPUT	14.01
85.12 = MESSAGE2	RO PTR1	14.16
85.13 = MESSAGE3	RELAY R02 OUTPUT	14.01
85.14 = MESSAGE4	RO PTR2	14.16
85.15 = MESSAGE5	RELAY R03 OUTPUT	14.01
1.17.5	RO PTR3	14.16
	DIO MOD1 R01	14.16
	RO P1M1	14.16
	DIO MOD1 R02	14.16
	RO P1M2	14.16
	DIO MOD2 R01	14.16
	RO P1M3	14.16
	DIO MOD2 R02	14.16
	RO P1M4	14.16
	DIO MOD3 R01	14.16
	RO P1M5	14.16
	DIO MOD3 R02	14.16
	RO P1M6	14.16
	ANALOGUE OUTPUT1	16.01
	ANAL1 PTR	16.11
	ANAL1 GROUP OUTPUT2	16.08
	ANAL2 PTR	16.11
	ANAL2 GROUP	16.08
	ANAL3 PTR	16.11
	ANAL3 GROUP	16.08
	FAULT RESET SEL	16.08
	FAULT RESET PTR	16.11
	MIN TO Q SEL	20.16
	TORQ MIN PTR	20.16
	MAX TORQ SEL	20.16
	TORQ MAX PTR	20.16
	ACC DEC SEL	22.08
	DEC PTR	22.08
	WOT WOD COMPENSATION	30.16
	WOT WOD COMP PTR	30.16
	ACTUAL IN/OUT SEL	40.16
	ACTUAL IN/OUT PTR	40.16
	TRIM REF SEL	42.16
	TRIM REF PTR	42.16
	FLUX REF PTR	20.08 C10000
	MSW B10 PTR	60.07 13.14.9
	MSW B13 PTR	62.08
	MSW B14 PTR	62.08

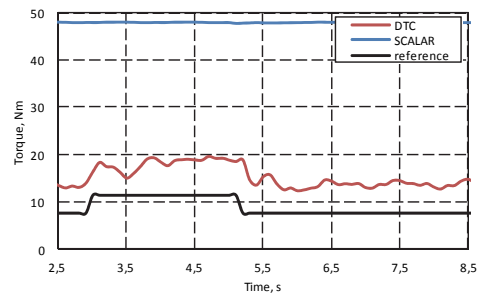
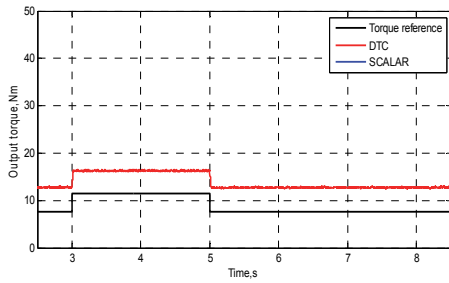
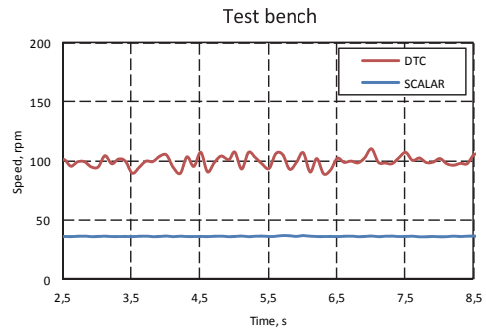
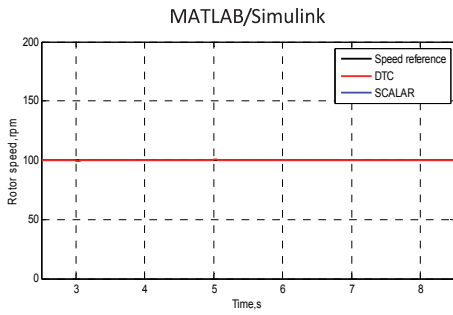
Time Level = 100 msec  
Software Version = AS9A1P1-0  
20.04  
33.32

Doc. No.	ECER15 Urban Dring Cycle
Rev. No.	1
Doc. No.	AB01
Doc. No.	PHD Thesis
Prepared on	Arizon Resistorlin
Customer	Arizon Resistorlin
Project Name	Research and Development of Local Instrumentation for Electric Propulsion Motor Drive
Cust. Doc. No.	11.32.2014
Date	11.32.2014

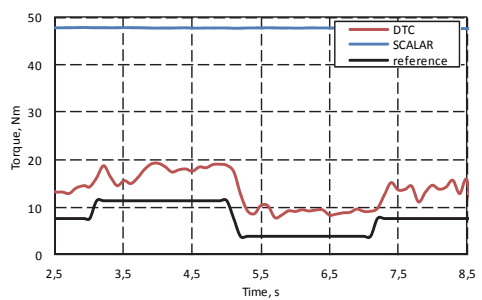
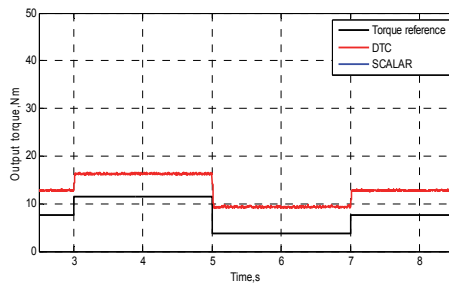
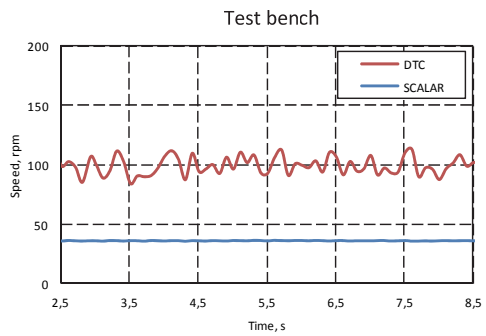
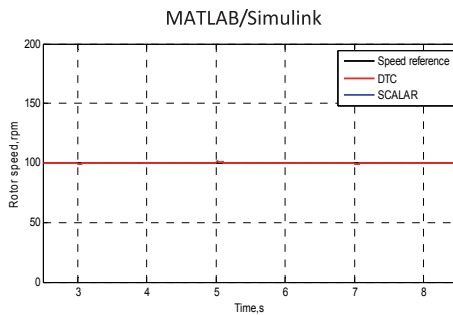


### **Appendix 3. Results observed from MATLAB/Simulink simulation and test bench experiments**

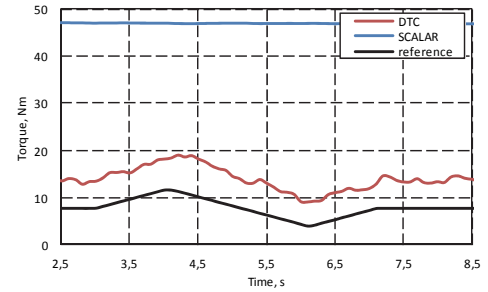
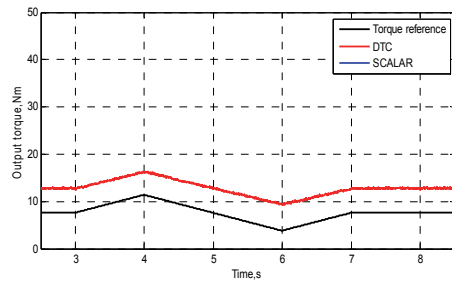
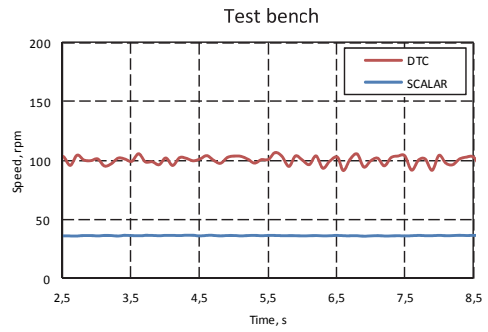
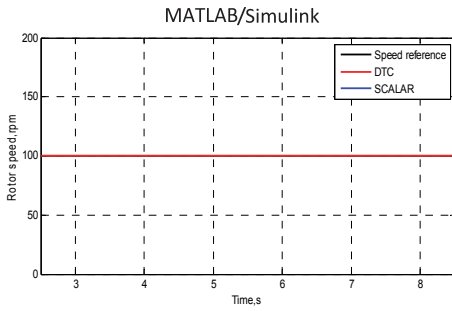
Speed response under different torque references on speed 100 rpm .....	114
Appendix 3. 1 - 3. 5;	
Speed response under different torque references on speed 1000 rpm .....	116
Appendix 3. 6 - 3. 10;	
Torque response under different speed references at zero speed .....	119
Appendix 3. 11 - 3. 14;	
Torque response under different speed references at 1000 rpm .....	121
Torque response under static load:	
Appendix 3. 15, 3. 17, 3. 19, 3. 21;	
Torque response under dynamic load:	
Appendix 3. 16, 3. 18, 3. 20, 3. 22.	



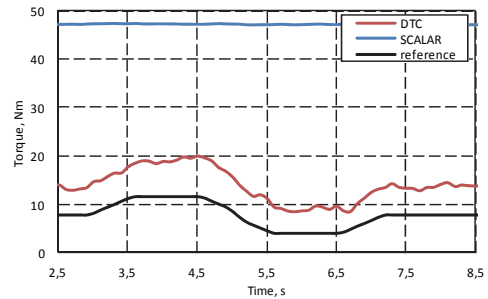
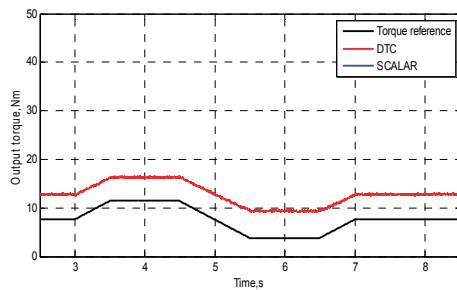
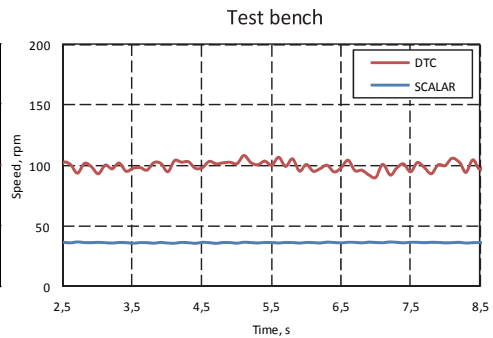
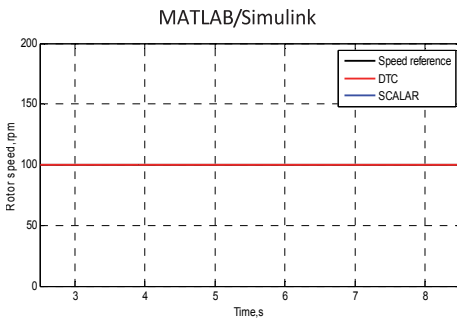
Appendix 3. 1. Speed response on torque pulse reference under different control modes



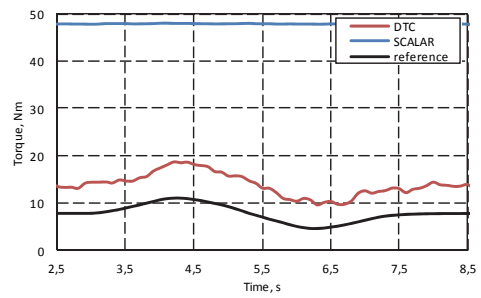
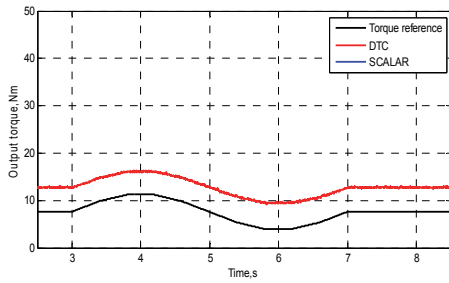
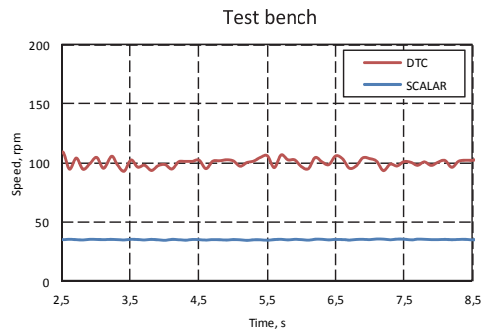
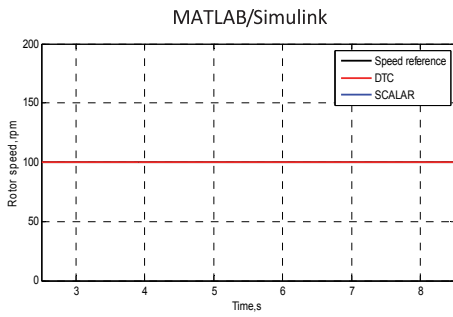
Appendix 3. 2. Speed response on torque meander reference under different control modes



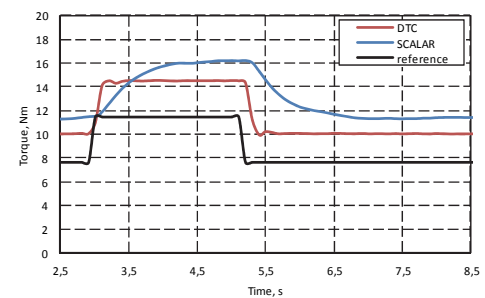
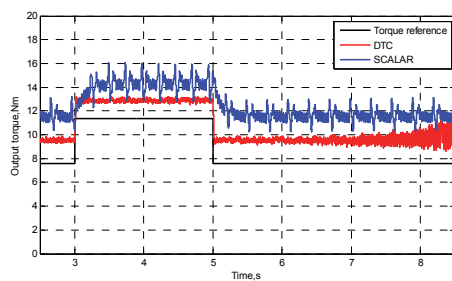
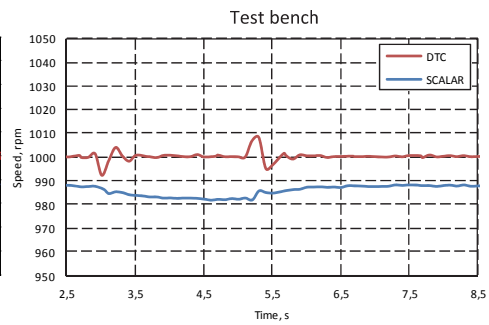
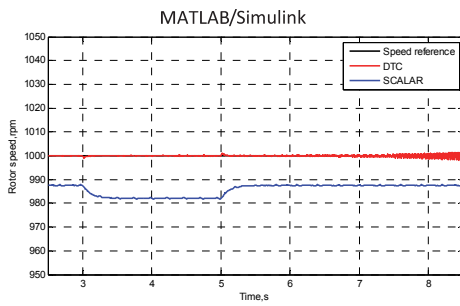
*Appendix 3. 3. Speed response on torque triangle reference under different control modes*



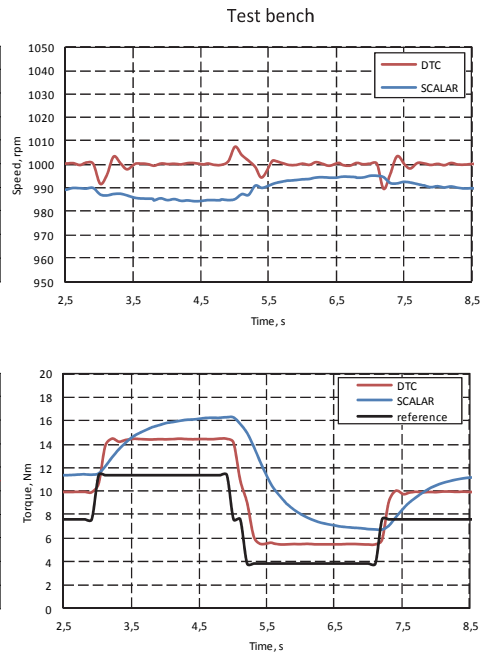
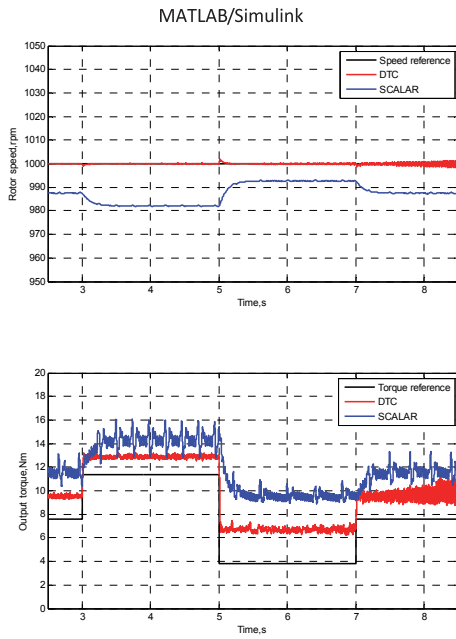
*Appendix 3. 4. Speed response on torque trapeze reference under different control modes*



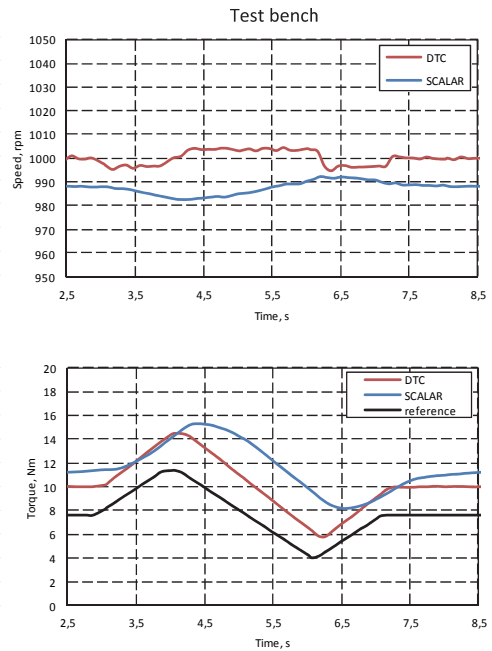
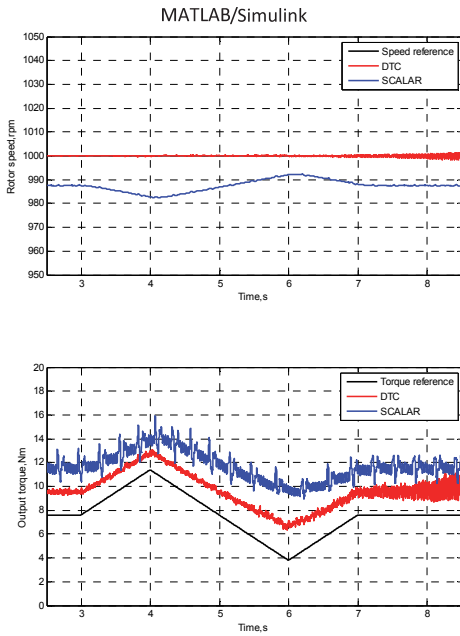
Appendix 3. 5. Speed response on torque sinusoidal reference under different control modes



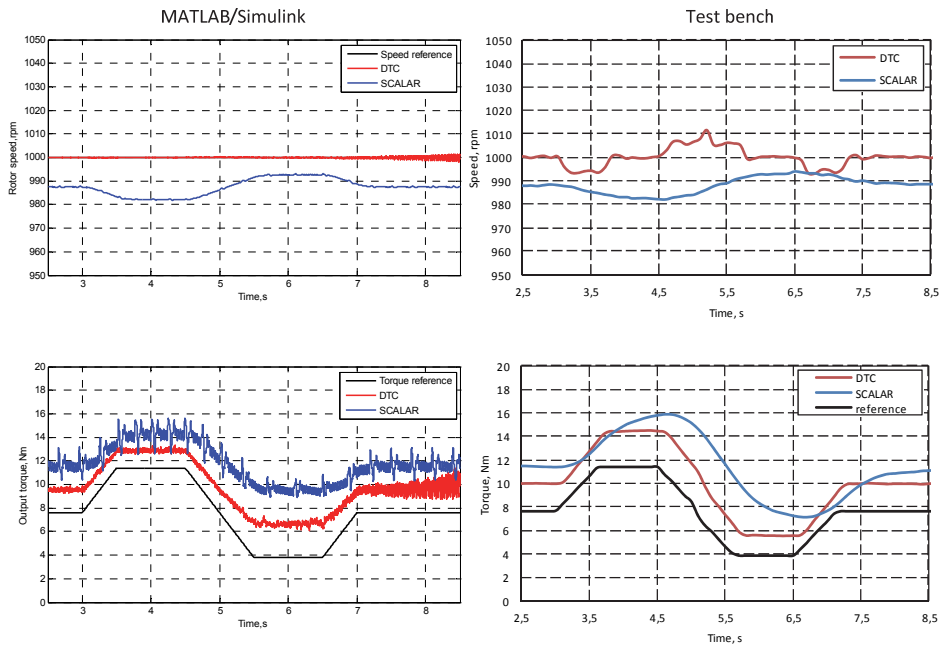
Appendix 3. 6. Speed response on torque pulse reference under different control modes



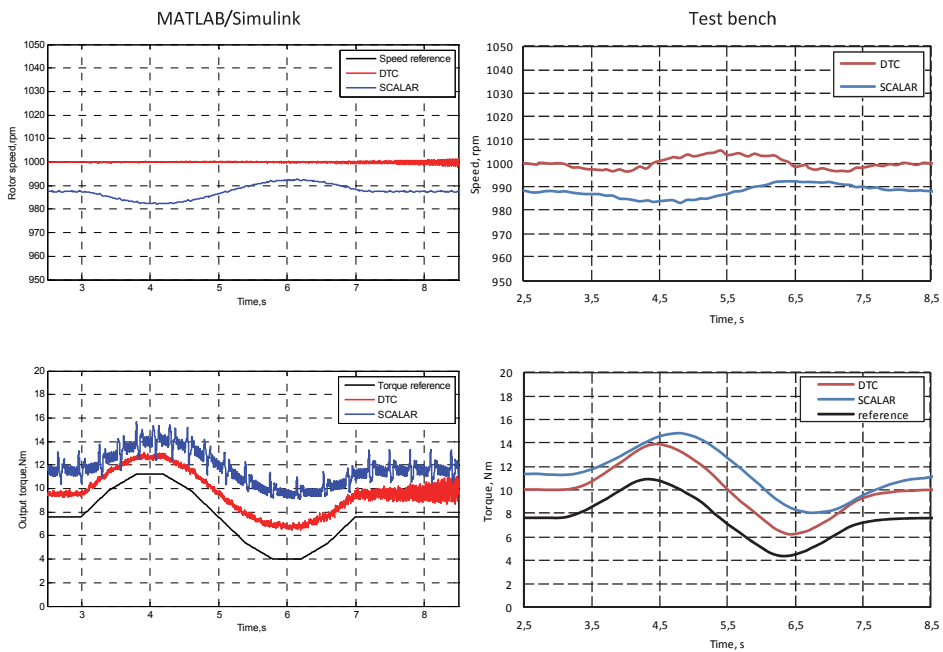
*Appendix 3. 7. Speed response on torque meander reference under different control modes*



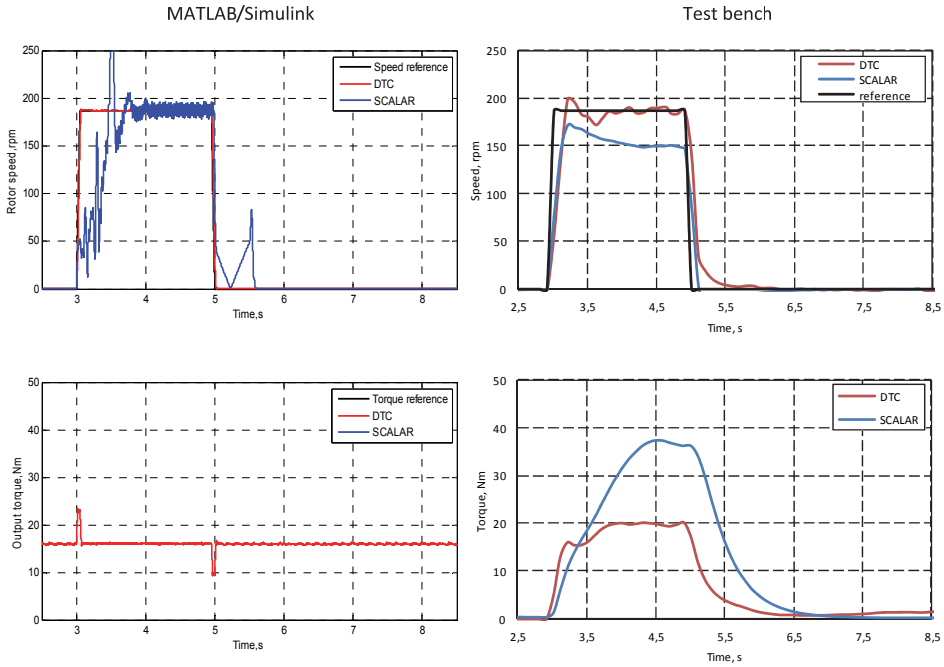
*Appendix 3. 8. Speed response on torque triangle reference under different control modes*



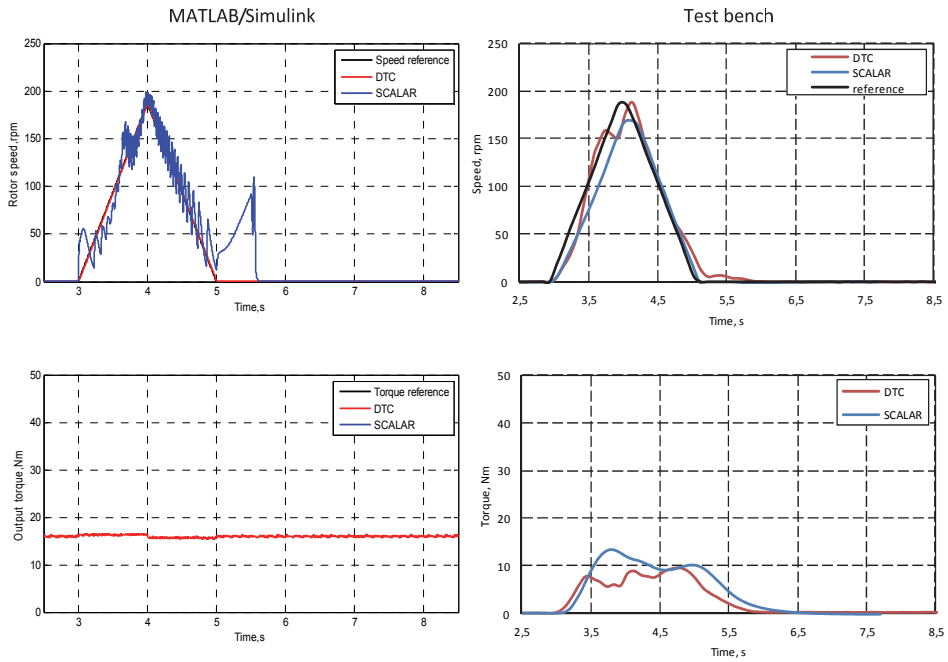
*Appendix 3. 9. Speed response on torque trapeze reference under different control modes*



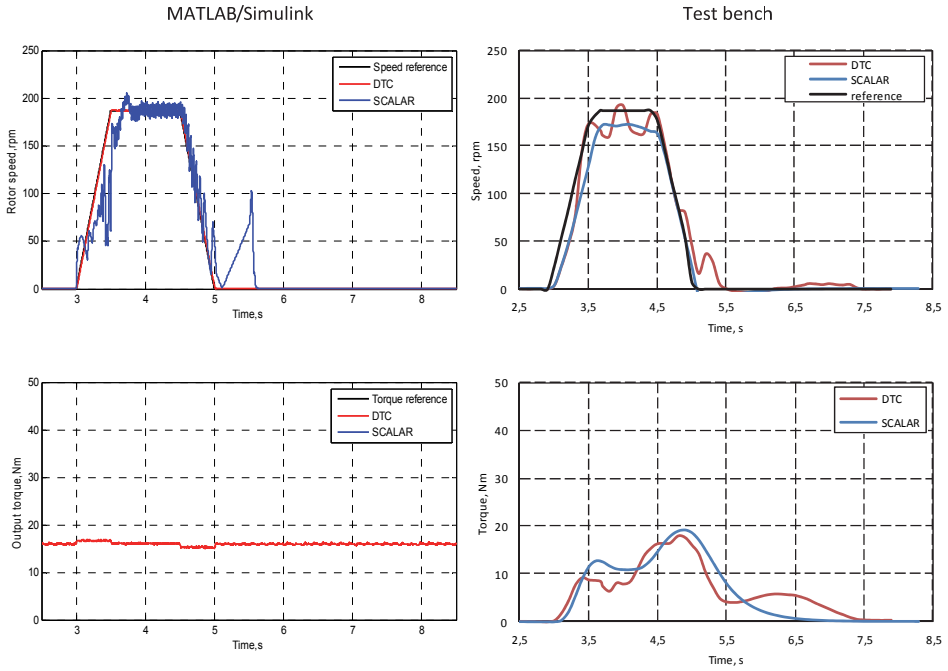
*Appendix 3. 10. Speed response on torque sinusoidal reference under different control modes*



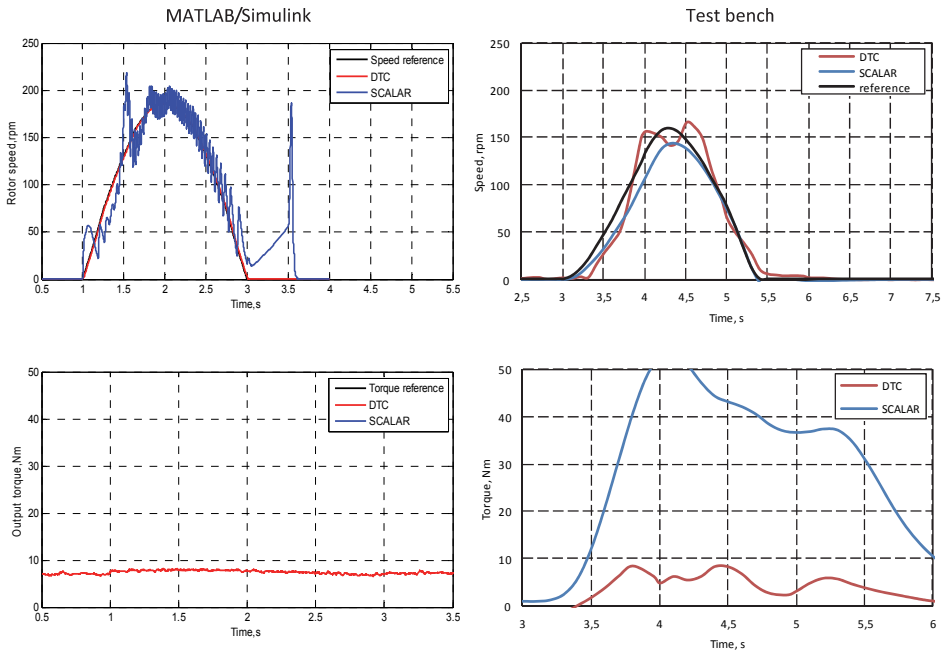
Appendix 3. 11. Torque response on speed pulse reference under different control modes



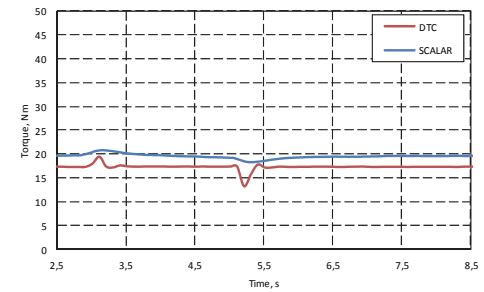
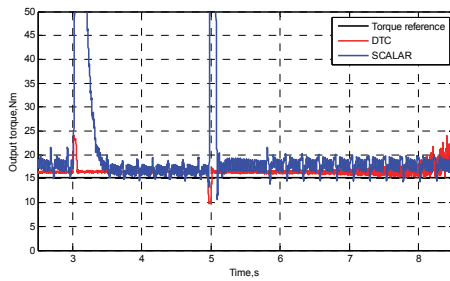
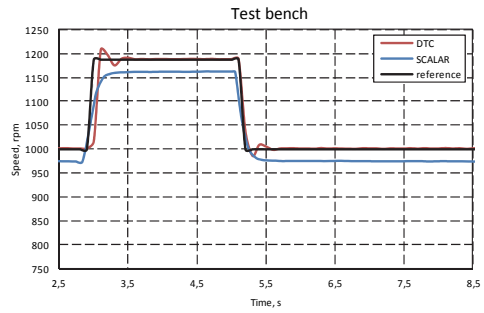
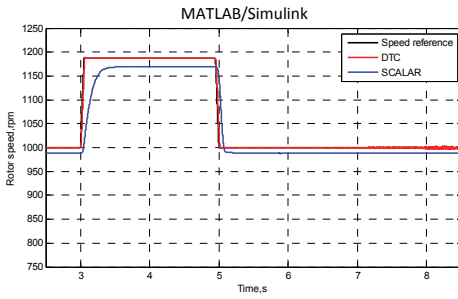
Appendix 3. 12. Torque response on speed triangle reference under different control modes



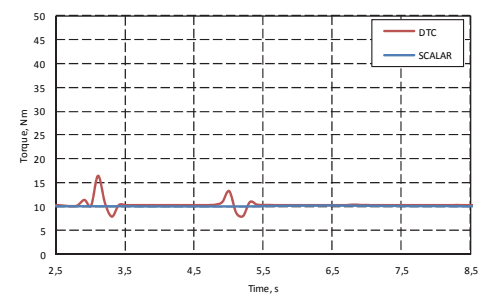
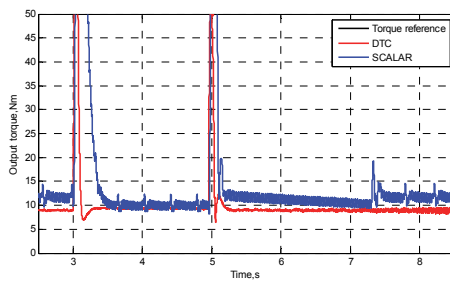
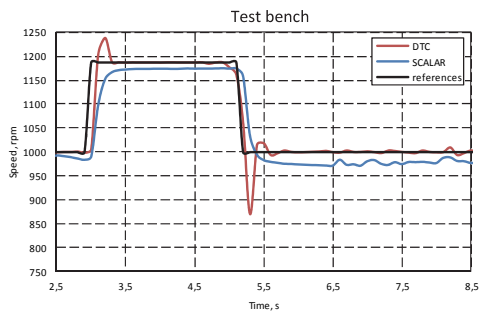
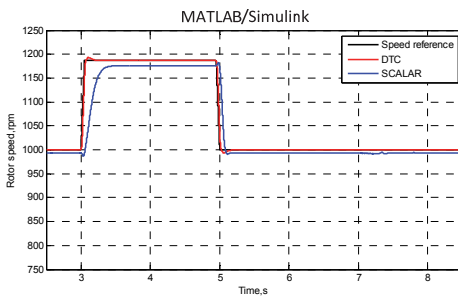
Appendix 3.13. Torque response on speed trapeze reference under different control modes



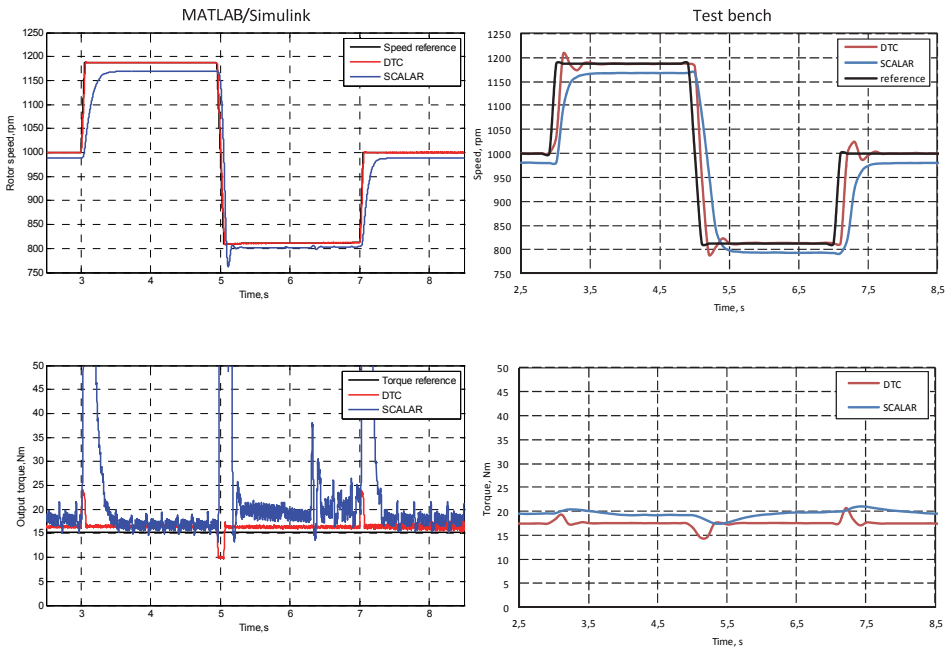
Appendix 3.14. Torque response on speed sinusoidal reference under different control modes



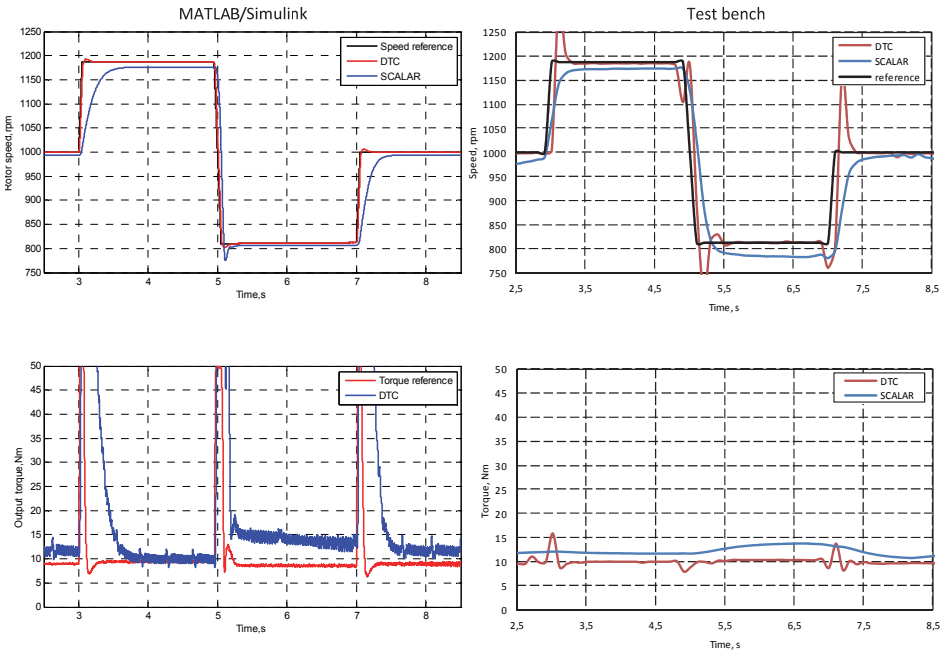
Appendix 3. 15. Torque response on speed pulse reference under different control modes



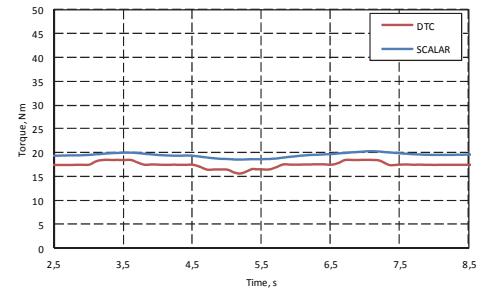
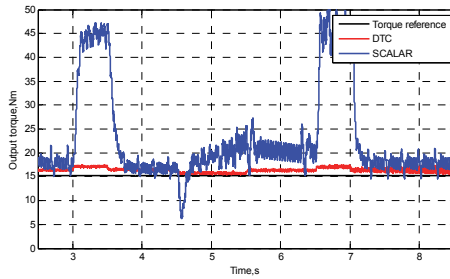
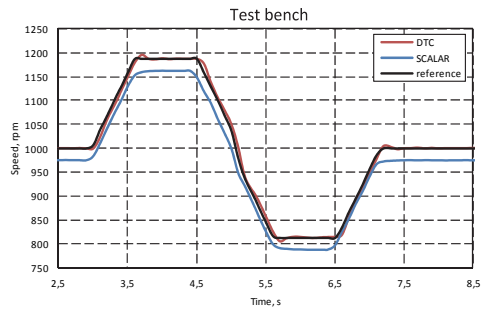
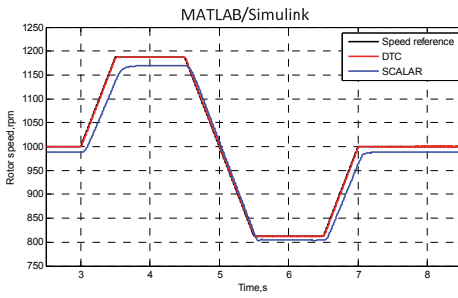
Appendix 3. 16. Torque response (dynamic load) on speed pulse reference under different control modes



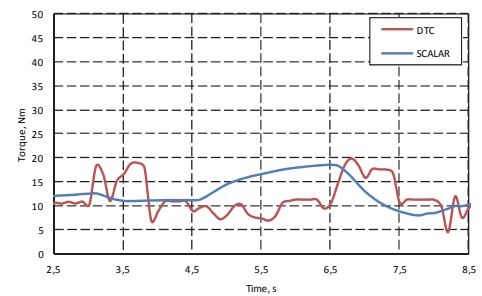
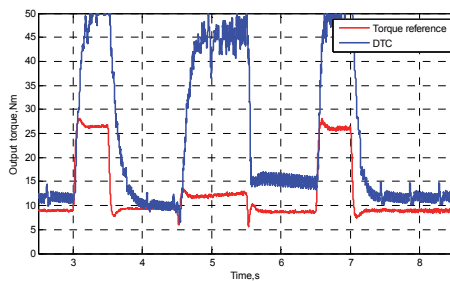
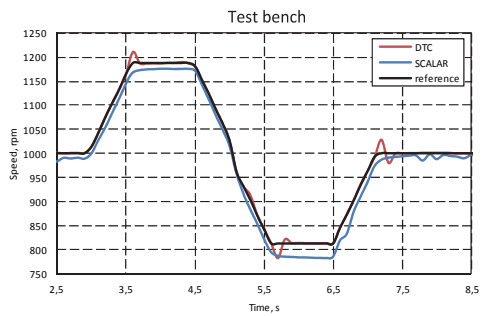
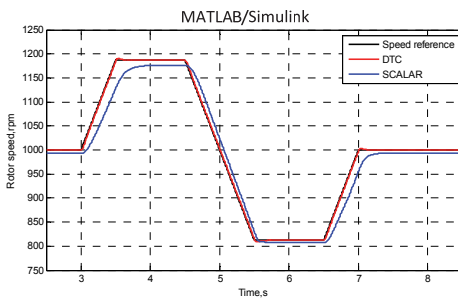
*Appendix 3. 17. Torque response on speed meander reference under different control modes*



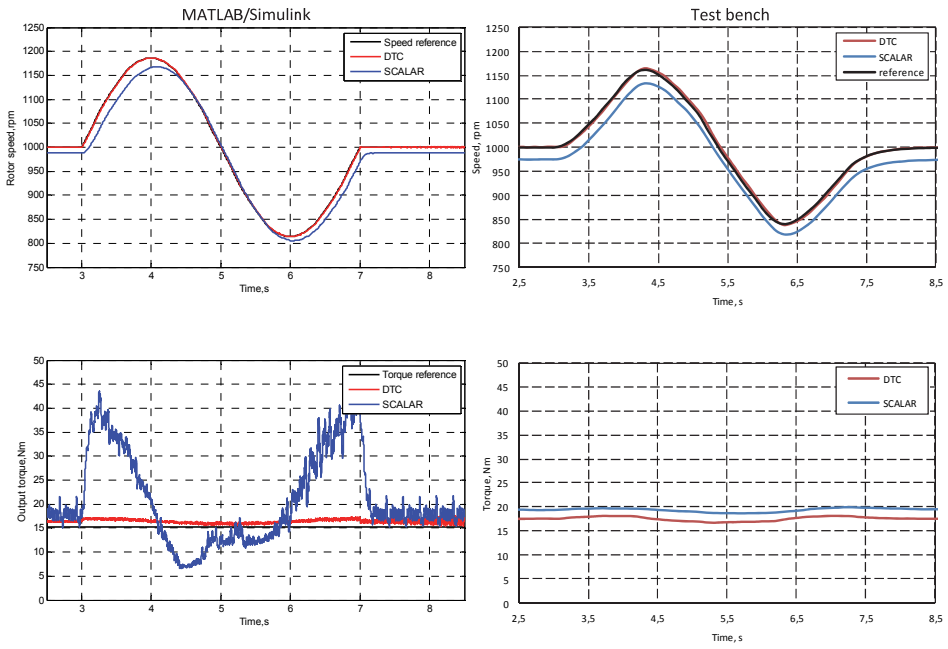
*Appendix 3. 18. Torque response (dynamic load) on speed meander reference under different control modes*



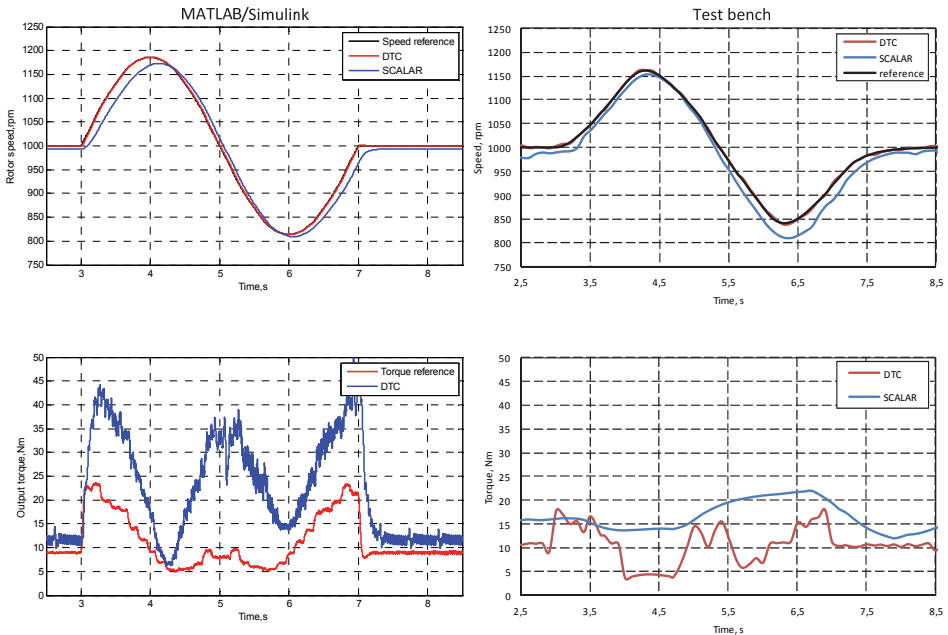
*Appendix 3. 19. Torque response on speed trapeze reference under different control modes*



*Appendix 3. 20. Torque response (dynamic load) on speed trapeze reference under different control modes*



Appendix 3. 21. Torque response on speed sinusoidal reference under different control modes



Appendix 3. 22. Torque response (dynamic load) on speed sinusoidal reference under different control modes

**DISSERTATIONS DEFENDED AT  
TALLINN UNIVERSITY OF TECHNOLOGY ON  
POWER ENGINEERING, ELECTRICAL ENGINEERING, MINING  
ENGINEERING**

1. **Jaan Tehver**. Boiling on Porous Surface. 1992.
2. Salastatud.
3. **Endel Risthein**. Electricity Supply of Industrial Plants. 1993.
4. **Tõnu Trump**. Some New Aspects of Digital Filtering. 1993.
5. **Vello Sarv**. Synthesis and Design of Power Converters with Reduced Distortions Using Optimal Energy Exchange Control. 1994.
6. **Ivan Klevtsov**. Strained Condition Diagnosis and Fatigue Life Prediction for Metals under Cyclic Temperature Oscillations. 1994.
7. **Ants Meister**. Some Phase-Sensitive and Spectral Methods in Biomedical Engineering. 1994.
8. **Mati Meldorf**. Steady-State Monitoring of Power System. 1995.
9. **Jüri-Rivaldo Pastarus**. Large Cavern Stability in the Maardu Granite Deposit. 1996.
10. **Enn Velmre**. Modeling and Simulation of Bipolar Semiconductor Devices. 1996.
11. **Kalju Meigas**. Coherent Photodetection with a Laser. 1997.
12. **Andres Udal**. Development of Numerical Semiconductor Device Models and Their Application in Device Theory and Design. 1998.
13. **Kuno Janson**. Paralleel- ja järjestikresonantsi parameetrilise vaheldumisega võrgusageduslik resonantsmuundur ja tema rakendamine. 2001.
14. **Jüri Joller**. Research and Development of Energy Saving Traction Drives for Trams. 2001.
15. **Ingo Valgma**. Geographical Information System for Oil Shale Mining – MGIS. 2002.
16. **Raik Jansikene**. Research, Design and Application of Magnetohydrodynamical (MHD) Devices for Automation of Casting Industry. 2003.
17. **Oleg Nikitin**. Optimization of the Room-and-Pillar Mining Technology for Oil-Shale Mines. 2003.
18. **Viktor Bolgov**. Load Current Stabilization and Suppression of Flicker in AC Arc Furnace Power Supply by Series-Connected Saturable Reactor. 2004.
19. **Raine Pajo**. Power System Stability Monitoring – An Approach of Electrical Load Modelling. 2004.
20. **Jelena Shuvalova**. Optimal Approximation of Input-Output Characteristics of Power Units and Plants. 2004.
21. **Nikolai Dorovatovski**. Thermographic Diagnostics of Electrical Equipment of Eesti Energia Ltd. 2004.
22. **Katrin Erg**. Groundwater Sulphate Content Changes in Estonian Underground Oil Shale Mines. 2005.

23. **Argo Rosin.** Control, Supervision and Operation Diagnostics of Light Rail Electric Transport. 2005.
24. **Dmitri Vinnikov.** Research, Design and Implementation of Auxiliary Power Supplies for the Light Rail Vehicles. 2005.
25. **Madis Lehtla.** Microprocessor Control Systems of Light Rail Vehicle Traction Drives. 2006.
26. **Jevgeni Šklovski.** LC Circuit with Parallel and Series Resonance Alternation in Switch-Mode Converters. 2007.
27. **Sten Suuroja.** Comparative Morphological Analysis of the Early Paleozoic Marine Impact Structures Kärddla and Neugrund, Estonia. 2007.
28. **Sergei Sabanov.** Risk Assessment Methods in Estonian Oil Shale Mining Industry. 2008.
29. **Vitali Boiko.** Development and Research of the Traction Asynchronous Multimotor Drive. 2008.
30. **Tauno Tammeoja.** Economic Model of Oil Shale Flows and Cost. 2008.
31. **Jelena Armas.** Quality Criterion of road Lighting Measurement and Exploring. 2008.
32. **Olavi Tammemäe.** Basics for Geotechnical Engineering Explorations Considering Needed Legal Changes. 2008.
33. **Mart Landsberg.** Long-Term Capacity Planning and Feasibility of Nuclear Power in Estonia under Certain Conditions. 2008.
34. **Hardi Torn.** Engineering-Geological Modelling of the Sillamäe Radioactive Tailings Pond Area. 2008.
35. **Aleksander Kilk.** Paljupooluselise püsimagnetitega sünkroongeneraator tuuleagregaatidele. 2008.
36. **Olga Ruban.** Analysis and Development of the PLC Control System with the Distributed I/Os. 2008.
37. **Jako Kilter.** Monitoring of Electrical Distribution Network Operation. 2009.
38. **Ivo Palu.** Impact of Wind Parks on Power System Containing Thermal Power Plants. 2009.
39. **Hannes Agabus.** Large-Scale Integration of Wind Energy into the Power System Considering the Uncertainty Information. 2009.
40. **Kalle Kilk.** Variations of Power Demand and Wind Power Generation and Their Influence to the Operation of Power Systems. 2009.
41. **Indrek Roasto.** Research and Development of Digital Control Systems and Algorithms for High Power, High Voltage Isolated DC/DC Converters. 2009.
42. **Hardi Hõimoja.** Energiatõhususe hindamise ja energiasalvestite arvutuse meetodika linna elektertranspordile. 2009.
43. **Tanel Jalakas.** Research and Development of High-Power High-Voltage DC/DC Converters. 2010.
44. **Helena Lind.** Groundwater Flow Model of the Western Part of the Estonian Oil Shale Deposit. 2010.
45. **Arvi Hamburg.** Analysis of Energy Development Perspectives. 2010.

46. **Mall Orru.** Dependence of Estonian Peat Deposit Properties on Landscape Types and Feeding Conditions. 2010.
47. **Erik Väli.** Best Available Technology for the Environmentally Friendly Mining with Surface Miner. 2011.
48. **Tarmo Tohver.** Utilization of Waste Rock from Oil Shale Mining. 2011.
49. **Mikhail Egorov.** Research and Development of Control Methods for Low-Loss IGBT Inverter-Fed Induction Motor Drives. 2011.
50. **Toomas Vinnal.** Eesti ettevõtete elektritarbimise uurimine ja soovitude väljatöötamine tarbimise optimeerimiseks. 2011.
51. **Veiko Karu.** Potential Usage of Underground Mined Areas in Estonian Oil Shale Deposit. 2012.
52. **Zoja Raud.** Research and Development of an Active Learning Technology for University-Level Education in the Field of Electronics and Power Electronics. 2012.
53. **Andrei Blinov.** Research of Switching Properties and Performance Improvement Methods of High-Voltage IGBT based DC/DC Converters. 2012.
54. **Paul Taklaja.** 110 kV õhuliinide isolatsiooni töökindluse analüüs ja töökindluse tõstmise meetodid. 2012.
55. **Lauri Kütt.** Analysis and Development of Inductive Current Sensor for Power Line On-Line Measurements of Fast Transients. 2012.
56. **Heigo Mölder.** Vedelmetalli juhitava segamisvõimaluse uurimine alalisvoolu kaarleekahjus. 2012.
57. **Reeli Kuhi-Thalfeldt.** Distributed Electricity Generation and its Possibilities for Meeting the Targets of Energy and Climate Policies. 2012.
58. **Irena Milaševski.** Research and Development of Electronic Ballasts for Smart Lighting Systems with Light Emitting Diodes. 2012.
59. **Anna Andrijanovitš.** New Converter Topologies for Integration of Hydrogen Based Long-Term Energy Storages to Renewable Energy Systems. 2013.
60. **Viktor Beldjajev.** Research and Development of the New Topologies for the Isolation Stage of the Power Electronic Transformer. 2013.
61. **Eduard Brindfeldt.** Visually Structured Methods and Tools for Industry Automation. 2013.
62. **Marek Mägi.** Development and Control of Energy Exchange Processes Between Electric Vehicle and Utility Network. 2013.
63. **Ants Kallaste.** Low Speed Permanent Magnet Slotless Generator Development and Implementation for Windmills. 2013.
64. **Igor Mets.** Measurement and Data Communication Technology for the Implementation in Estonian Transmission Network. 2013.
65. **Julija Šommet.** Analysis of Sustainability Assessment in Carbonate Rock Quarries. 2014.